Supplementary Information

Precise Assembly/Disassembly of Homo-Type and Hetero-Type Macrocycles with Photoresponsive and Non-Photoresponsive Dynamic Covalent Bonds

Junmiao Deng[a,b], Hanwei Lu[a], Hebo Ye[a], Yu Hai[a], Zimu Liu[a,b], and Lei You[a,c,*]

a. State Key Laboratory of Structural Chemistry, Fujian Institute of Research on the Structure of Matter, Chinese Academy of Sciences, Fuzhou 350002, China.

b. College of Chemistry and Material Science, Fujian Normal University, Fuzhou 350007, China.

c. University of Chinese Academy of Sciences, Beijing 100049, China.

*E-mail: lyou@fjirsm.ac.cn

TABLE OF CONTENTS

1. General Methods

^{1}H NMR and ^{13}C NMR spectra were recorded on a 400 MHz Bruker Biospin avance III HD spectrometer or a 600 MHz JEOL JNM-ECZ600S spectrometer. Deuterated reagents for characterization and *in situ* reactions were purchased from Sigma-Aldrich Chemical Co. and Cambridge Isotope Laboratories, Inc. (purity ≥ 99.9%). The chemical shifts (δ) for ^{1}H NMR spectra, given in ppm, are referenced to the residual proton signal of the deuterated solvent. Mass spectra were recorded on a Bruker IMPACT-II or Thermo Scientific LCQ Fleet spectrometer. The UV-Vis spectra were recorded on a Shimadzu UV-1700i spectrometer. All other reagents were obtained from commercial sources and used without further purification, unless indicated otherwise.

Irradiation experiments. The UV and Visible light irradiation experiments were carried out on a CEL−HXF300 xenon lamp with bandpass filters at 313 ± 10 and 650 ± 10 nm, respectively.

Dynamic covalent reactions in solution. Dynamic Covalent Reactions (DCRs) were performed *in situ* in $CDCl_3$ at room temperature without isolation and purification, and the mixture was characterized by ^{1}H NMR (400 MHz). See specific conditions in figure or scheme captions of the main text or supplementary information if necessary.

The regulation of macrocycles. The regulation of macrocycles was performed *in situ* in $CDCl_3$ at room temperature, and the mixture was characterized by ^{1}H NMR (400 MHz). See specific conditions in figure captions of the main text or supplementary information if necessary.

2. Synthesis and Characterization

Scheme S1. Synthesis of $\mathbf{1}_o$

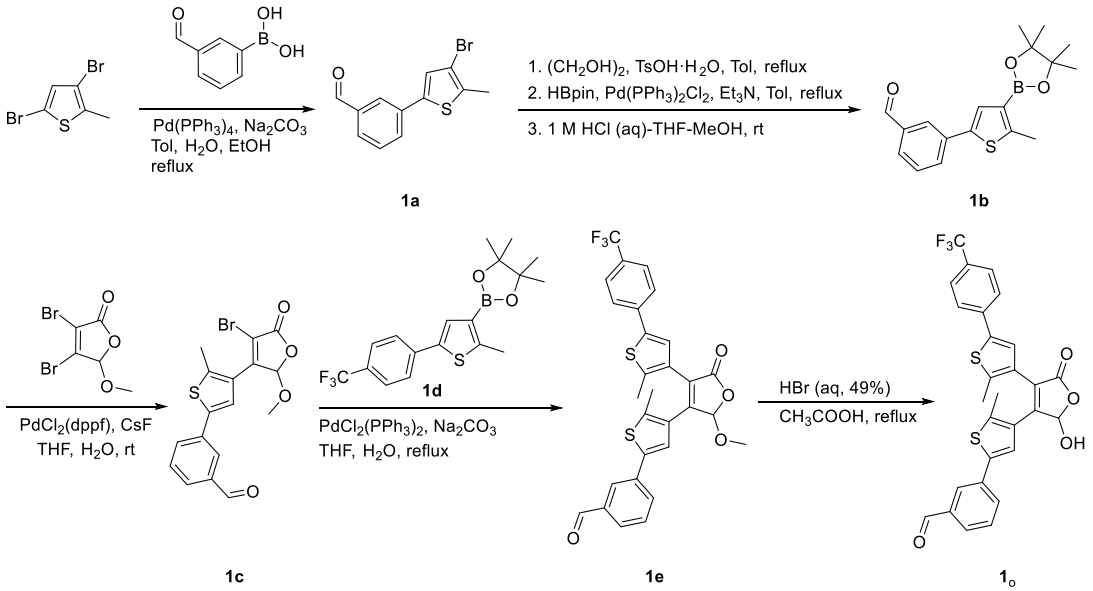

1a: 3,5-dibromo-2-methylthiophene (prepared according to the literature procedure,[S1] (5.12 g, 20.2 mmol) and 3-formylphenylboronic acid (3.60 g, 24.0 mmol) were dissolved in toluene/ethanol (6:1, 70 mL). $Pd(PPh_3)_4$ (185 mg, 0.16 mmol), Na_2CO_3 (8.48 g, 80.0 mmol), and water (5 mL) were then added. The resulting mixture was refluxed for 12 h. After the completion of reaction, the mixture was diluted by ethyl acetate (150 mL). The combined organic layer was dried over Na_2SO_4, and the solvents were evaporated *in vacuo*. The residue was purified by silica gel column chromatography (petroleum ether/dichloromethane 20:1 to 8:1) to give the product **1a** (4.52 g, 80 %) as a white solid. ^{1}H NMR (400 MHz, $CDCl_3$): δ = 10.04 (s, 1H), 8.00 (s, 1H), 7.82 – 7.72 (m, 2H), 7.55 (t, *J* = 7.7 Hz, 1H), 7.21 (s, 1H), 2.44 (s, 3H). ^{13}C{^{1}H} NMR (101 MHz, $CDCl_3$): 192.0, 139.5, 137.1, 135.0, 134.6, 131.0, 129.8, 129.1, 126.7, 126.1, 110.4, 15.1. APCI-HRMS: *m/z* calculated for $C_{12}H_{10}BrOS$ $[M + H]^+$: 280.9630; found: 280.9641.

1b: To a solution of **1a** (2.31 g, 8.25 mmol) in toluene (120 mL), were added ethylene glycol (5.12 g, 82.5 mmol) and *p*-TsOH·H_2O (157 mg, 0.82 mmol). The resulting mixture was refluxed in a Dean-Stark trap until water ceased to be removed (16 h). After the completion of reaction, Et_3N (10 mL) was added. The mixture was washed with brine (3 × 50 mL), and the organic layer was dried over Na_2SO_4 and evaporated *in vacuo* to give a yellow oil. The obtained crude product and $PdCl_2(PPh_3)_2$ (288 mg, 0.41 mmol) were dissolved in degassed toluene (70 mL), and then pinacolborane (4.5 mL, 30.9 mmol) and Et_3N (9.6 mL, 69.3 mmol) were added. The reaction was refluxed for 13 h, cooled down, and then quenched with water (10 ml). The mixture was filtered

through a pad of silica gel, and the solvents were washed with brine (3 × 50 mL) and dried over Na_2SO_4. Evaporation of the solvents *in vacuo* gave the product as a black oil. The obtained crude product was dissolved in tetrahydrofuran (40 mL), and HCl aqueous solution (1 M, 10 mL) and MeOH (5 mL) was added. The resulting mixture was stirred for 4 h at room temperature. After the completion of reaction, the mixture was diluted by ethyl acetate (150 mL) and washed with brine (3 × 50 mL). The combined organic layer was dried over Na_2SO_4 and evaporated *in vacuo*. The residue was purified by silica gel column chromatography (petroleum ether/ethyl acetate 40:1 to 20:1) to give the product **1b** (1.21 g, 45 %) as a white solid. ^{1}H NMR (400 MHz, $CDCl_3$): δ = 10.03 (s, 1H), 8.06 (s, 1H), 7.81 (d, *J* = 7.8 Hz, 1H), 7.73 (d, *J* = 7.6 Hz, 1H), 7.53 (s, 1H), 7.50 (t, *J* = 7.7 Hz, 1H), 2.72 (s, 3H), 1.34 (s, 12H). ^{13}C{^{1}H} NMR (101 MHz, $CDCl_3$): δ = 192.4, 153.5, 139.2, 137.0, 135.6, 131.4, 130.2, 129.6, 128.0, 126.7, 83.6, 25.1, 16.1. ESI-HRMS: *m/z* calculated for $C_{18}H_{22}BO_3S$ $[M + H]^+$: 329.1377; found: 329.1385.

1c: 3,4-dibromo-5-methoxyfuran-2(5H)-one (prepared according to the literature procedure,[S2] 0.66 g, 2.4 mmol), $Pd(dppf)Cl_2$ (0.15 g, 0.20 mmol), and **1b** (0.65 g, 2.0 mmol) were dissolved in tetrahydrofuran (50 mL), and cesium fluoride (0.91 g, 6.0 mmol) and water (5 mL) were added. The reaction mixture was stirred at room temperature for 48 h. After the completion of reaction, the mixture was diluted by ethyl acetate (150 mL). The combined organic layer was washed with brine (3 × 20 mL), dried over Na_2SO_4, and evaporated *in vacuo*. The residue was purified by silica gel column chromatography (petroleum ether/ethyl acetate 20:1 to 10:1) to give the product **1c** (0.39 g, 50%) as a white solid. ^{1}H NMR (400 MHz, $CDCl_3$): δ = 10.06 (s, 1H), 8.05 (s, 1H), 7.83 – 7.80 (m, 2H), 7.58 (t, *J* = 7.7 Hz, 1H), 7.55 (s, 1H), 6.11 (s, 1H), 3.60 (s, 3H), 2.58 (s, 3H). ^{13}C{^{1}H} NMR (101 MHz, $CDCl_3$): δ = 192.0, 166.3, 153.0, 142.5, 140.3, 137.1, 134.4, 131.4, 129.9, 129.5, 127.6, 126.2, 123.6, 112.8, 103.8, 56.7, 15.9. ESI-HRMS: *m/z* calculated for $C_{17}H_{12}BrO_4S$ $[M - H]^-$: 390.9645; found: 390.9644.

1e: **1c** (0.87 g, 2.22 mmol) and **1d** (prepared according to the literature procedure,[S3] 2.45 g, 6.66 mmol) were disssolved in THF/H_2O (10:1, 75 mL), and then $PdCl_2(PPh_3)_2$ (0.16 g, 0.22 mmol) and Na_2CO_3 (0.94 g, 8.88 mmol) were added. The reaction mixture was refluxed for 10 h. The mixture was diluted by ethyl acetate (250 mL). The organic layer was washed with brine (3 × 50 mL), dried over Na_2SO_4, and evaporated *in vacuo*. The residue was purified by silica gel column chromatography (petroleum ether/ethyl acetate 20:1 to 10:1) to give the product **1e** (1.01 g, 82%) as a white solid. ^{1}H NMR (400 MHz, $CDCl_3$): δ = 10.05 (s, 1H), 8.02 (s, 1H), 7.80 (d, *J* = 7.6 Hz, 1H), 7.76 (d, *J* = 7.8 Hz, 1H), 7.66 – 7.54 (m, 5H), 7.35 (m, 2H), 6.12 (s, 1H), 3.69 (s, 3H), 2.09 (s, 3H), 2.06 (s, 3H). ^{19}F NMR (376 MHz, $CDCl_3$): δ = -62.54. ^{13}C{^{1}H} NMR (101 MHz, $CDCl_3$): δ = 191.9, 170.0, 150.4, 141.8, 140.8, 140.4, 139.6, 137.1, 137.0, 134.4, 131.2, 129.8, 129.4, 129.4, 129.1, 128.2, 125.9, 125.9, 125.9, 125.8, 125.6, 125.5, 125.4, 125.2, 123.5, 122.7, 102.9, 56.9, 14.8. ESI-HRMS: *m/z* calculated for $C_{29}H_{20}F_3O_4S_2$, $[M - H]^-$:

553.0761; found: 553.0760.

1$_o$: **1e** (0.50 g, 0.9 mmol) was dissolved in acetic acid (30 mL), and 48% HBr (6 mL) was added. The resulting mixture was refluxed for 14 h. After the completion of reaction, the mixture was diluted with ethyl acetate (150 ml). The organic layer was washed with saturated $NaHCO_3$ solution and then brine, dried over Na_2SO_4, and evaporated *in vacuo*. The residue was purified by silica gel column chromatography (petroleum ether/ethyl acetate 20:1 to 10:1) to give the product **1**$_o$ (0.41 g, 85%) as a white solid. ^{1}H NMR (400 MHz, CD_3CN): δ = 10.00 (s, 1H), 8.02 (s, 1H), 7.81 (t, *J* = 6.8 Hz, 2H), 7.72 (d, *J* = 8.1 Hz, 2H), 7.66 (d, *J* = 8.2 Hz, 2H), 7.58 (t, *J* = 7.7 Hz, 1H), 7.46 (s, 1H), 7.41 (s, 1H), 6.52 (s, 1H), 5.60 (s, 1H), 2.11 (s, 3H), 2.08 (s, 3H). ^{19}F NMR (376 MHz, CD_3CN): δ = -63.03. ^{13}C{^{1}H} NMR (101 MHz, CD_3CN): δ = 193.3, 170.8, 154.2, 142.6, 141.6, 140.6, 139.7, 138.3, 138.2, 135.2, 131.8, 130.91, 130.87, 129.96, 129.5, 129.5, 129.2, 127.3, 126.9, 126.7, 126.6, 126.5, 125.4, 125.3, 124.0, 98.4, 14.9, 14.6. ESI-HRMS: m/z calculated for $C_{28}H_{18}F_3O_4S_2$ [M - H]$^-$: 539.0604; found: 539.0602.

Scheme S2. Synthesis of **6**$_o$ and **10**$_o$.

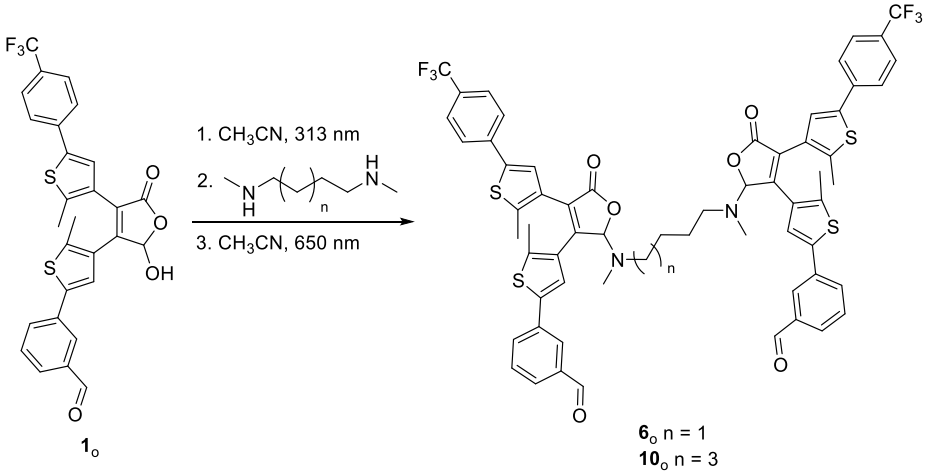

6$_o$: A solution of **1**$_o$ (32.5 mg, 0.060 mmol) in CH_3CN (6.0 mL) was irradiated at 313 nm for 3 h, and *N*,*N*'-dimethyl-1,4-butanediamine (3.15 mg, 0.027 mmol) was added. The reaction was stirred under dark for 12 h at room temperature, and then diluted with CH_3CN (12 mL). The resulting mixture was irradiated at 650 nm until the suspension turned from black to red. The solvents were evaporated *in vacuo*. The residue was purified by silica gel column chromatography ($CHCl_3$) to give the product **6**$_o$ (17.4 mg, 56%) as a white solid. ^{1}H NMR (400 MHz, $CDCl_3$): δ = 9.97 (s, 2H), 7.92 (s, 2H), 7.72 (d, *J* = 7.7 Hz, 2H), 7.68 – 7.64 (m, 2H), 7.62 (d, *J* = 8.4 Hz, 4H), 7.57 (d, *J* = 8.3 Hz, 4H), 7.52 – 7.45 (m, 2H), 7.32 (s, 2H), 7.20 (d, *J* = 3.8 Hz, 2H), 6.06 (s, 2H), 2.77 – 2.58 (m, 4H), 2.24 (s, 6H), 2.02 (s, 6H), 1.99 (s, 6H), 1.45 – 1.26 (m, 4H). ^{19}F NMR (376 MHz, $CDCl_3$): δ = -62.52. ^{13}C{^{1}H} NMR (101 MHz, $CDCl_3$): δ = 191.9, 170.9, 151.5, 141.2, 140.4, 140.02, 139.6, 137.3, 137.1, 134.5, 131.2, 130.3, 129.9, 129.8, 129.5, 129.1, 129.0, 126.2, 126.00, 125.8, 125.7, 125.5, 125.4, 124.0, 122.9, 98.6, 52.7, 34.7, 24.9, 15.1, 14.9. ESI-HRMS: m/z calculated for $C_{62}H_{50}N_2O_6S_4F_6Na$ [M + Na]$^+$,

1183.2348; found: 1183.2307.

10$_o$: **10**$_o$ was synthesized from **1**$_o$ (32.5 mg, 0.060 mmol) and *N*,*N*'-dimethyl-1,6-hexanediamine (3.90 mg, 0.027 mmol) according to the procedure of **6**$_o$. The residue was purified by silica gel column chromatography ($CHCl_3$) to give the product **10**$_o$ (18.2 mg, 57%) as a white solid. ^{1}H NMR (400 MHz, $CDCl_3$): δ = 10.00 (s, 2H), 7.97 (s, 2H), 7.75 (d, *J* = 7.5 Hz, 2H), 7.70 (d, *J* = 7.7 Hz, 2H), 7.64 (d, *J* = 8.4 Hz, 4H), 7.59 (d, *J* = 8.3 Hz, 4H), 7.52 (t, *J* = 7.7 Hz, 2H), 7.37 (s, 2H), 7.24 (s, 2H), 6.07 (s, 2H), 2.80 – 2.59 (m, 2H), 2.31 (s, 6H), 2.06 (s, 6H), 2.04 (s, 6H), 1.48 – 1.33 (m, 4H), 1.22 – 1.05 (m, 4H). ^{19}F NMR (376 MHz, $CDCl_3$): δ = -62.53.^{13}C{^{1}H} NMR (101 MHz, $CDCl_3$): δ = 191.9, 171.0, 151.6, 141.2, 140.4, 139.9, 139.5, 137.3, 137.1, 134.6, 131.2, 130.3, 129.9, 129.6, 129.4, 129.1, 129.1, 126.1, 126.0, 125.8, 125.7, 125.6, 124.1, 122.9, 98.6, 53.1, 34.8, 27.6, 27.0, 15.1, 14.9. ESI-HRMS: m/z calculated for $C_{64}H_{54}N_2O_4S_4F_6Na$ $[M + Na]^+$, 1211.2661; found: 1211.2662.

^{1}H NMR and ^{13}C NMR Spectra

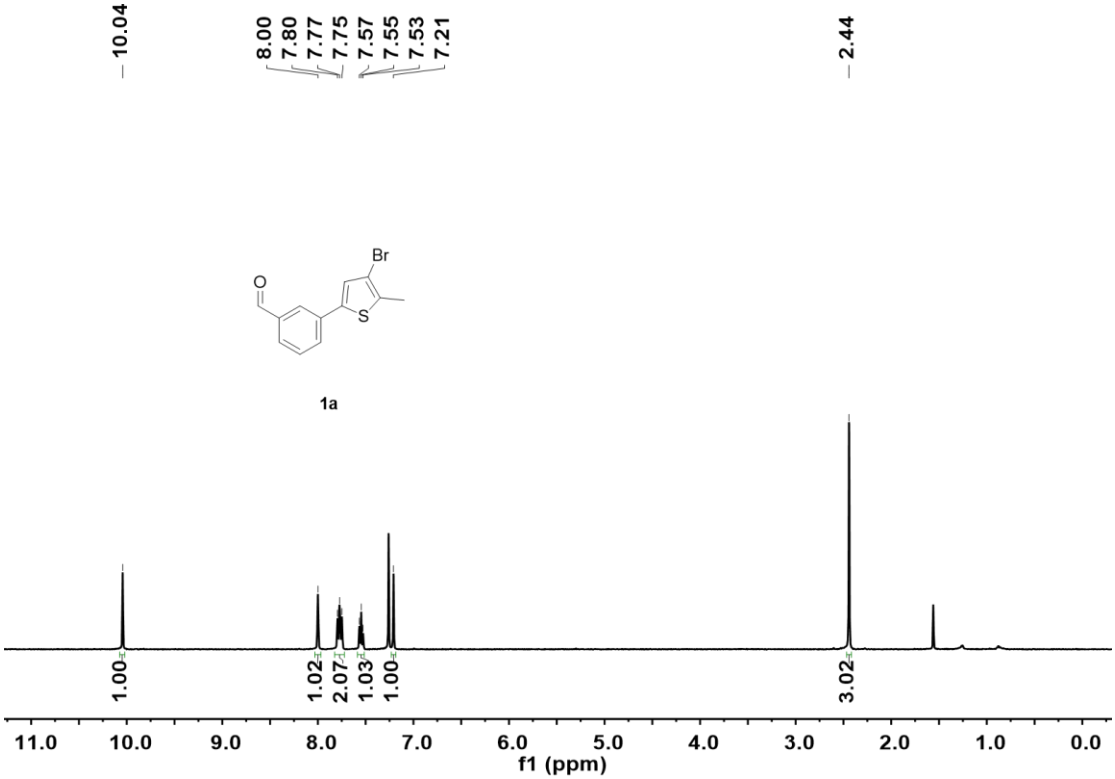

Figure S1. ^{1}H NMR spectrum of **1a** in $CDCl_3$.

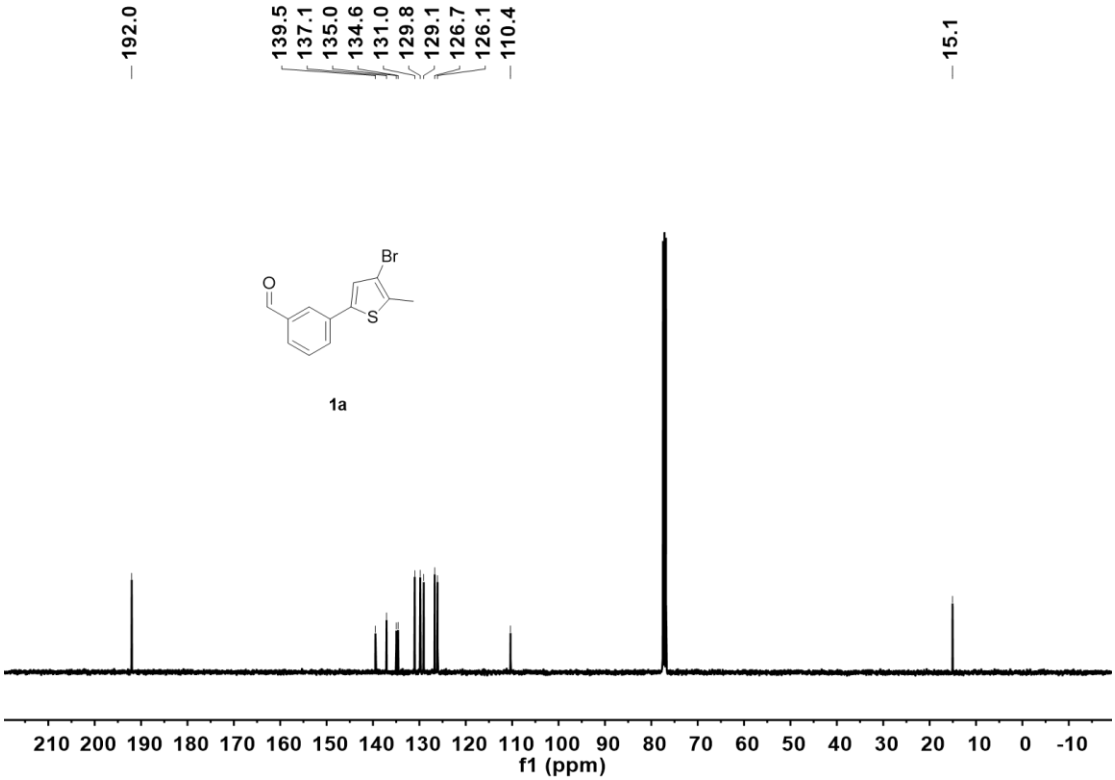

Figure S2. ^{13}C NMR spectrum of **1a** in $CDCl_3$.

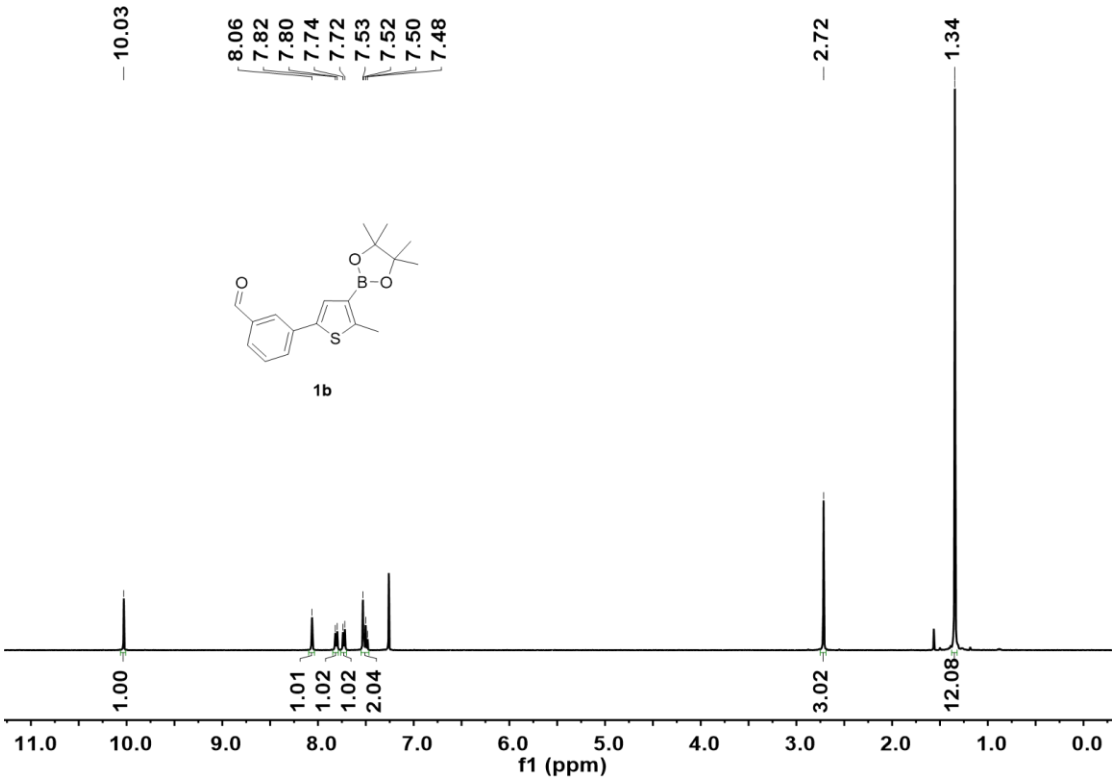

Figure S3. ^{1}H NMR spectrum of **1b** in $CDCl_3$.

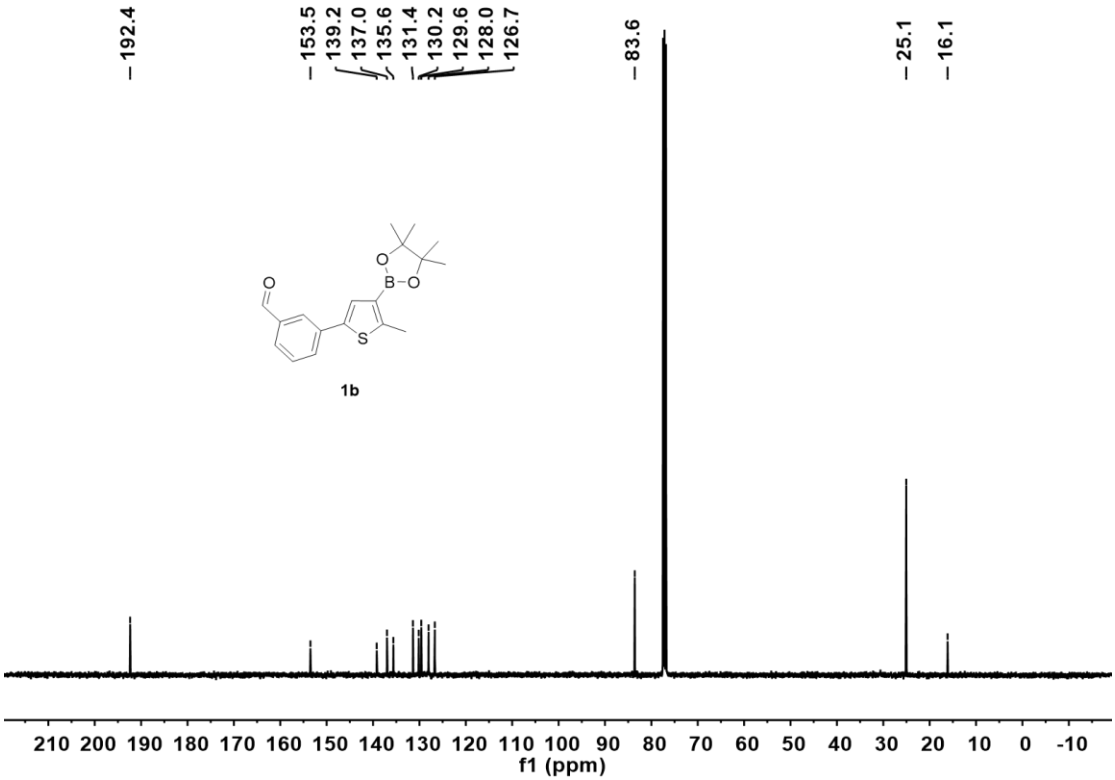

Figure S4. ^{13}C NMR spectrum of **1b** in $CDCl_3$.

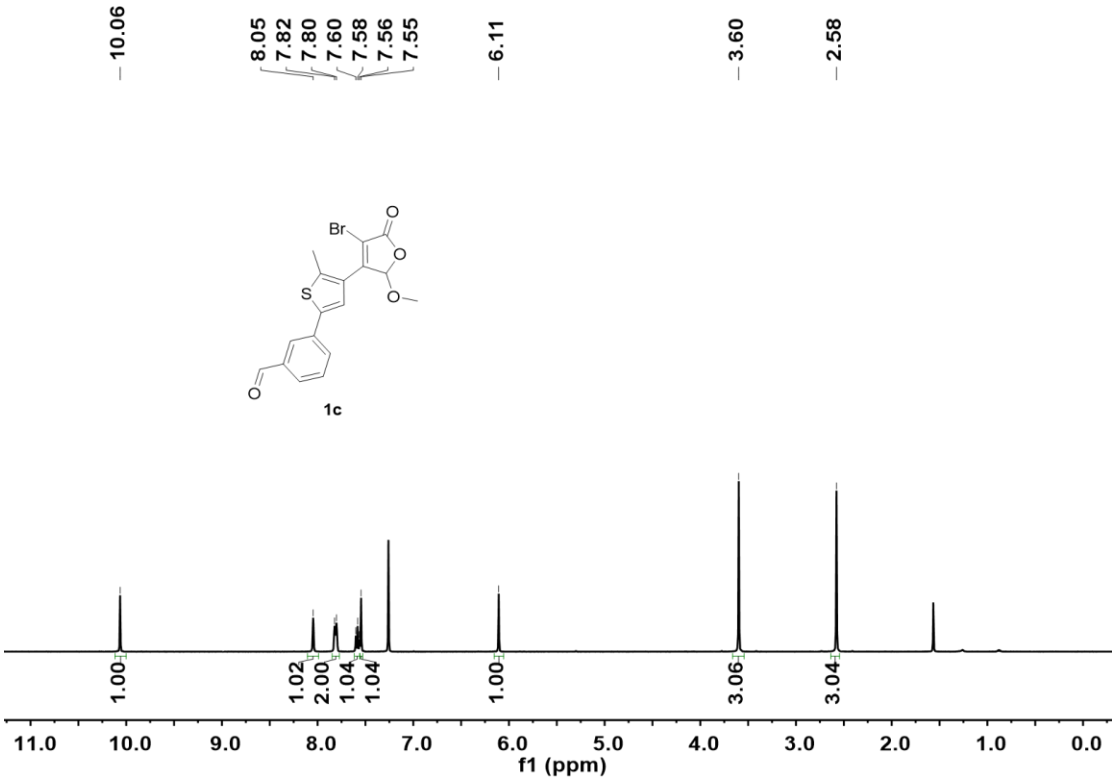

Figure S5. ^{1}H NMR spectrum of **1c** in $CDCl_3$.

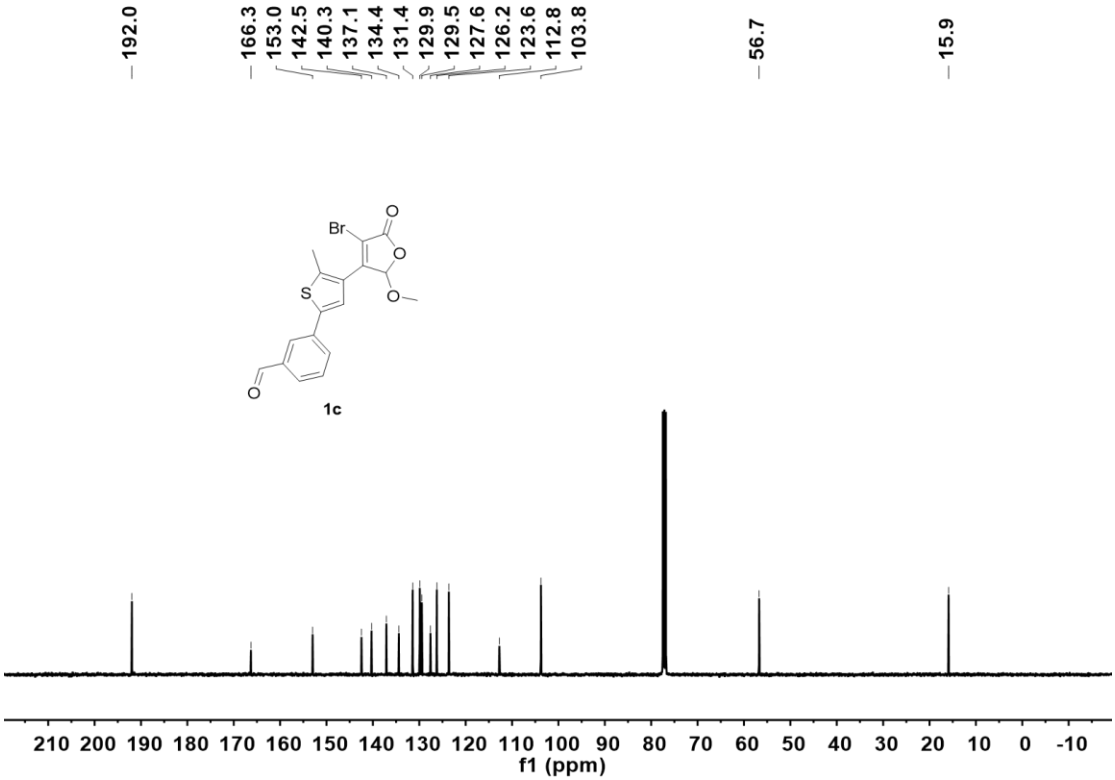

Figure S6. ^{13}C NMR spectrum of **1c** in $CDCl_3$.

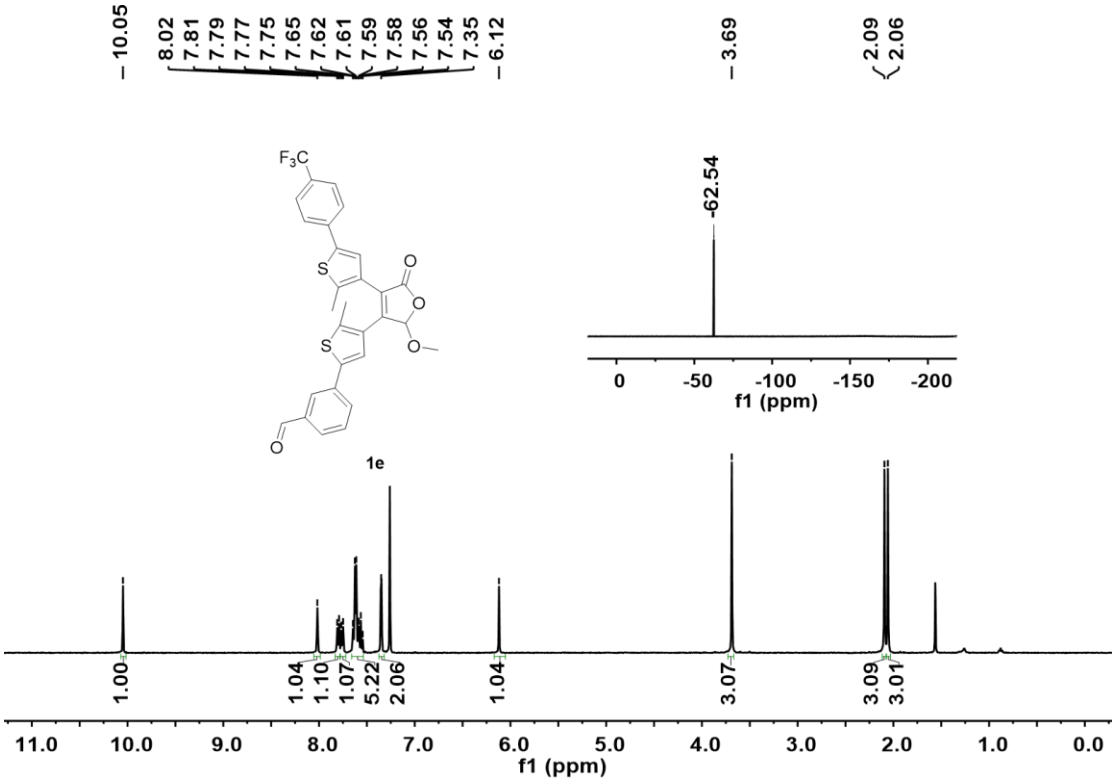

Figure S7. ^{1}H NMR spectrum of **1e** in $CDCl_3$. Inset: ^{19}F NMR spectrum of **1e** in $CDCl_3$.

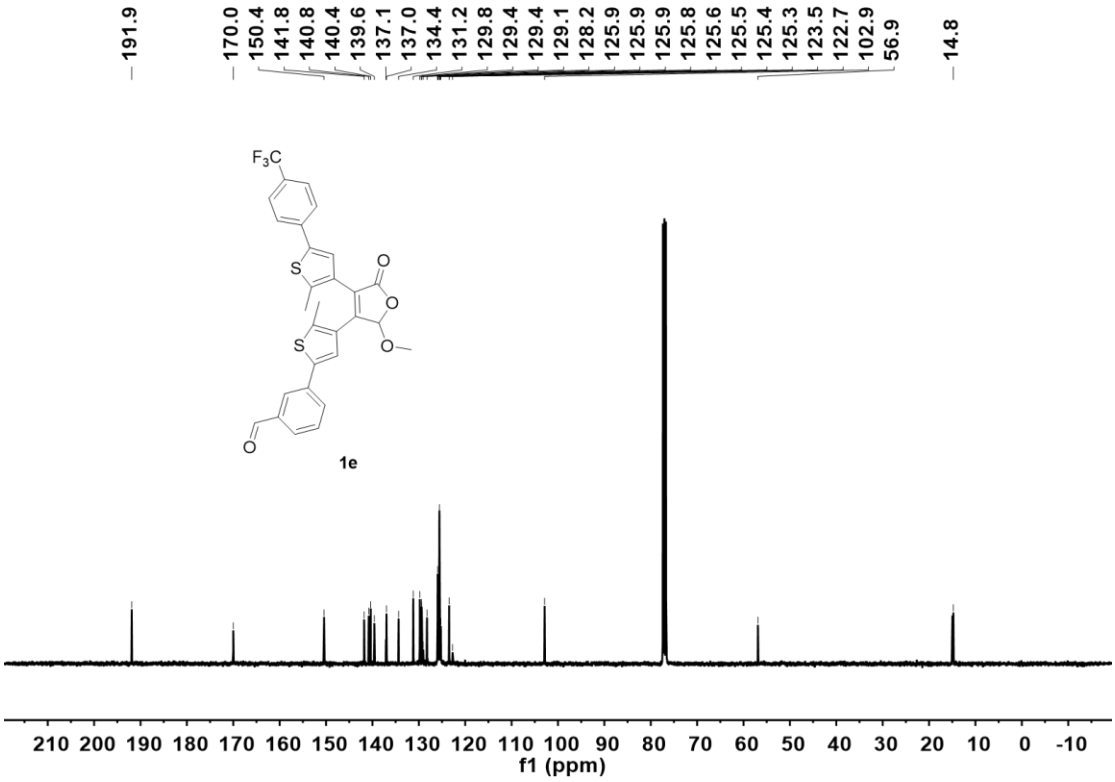

Figure S8. ^{13}C NMR spectrum of **1e** in $CDCl_3$.

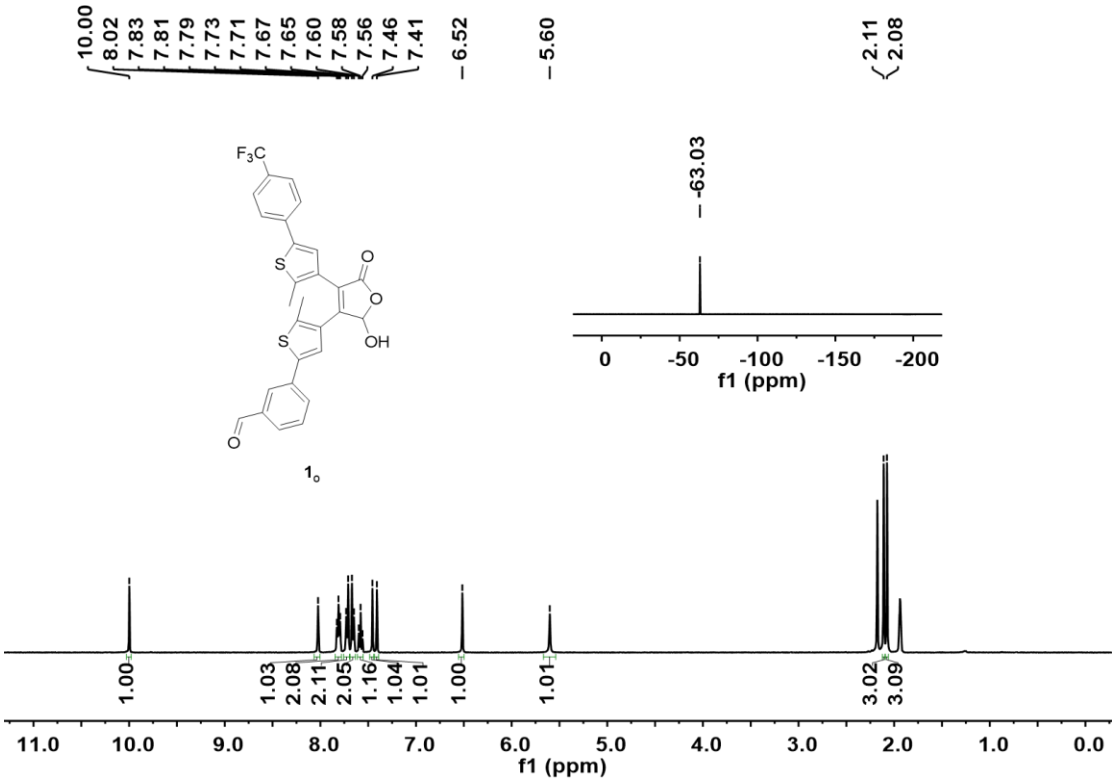

Figure S9. ^{1}H NMR spectrum of **1**$_{o}$ in CD_3CN. Inset: ^{19}F NMR spectrum of **1**$_{o}$ in CD_3CN.

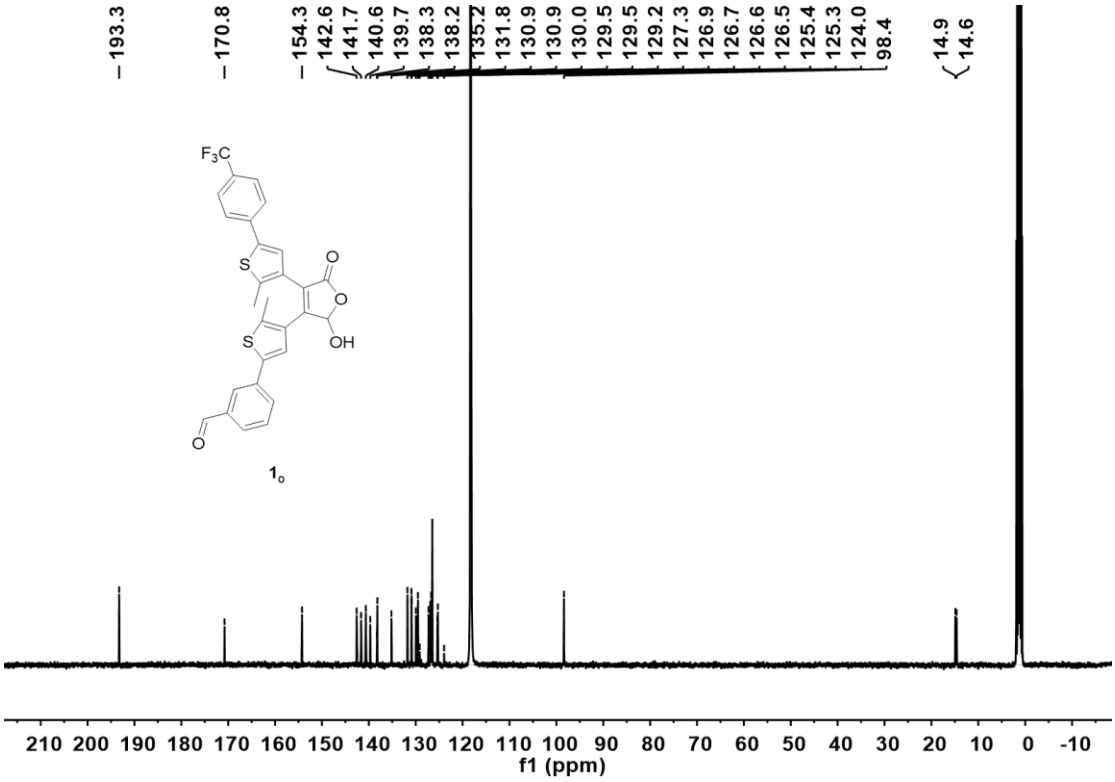

Figure S10. ^{13}C NMR spectrum of **1**$_{o}$ in CD_3CN.

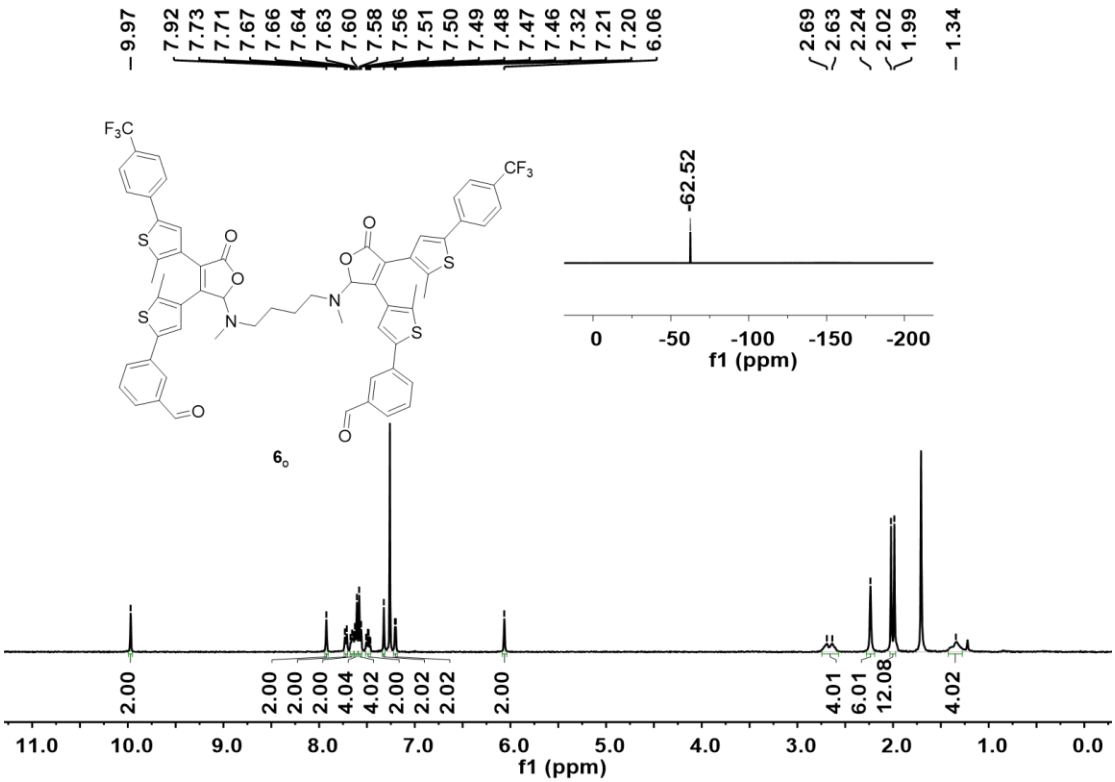

Figure S11. ^{1}H NMR spectrum of **6**$_{o}$ in $CDCl_3$. Inset: ^{19}F NMR spectrum of **6**$_{o}$ in $CDCl_3$.

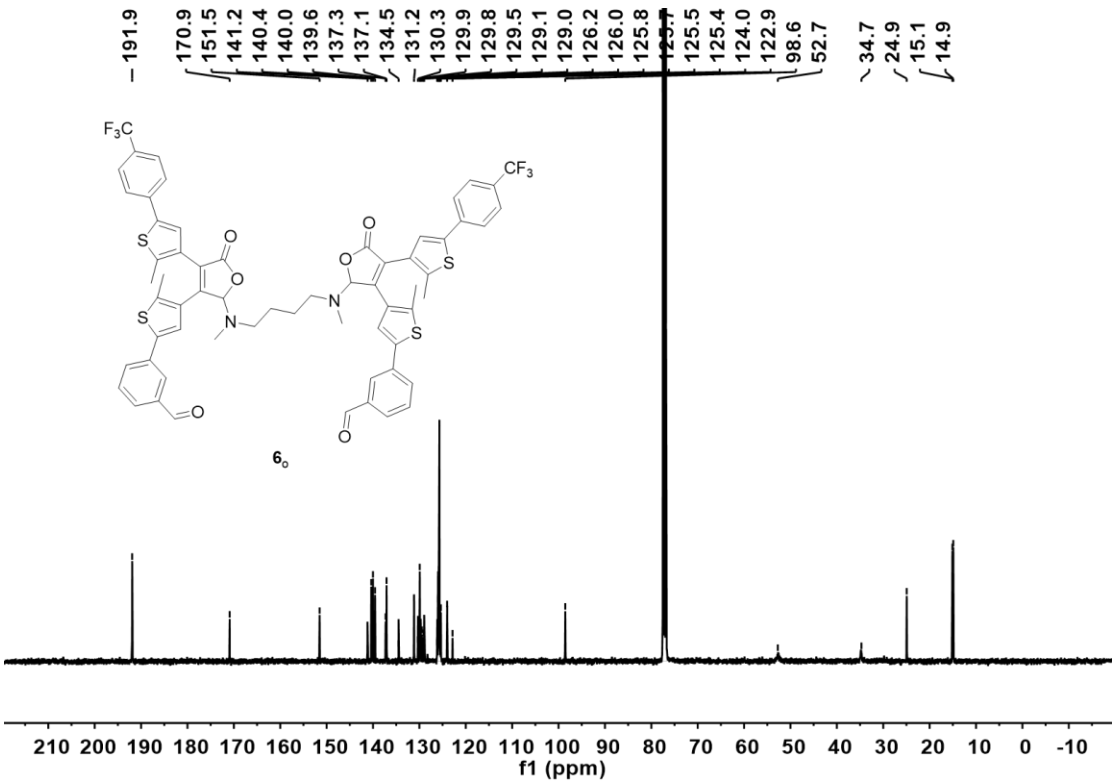

Figure S12. ^{13}C NMR spectrum of **6**$_{o}$ in $CDCl_3$.

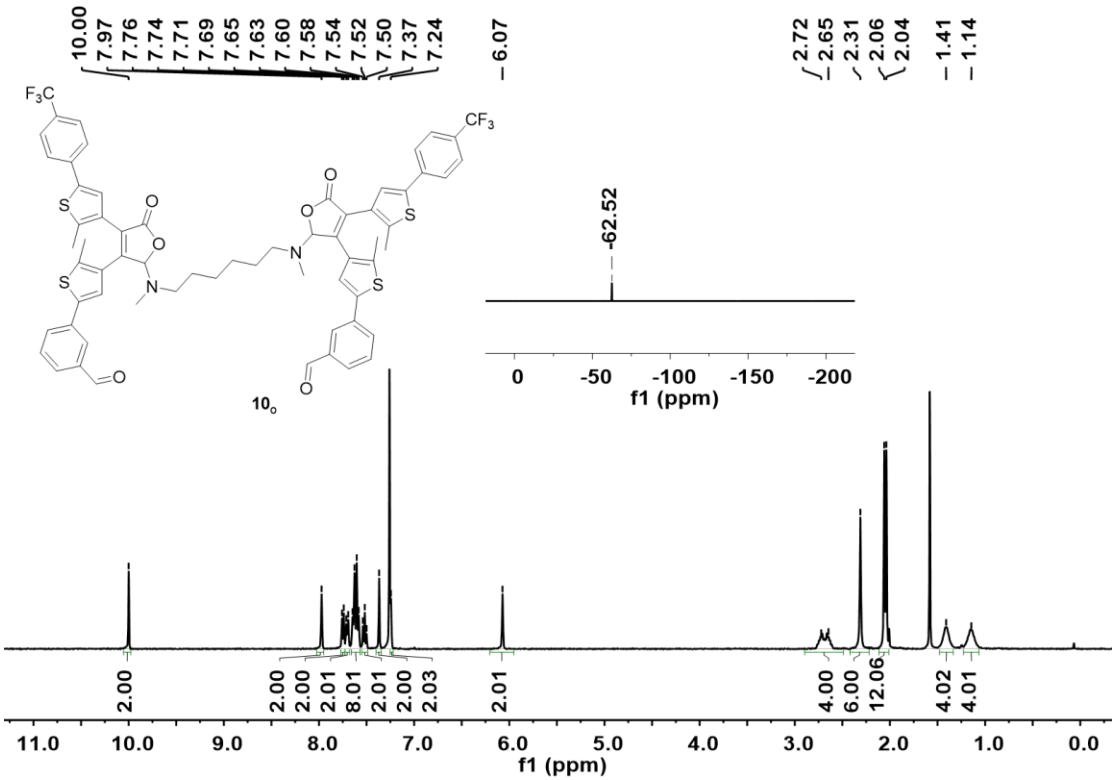

Figure S13. ^{1}H NMR spectrum of **10**$_{o}$ in $CDCl_3$. Inset: ^{19}F NMR spectrum of **10**$_{o}$ in $CDCl_3$.

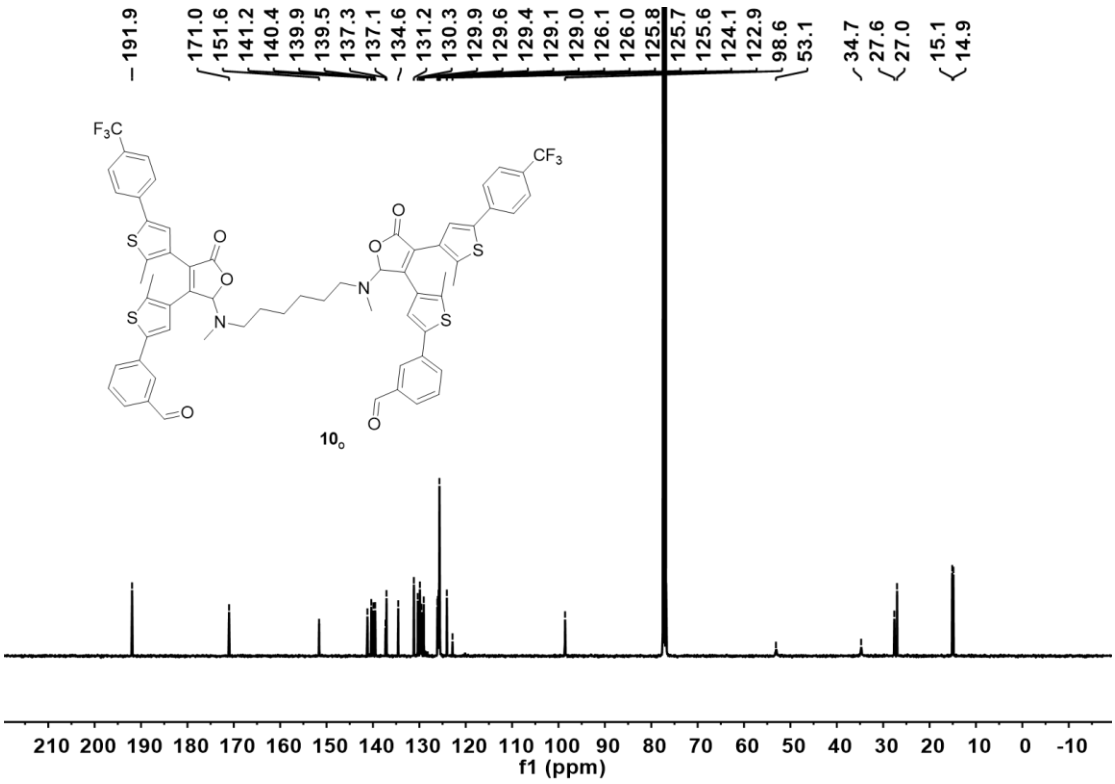

Figure S14. ^{13}C NMR spectrum of **10**$_{o}$ in $CDCl_3$.

Table S1. Summary of crystallographic data.

Compound	**1**$_o$
Formula	$C_{56}H_{38}F_6O_8S_4$
Formula weight	1081.10
T/*K*	100.00(13)
Crystallization solvent	acetonitrile
Color	colorless
Crystal system	triclinic
Space group	*P*-1
a / Å	10.8235(3)
b / Å	15.9748(5)
c / Å	17.4694(5)
α / °	63.306(3)
β / °	80.700(2)
γ / °	87.091(2)
V/ Å^3	2662.30(15)
Z	2
*D*x / g cm^{-3}	1.349
μ / mm^{-1}	1.491
F(000)	1112.0
θ range / º	4.984 to 110.376
GOF on F^2	1.351
R_1 [$I > 2\sigma(I)$]	0.1015
wR_2 (all data)	0.3378

Photoswitching Experiment

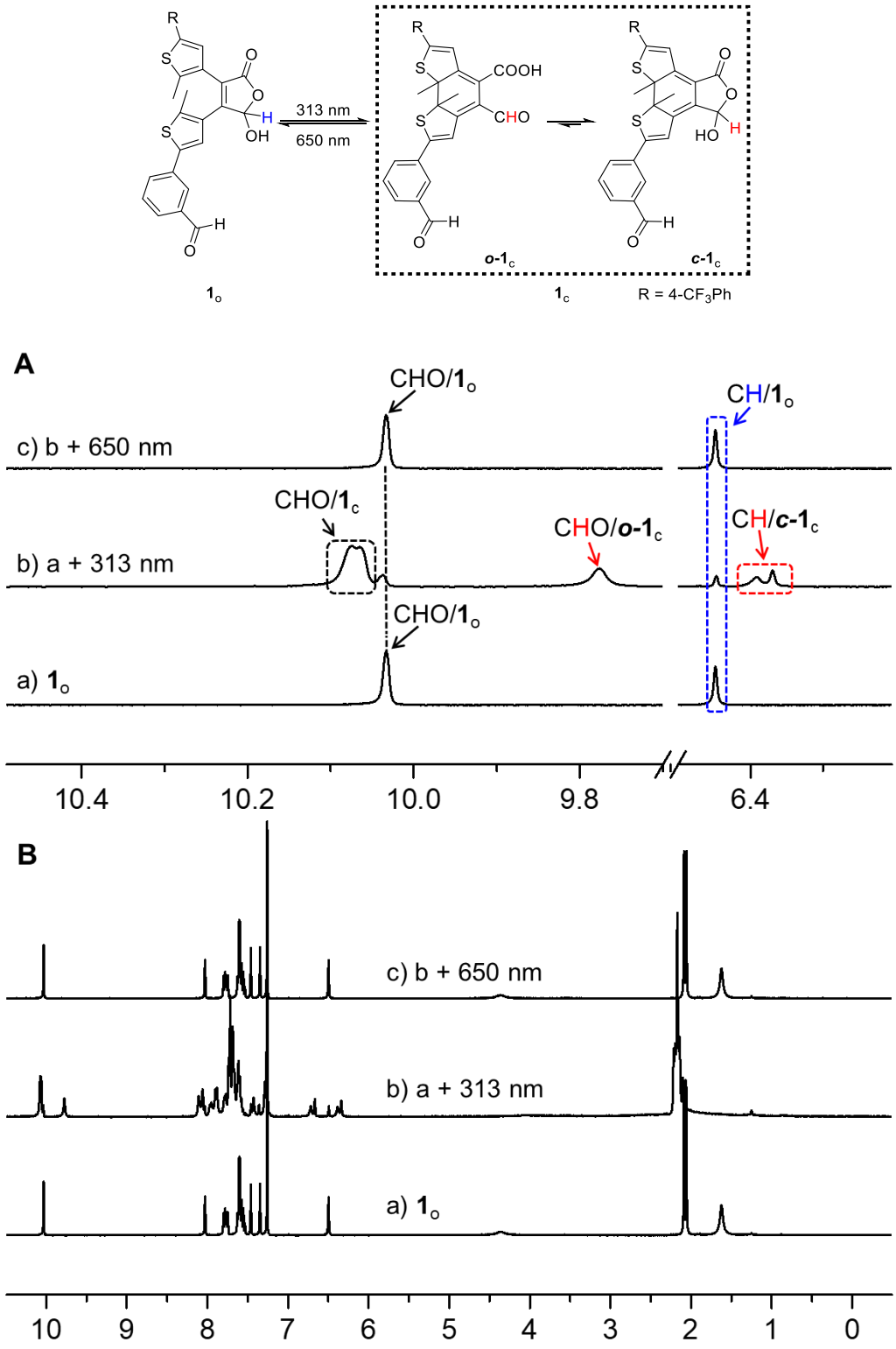

Figure S15. Photoswitching of $\mathbf{1}_o$ (10 mM) in $CDCl_3$. (A) (a) ^1H NMR spectrum of $\mathbf{1}_o$ (10 mM) in $CDCl_3$; (b) Irradiation of $\mathbf{1}_o$ with UV light (313 nm, 150 min), the ratio of $\mathbf{1}_o$ and $\mathbf{1}_c$ is 4:96, and the ratio of ***c*-1**$_c$ and ***o*-1**$_c$ is 57:43; (c) Further irradiation with visible light (650 nm, 150 min). (B) The full ^1H NMR spectra of A.

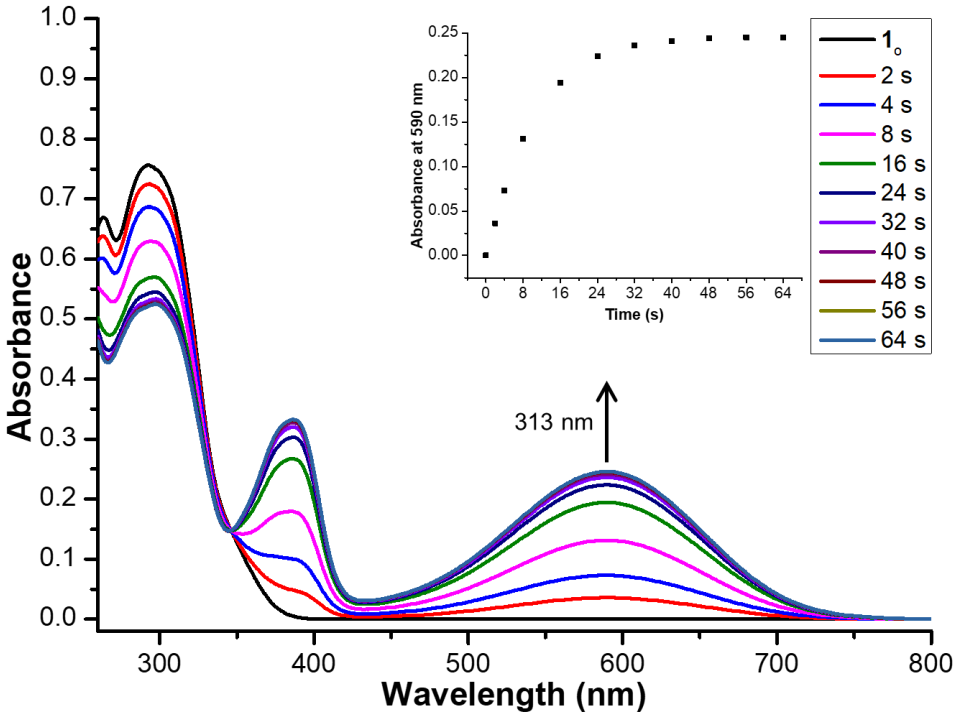

Figure S16. Photocyclization of $\mathbf{1}_o$ to give $\mathbf{1}_c$: changes in absorption spectra upon irradiation of $\mathbf{1}_o$ (25 μM, $CHCl_3$) with 313 nm light. Inset: the change of absorbance at 590 nm with irradiation time.

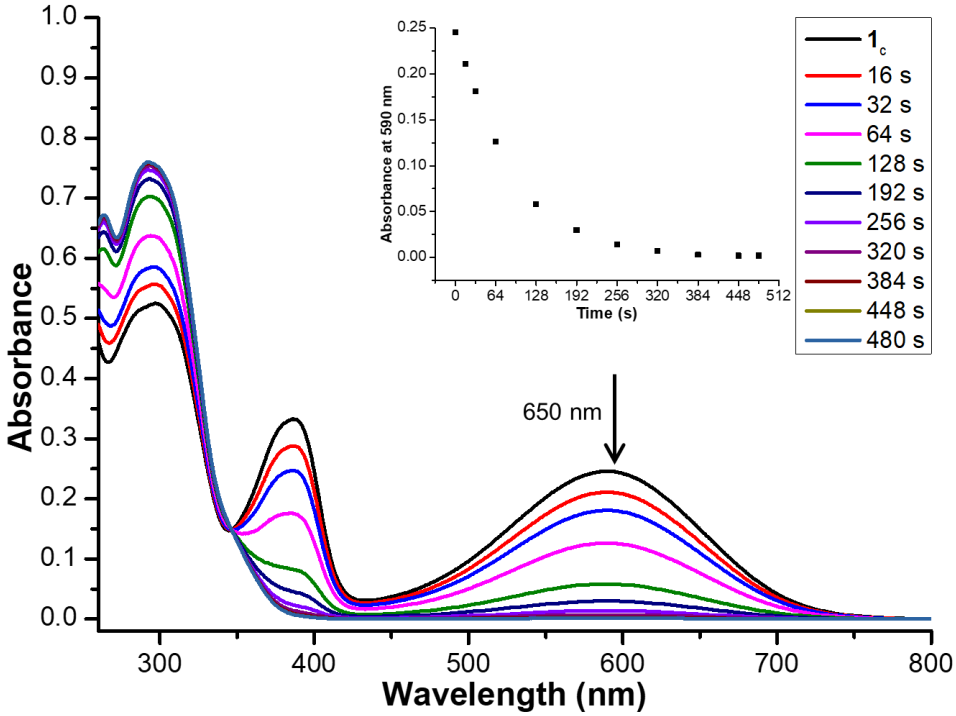

Figure S17. Photocycloreversion of $\mathbf{1}_c$ to give $\mathbf{1}_o$: changes in absorption spectra upon irradiation of $\mathbf{1}_c$ (25 μM, $CHCl_3$) with 650 nm light. Inset: the change of absorbance at 590 nm with irradiation time.

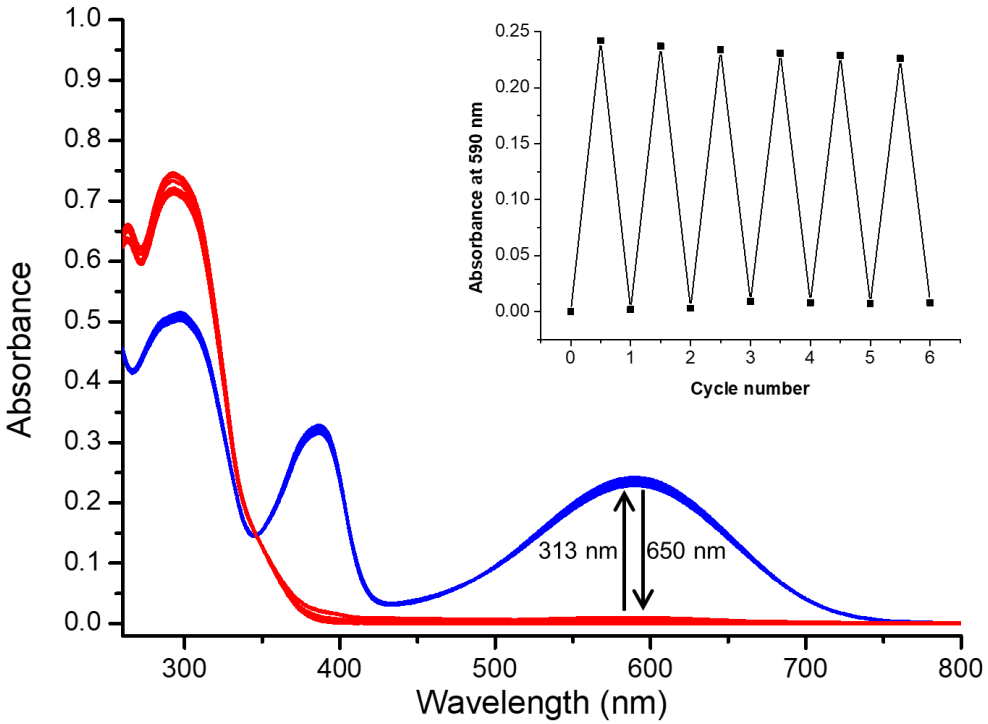

Figure S18. The UV-Vis absorbance spectra of $\mathbf{1}_o$ (25 μM, $CHCl_3$) after multiple alternating irradiations at 313 nm (64 s) and 650 nm (8 min). Inset: the change of absorbance at 590 nm after alternating irradiations.

3. Formation and Characterization of [1+1] Macrocycles

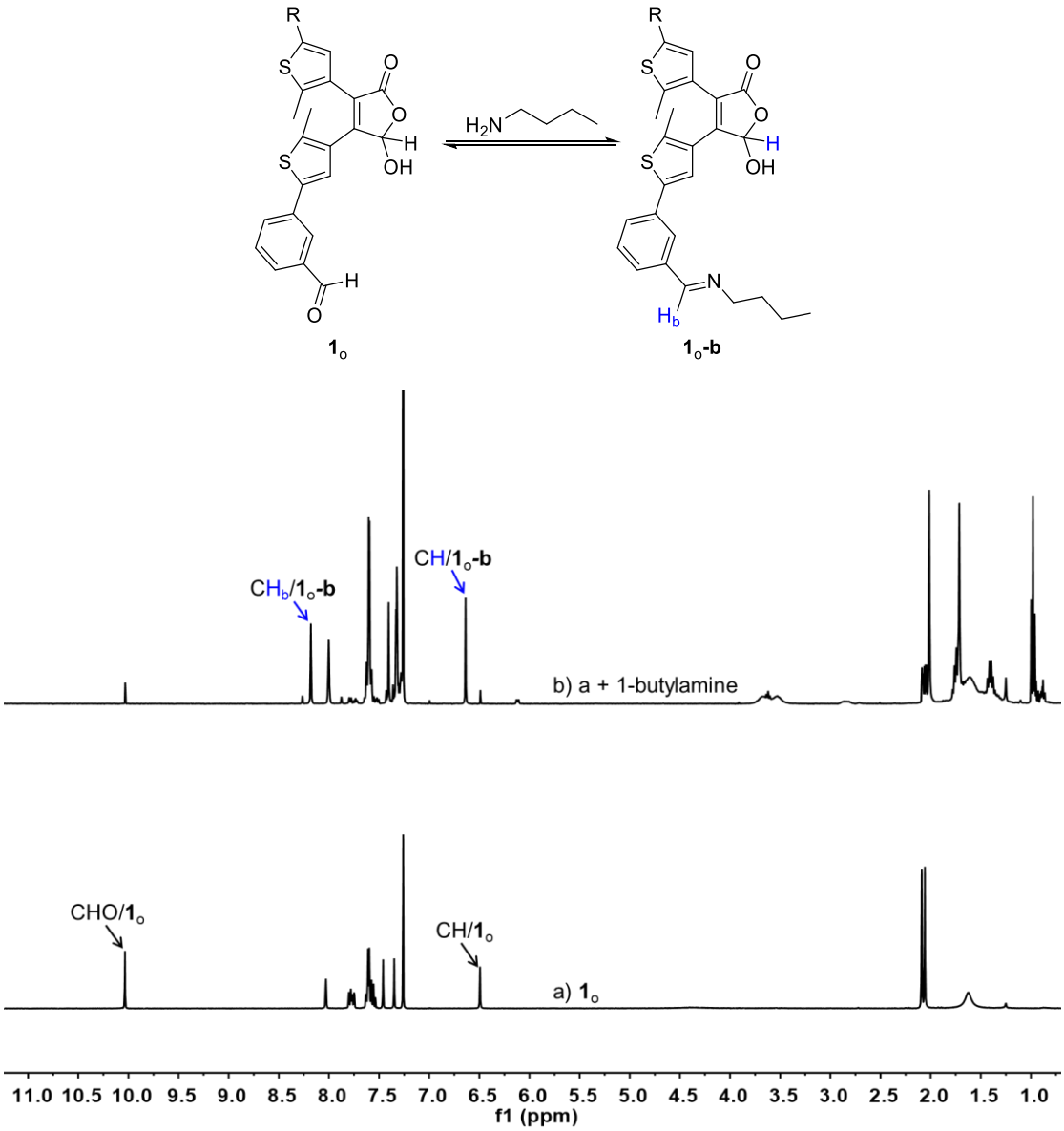

Figure S19. The reaction of $\mathbf{1}_o$ with primary monoamine. (a) ^{1}H NMR spectrum of $\mathbf{1}_o$ (10 mM) in $CDCl_3$; (b) The addition of 1-butylamine (1.0 equiv.) to panel a. $\mathbf{1}_o$ converted to $\mathbf{1}_o$**-b** after 1 day, and the conversion of reaction was 82%. The hemiacetal from site a remained nearly unreactive.

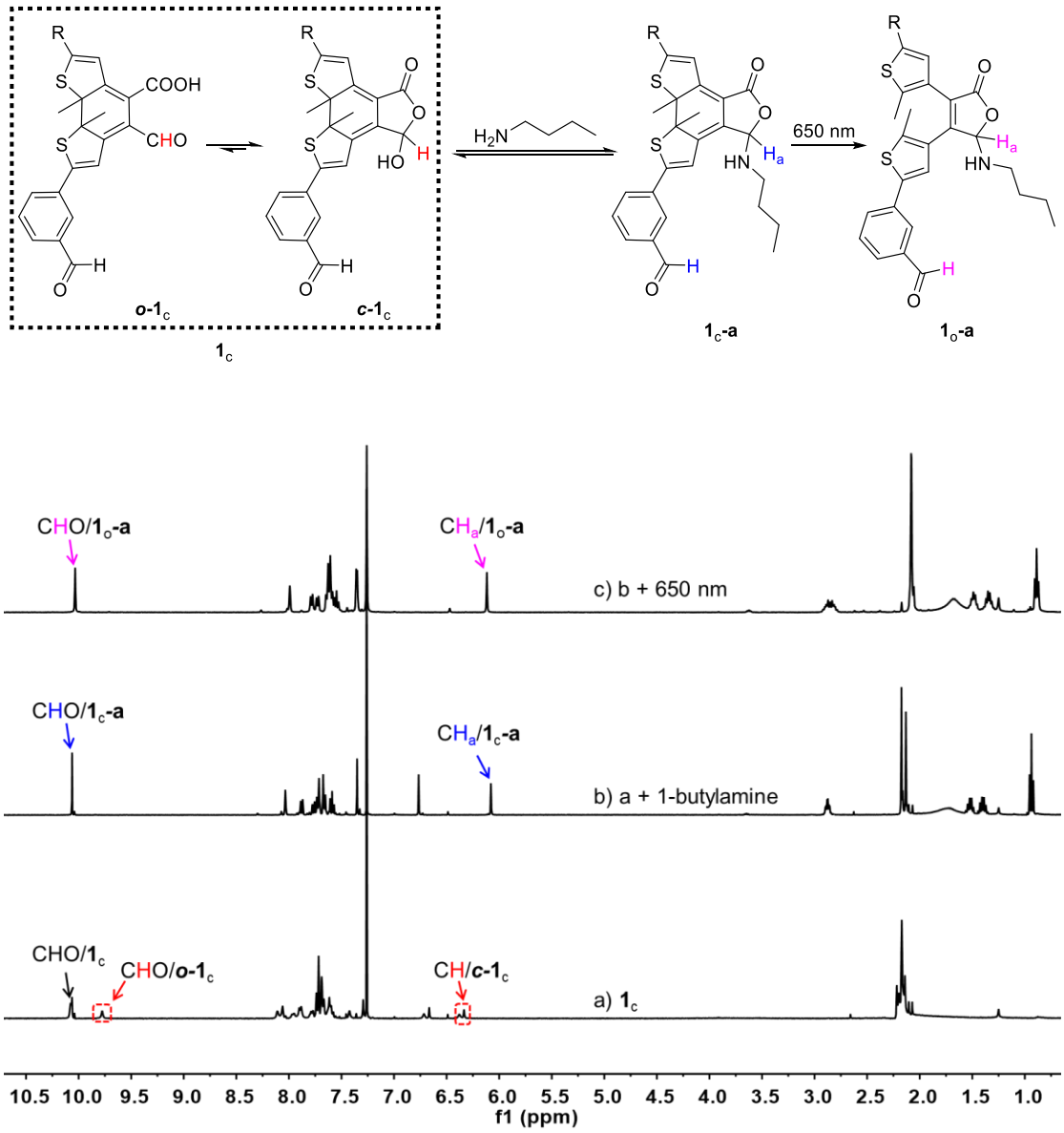

Figure S20. The reaction of $\mathbf{1}_c$ with primary monoamine. (a) ^{1}H NMR spectrum of $\mathbf{1}_c$ (10 mM, created from the irradiation of $\mathbf{1}_o$ at 313 nm) in $CDCl_3$; (b) The addition of 1-butylamine (1.0 equiv.) to panel a. $\mathbf{1}_c$ converted to $\mathbf{1}_c$**-a** within 3 min. (c) Irradiation of panel b at 650 nm for 120 min to give $\mathbf{1}_o$**-a**. The aldehyde from site b remained nearly unreactive.

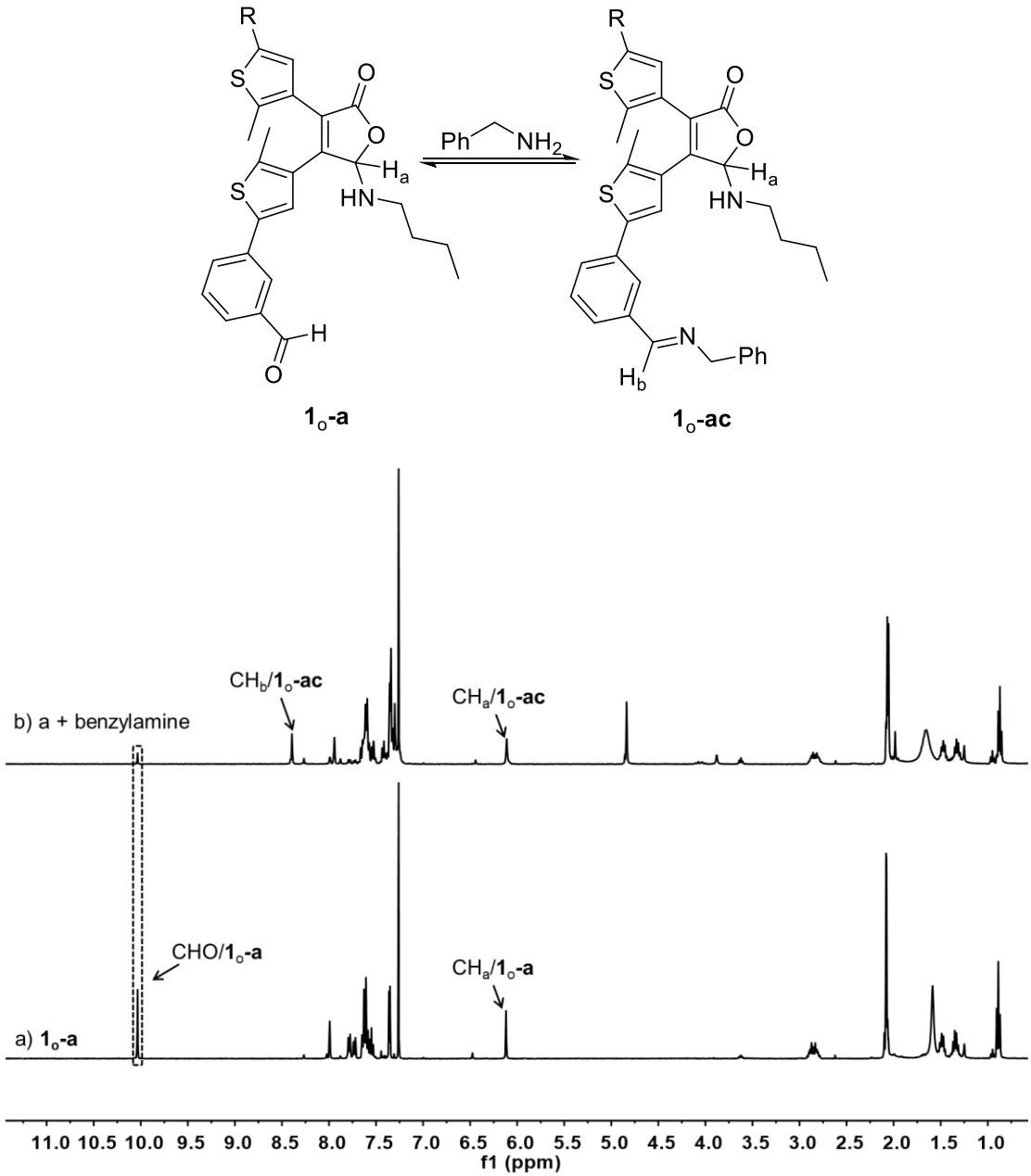

Figure S21. The exchange reaction of **1$_o$-a** with primary monoamine. (a) ^{1}H NMR spectrum of **1$_o$-a** (10 mM, as the procedure in Figure S20) in $CDCl_3$; (b) The addition of benzylamine (1.0 equiv.) to panel a. **1$_o$-a** converted to **1$_o$-ac** after 2 days, and the conversion of reaction was 90%. The hemiaminal ether from site a remained nearly unreactive. In Figures S21 and S22, the a and c refer to the amine adducts from 1-butylamine and benzylamine, respectively.

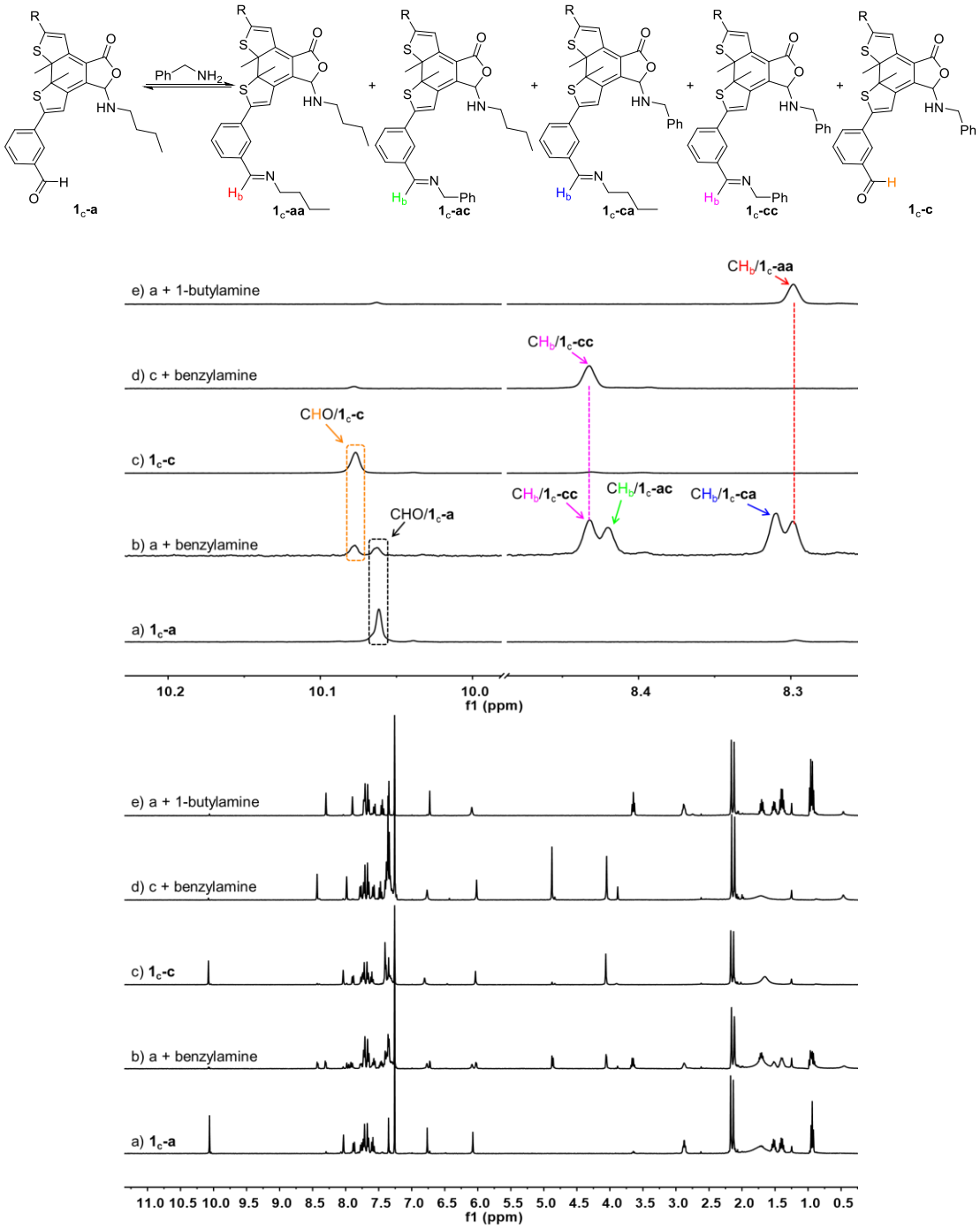

Figure S22. The exchange reaction of **1$_c$-a** with primary monoamine. (a) ^{1}H NMR spectrum of **1$_c$-a** (10 mM, as the procedure in Figure S20) in $CDCl_3$; (b) The addition of benzylamine (1.0 equiv.) to panel a. The system reached equilibrium in 2 days; (c) ^{1}H NMR spectrum of **1$_c$-c** (10 mM, created *in situ* from **1$_c$** and benzylamine (1.0 equiv.) for 3 min) in $CDCl_3$ for comparison; (d) The addition of benzylamine (1.1 equiv.) to panel c. **1$_c$-c** converted to **1$_c$-cc** after 1 day; (e) The addition of 1-butylamine (1.1 equiv.) to panel a. **1$_c$-a** converted to **1$_c$-aa** after 1 day; (B) The full ^{1}H NMR spectra of A. The amine exchange of hemiaminal ether from site a remained occurred.

Scheme S3. (A) Synthesis of [1+1] type macrocycles. (B) List of the selected diamines for the formation of [1+1] type macrocycles.

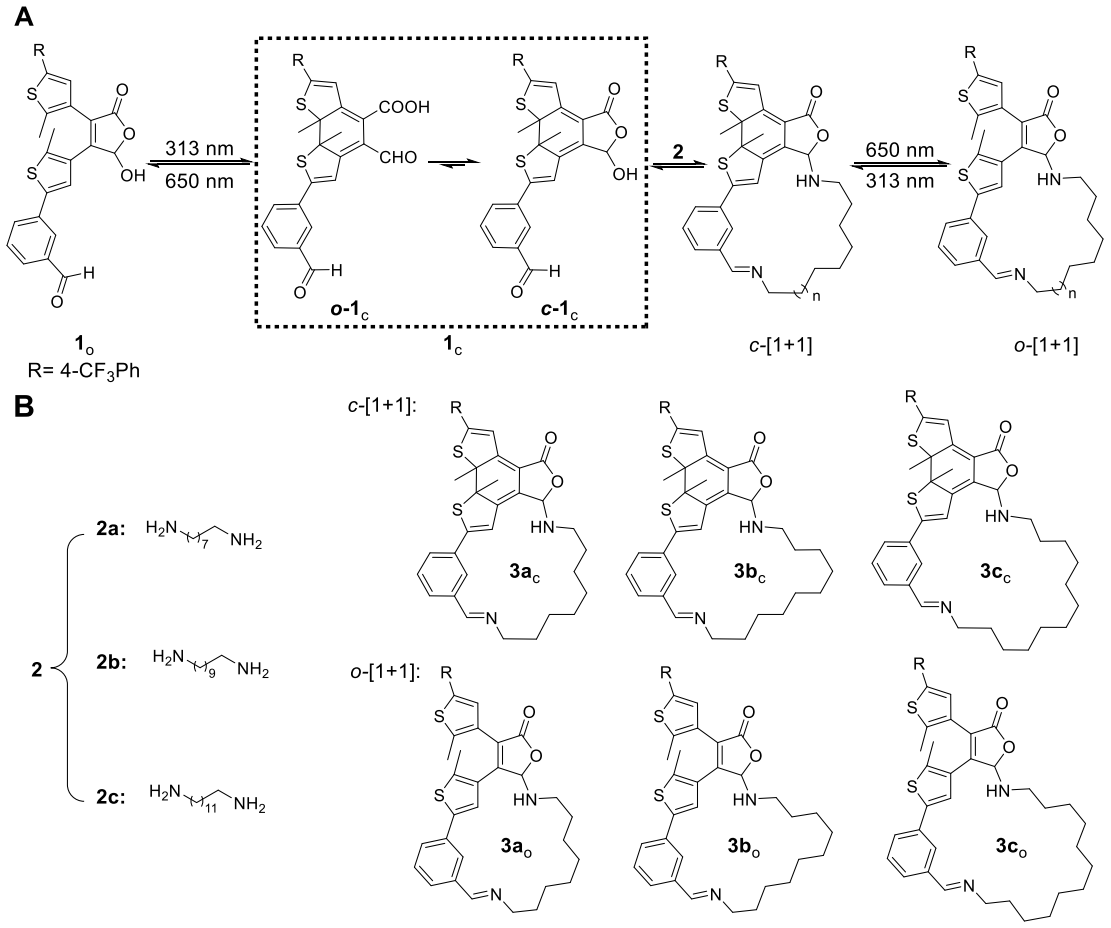

Synthesis of *c*-[1+1] type macrocycles: The *c*-[1+1] type macrocycles were created *in situ*. A solution of $\mathbf{1}_o$ (10 mM, $CDCl_3$) was irradiated at 313 nm for 150 min. The primary diamine (1.0 eq.) was then added, and the resulting mixture was stirred under dark for 70 min at room temperature. The yield of *c*-[1+1] macrocycles was nearly quantitative.

Synthesis of *o*-[1+1] type macrocycles: The *o*-[1+1] type macrocycles were created by irradiation of *c*-[1+1] macrocycles at 650 nm for 75 min. The conversion of *c*-[1+1] to *o*-[1+1] macrocycles was quantitative.

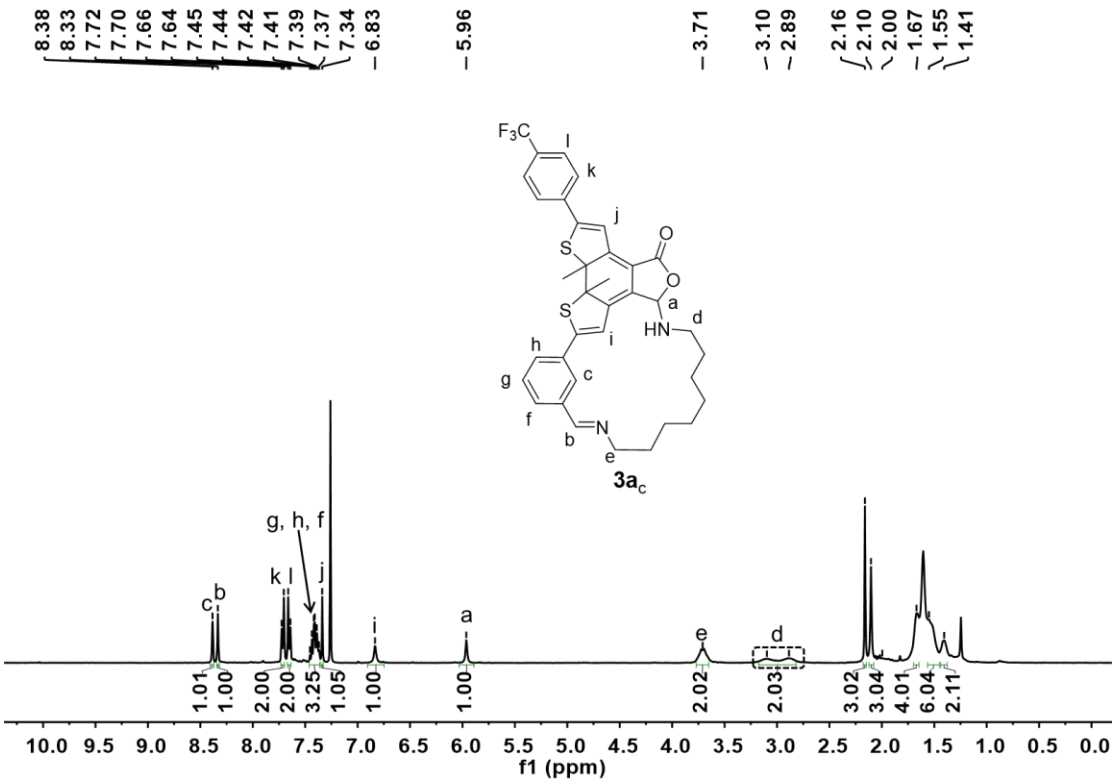

Figure S23. ^{1}H NMR spectra of **3a**$_c$ (created *in situ* from **1**$_c$ (10 mM) and **2a** (1,8-diaminooctane, 1.0 equiv.) for 1 h) in $CDCl_3$.

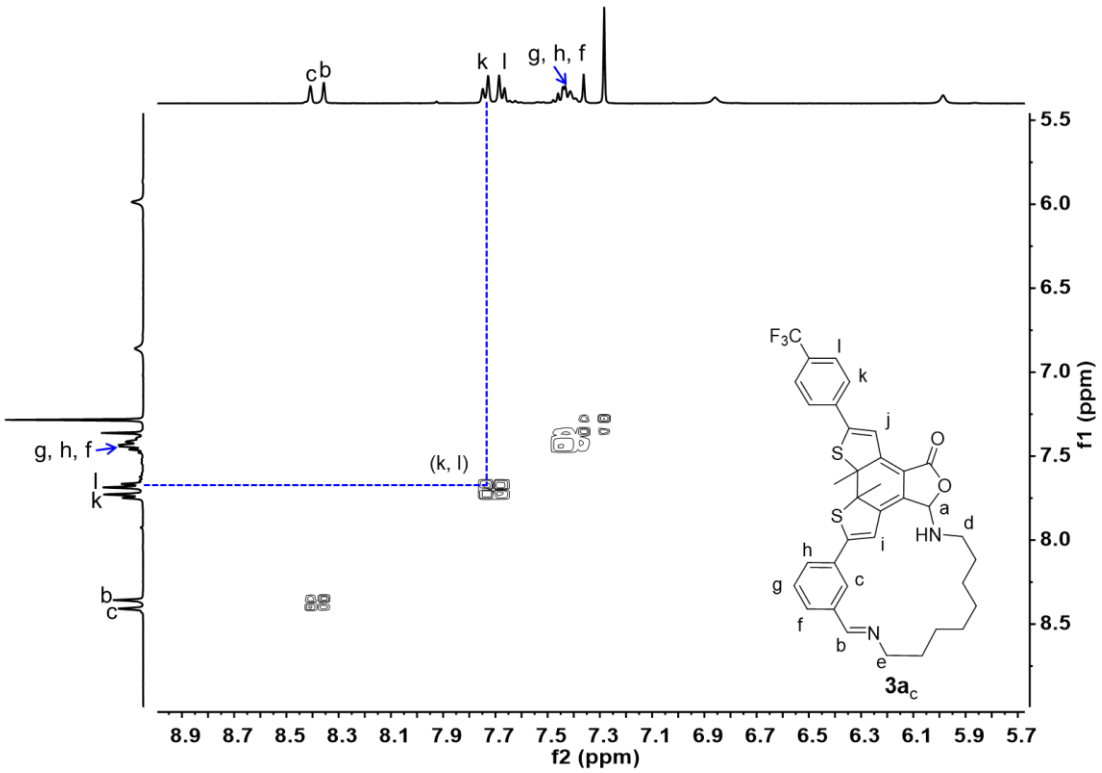

Figure S24. Partial 2D ^{1}H-^{1}H COSY NMR spectrum of **3a**$_c$ (created *in situ* from **1**$_c$ (10 mM) and **2a** (1.0 equiv.) for 1 h) in $CDCl_3$.

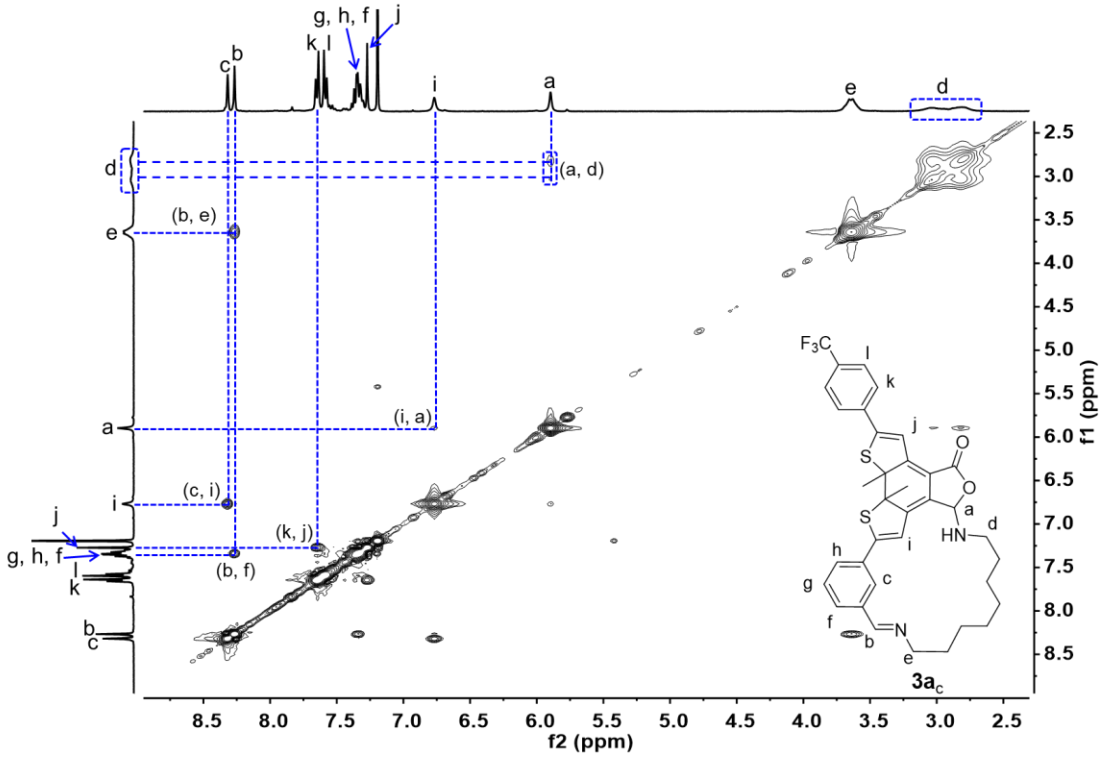

Figure S25. Partial 2D ^{1}H-^{1}H NOESY NMR spectrum of **3a**$_c$ (created *in situ* from **1**$_c$ (10 mM) and **2a** (1.0 equiv.) for 1 h) in $CDCl_3$.

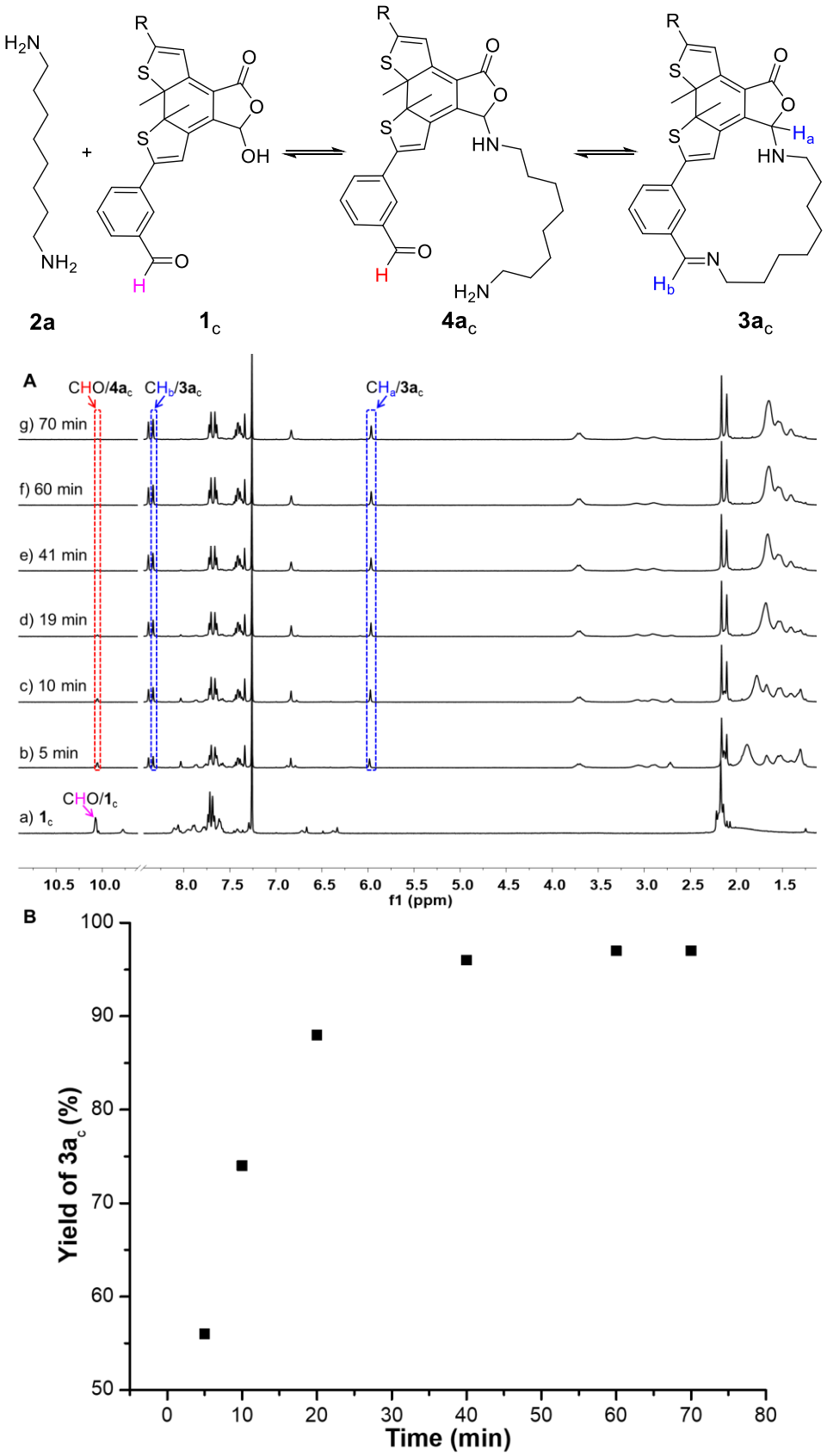

Figure S26. (A) Stacked ^{1}H NMR spectra of the reaction of $\mathbf{1}_c$ (10 mM) with **2a** (1.0 equiv.) in $CDCl_3$. The conversion of reaction was 97%. (B) The kinetics profile of the reaction of $\mathbf{1}_c$ with **2a** in 70 min.

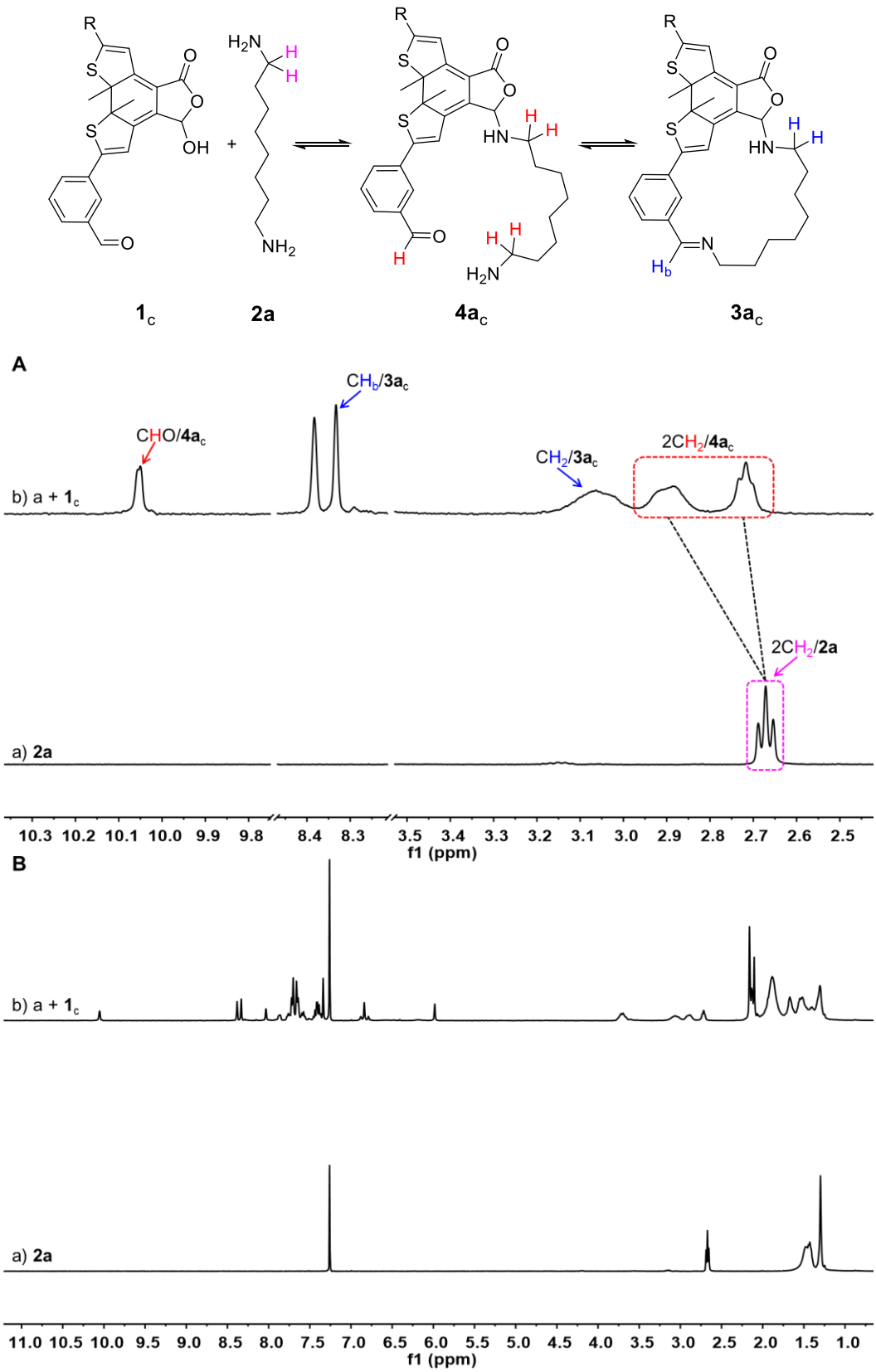

Figure S27. The reaction progress of $\mathbf{1}_c$ and **2a**. (A) (a) ^{1}H NMR spectrum of **2a** (10 mM) in $CDCl_3$; (b) The addition of **2a** (1.0 equiv.) to $\mathbf{1}_c$ (10 mM, $CDCl_3$). After the reaction for 5 min, the peak at 2.67 ppm (CH_2/**2a**) disappeared, with the formation of intermediate $\mathbf{4a}_c$ and macrocycle $\mathbf{3a}_c$; (B) The full ^{1}H NMR spectra of A.

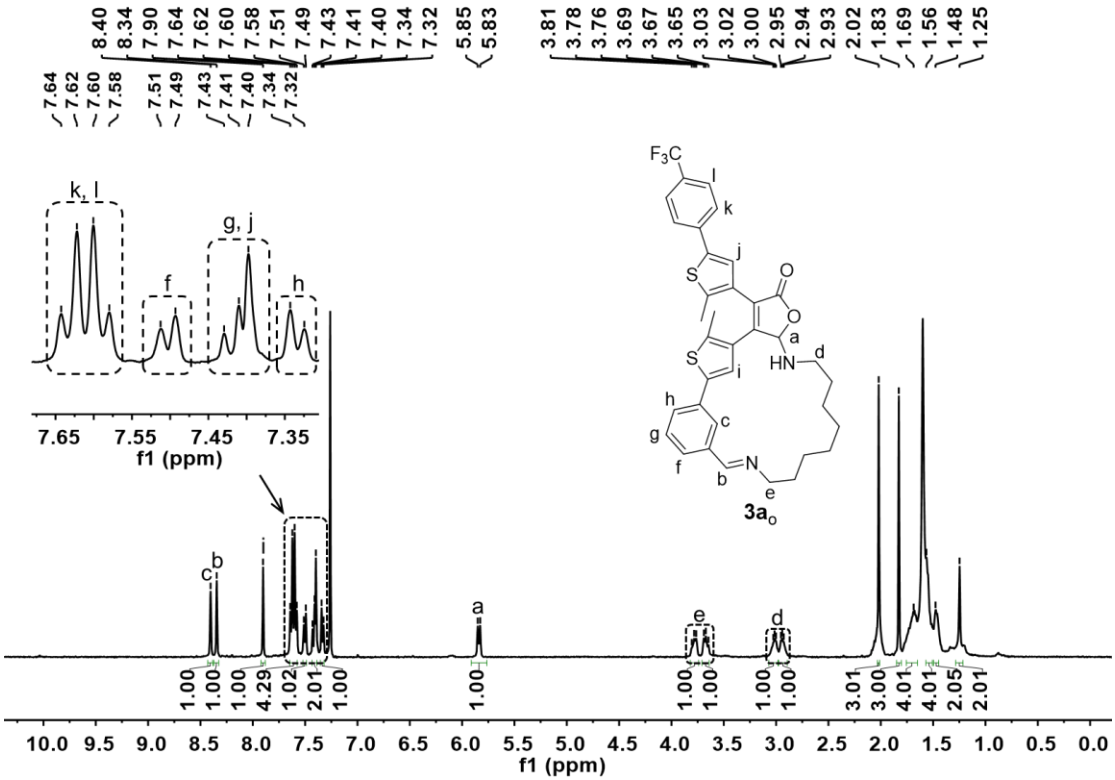

Figure S28. ^{1}H NMR spectra of **3a**$_o$ (10 mM, created by irradiation of **3a**$_c$ at 650 nm for 75 min) in $CDCl_3$.

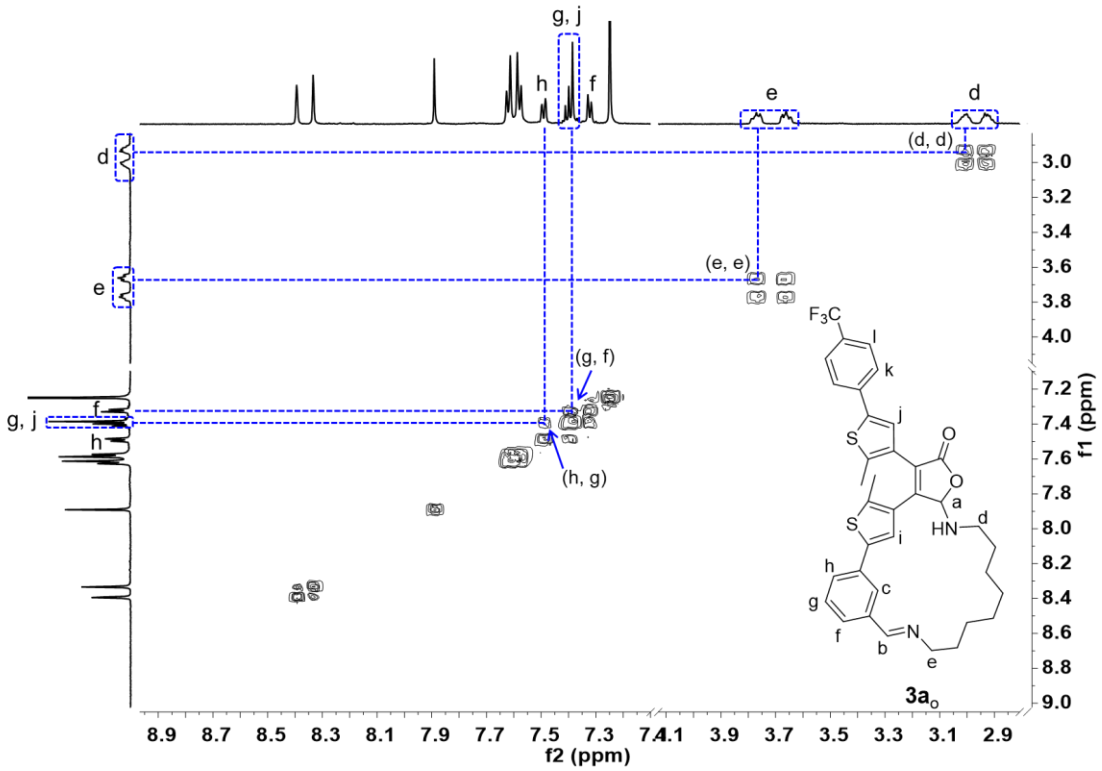

Figure S29. Partial 2D ^{1}H-^{1}H COSY NMR spectrum of **3a**$_o$ (10 mM, created by irradiation of **3a**$_c$ at 650 nm for 75 min) in $CDCl_3$.

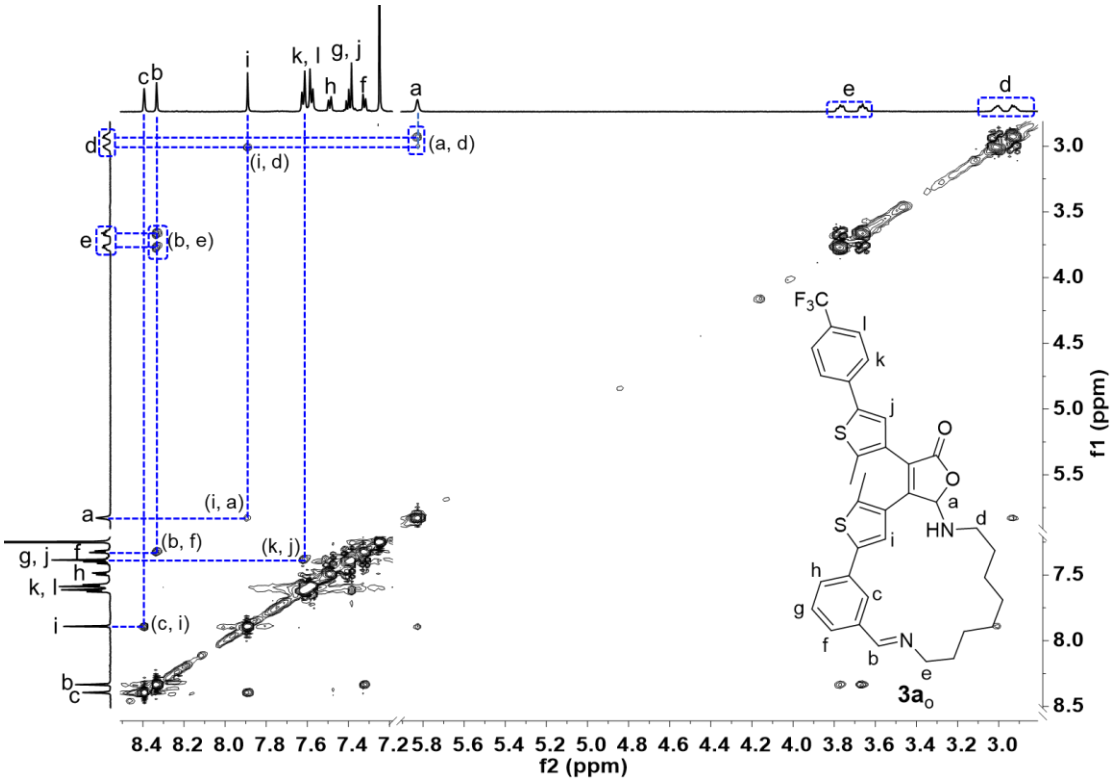

Figure S30. Partial 2D ^{1}H-^{1}H NOESY NMR spectrum of **3a**$_o$ (10 mM, created by irradiation of **3a**$_c$ at 650 nm for 75 min) in $CDCl_3$.

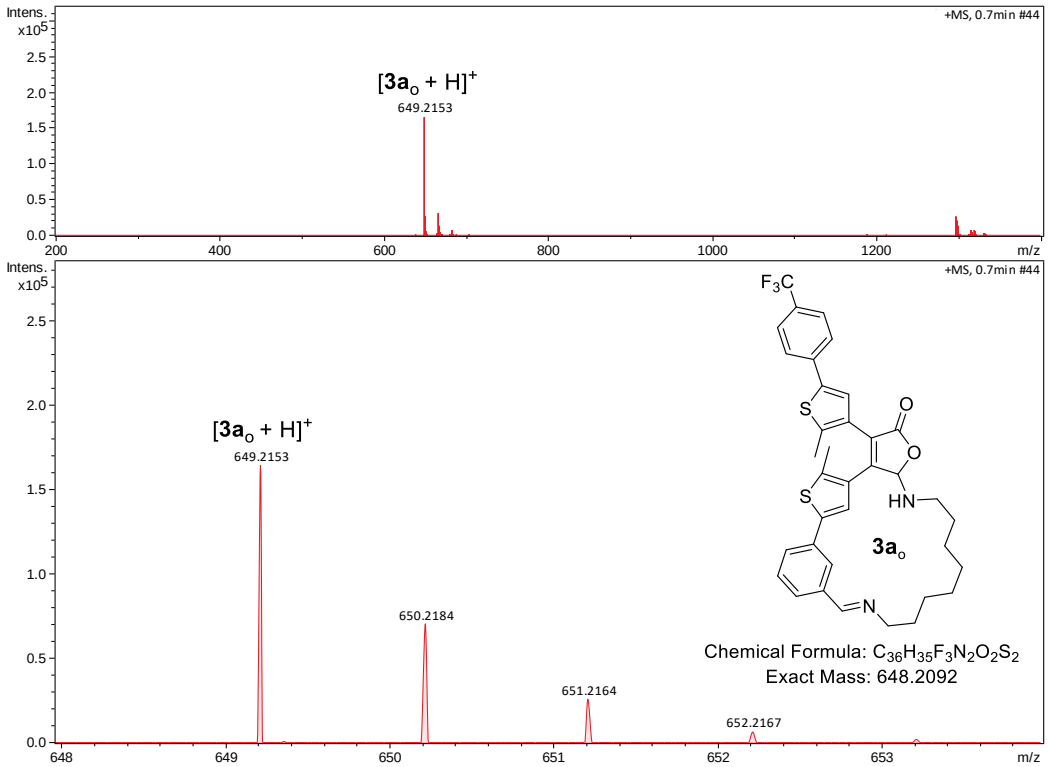

Figure S31. ESI mass spectrum of **3a**$_o$ (created by irradiation of **3a**$_c$ at 650 nm for 75 min).

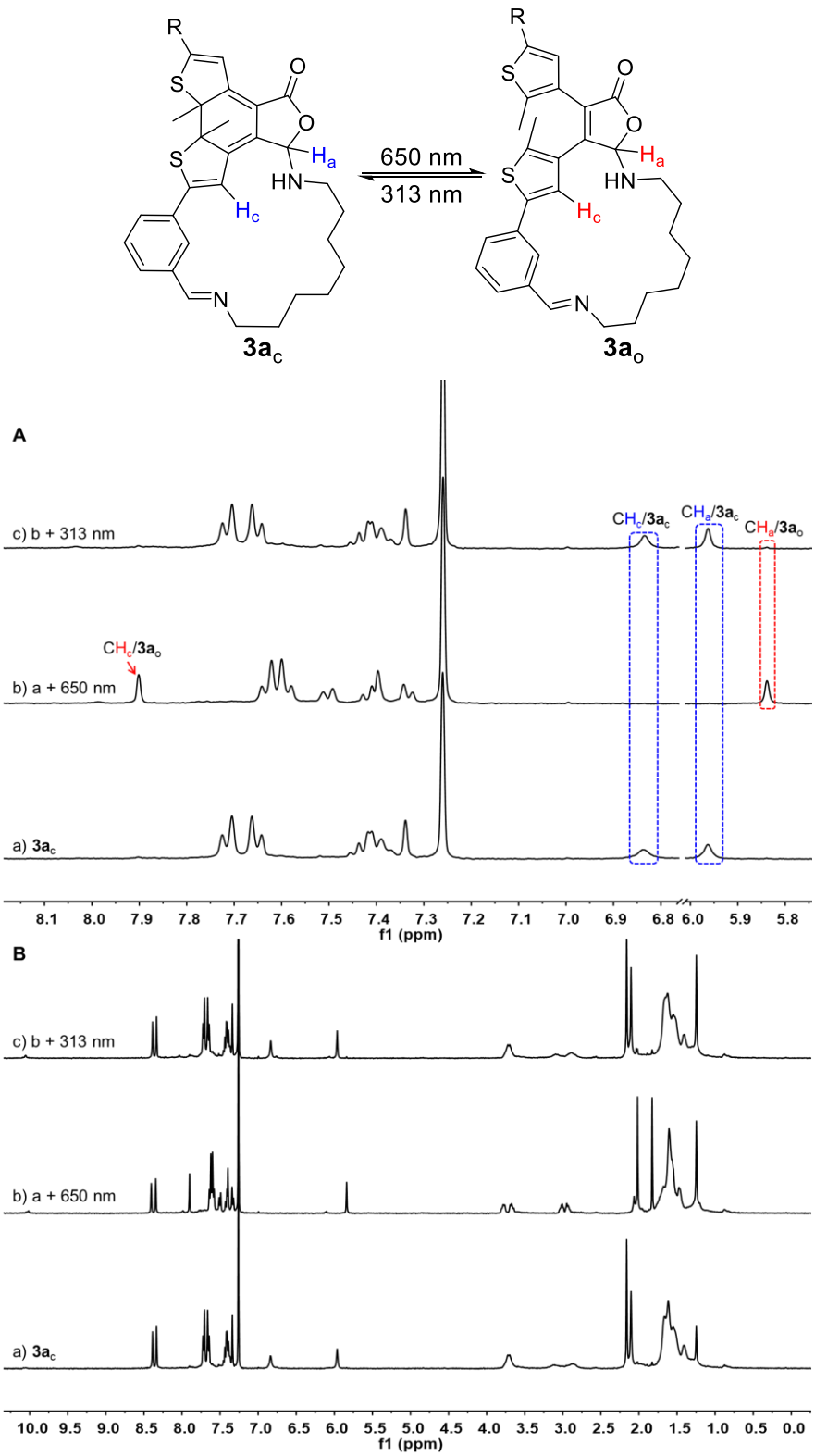

Figure S32. The changes of ^{1}H NMR spectrum of **3a** with photoswitching. (A) (a) ^{1}H NMR spectrum of **3a**$_c$ (10 mM, created *in situ* from **1**$_c$ and **2a**) in $CDCl_3$; (b) Irradiation of **3a**$_c$ at 650 nm for 75 min to give **3a**$_o$. The conversion of **3a**$_c$ to **3a**$_o$ was quantitative; (c) Further irradiation with UV light (313 nm, 120 min) to restore **3a**$_c$. The ratio of **3a**$_c$ and **3a**$_o$ is 98:2. (B) The full ^{1}H NMR spectra of A.

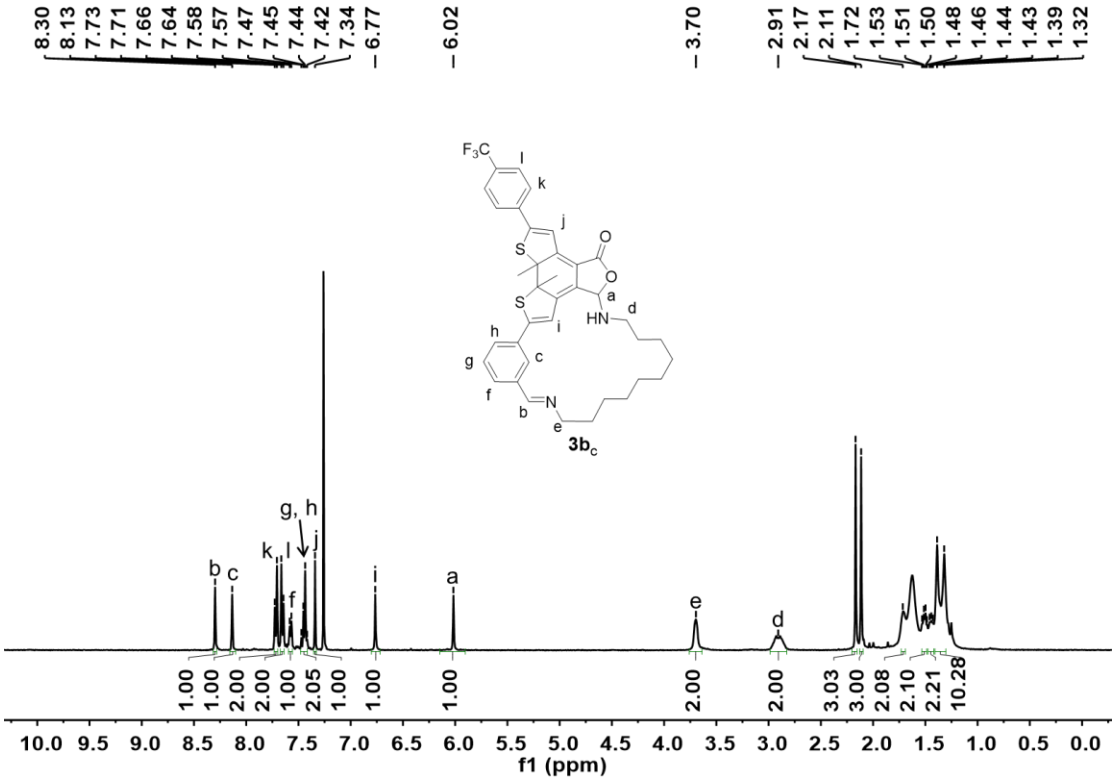

Figure S33. ^{1}H NMR spectra of **3b**$_c$ (created *in situ* from **1**$_c$ (10 mM) and **2b** (1,10-diaminodecane, 1.0 equiv.) for 1 h) in $CDCl_3$.

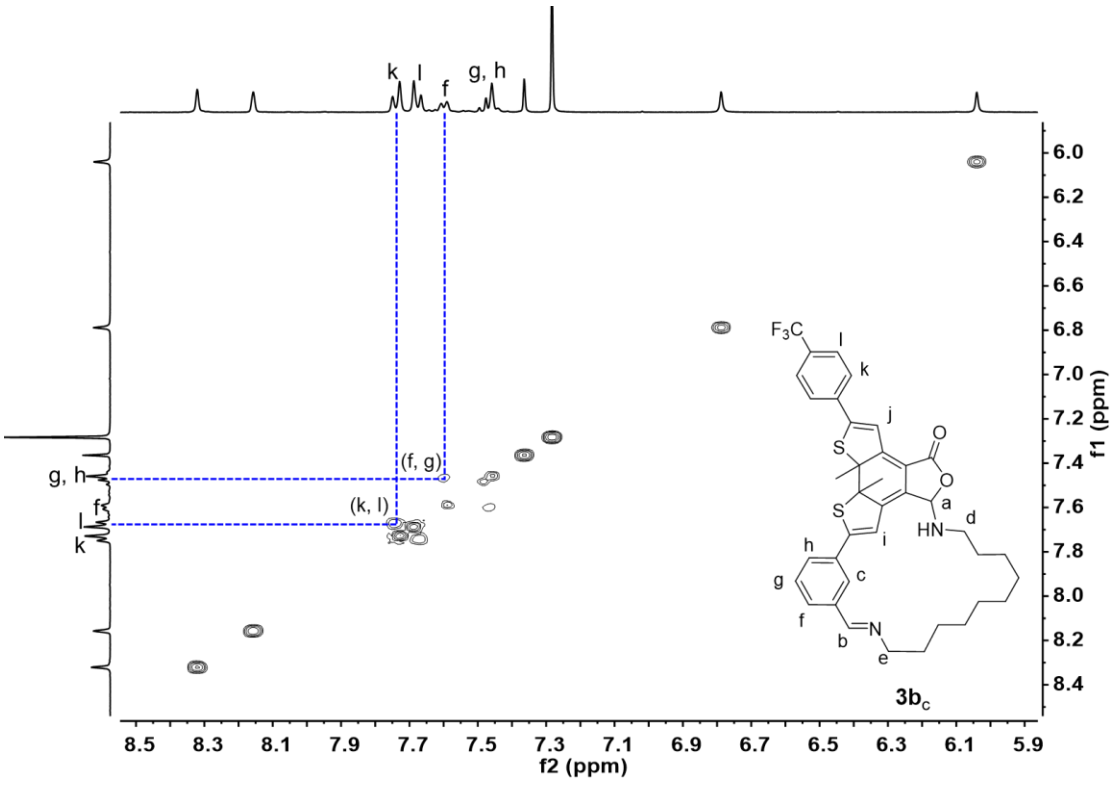

Figure S34. Partial 2D ^{1}H-^{1}H COSY NMR spectrum of **3b**$_c$ (created *in situ* from **1**$_c$ (10 mM) and **2b** (1.0 equiv.) for 1 h) in $CDCl_3$.

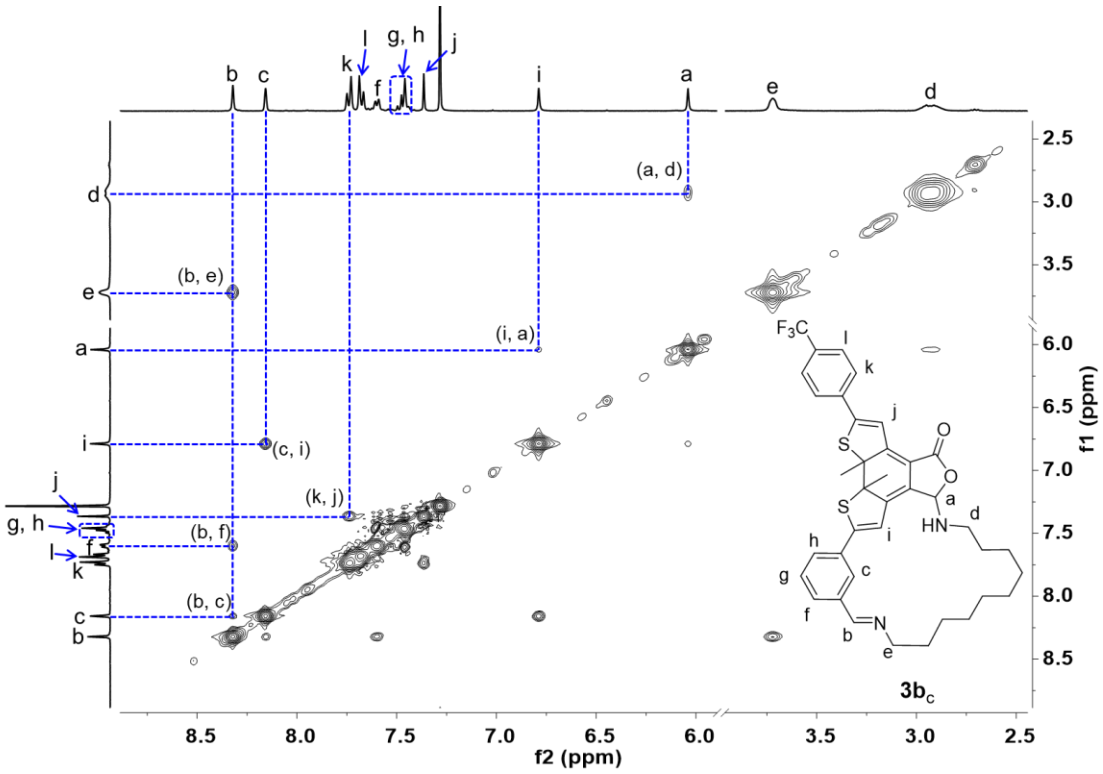

Figure S35. Partial 2D ^{1}H-^{1}H NOESY NMR spectrum of **3b**$_c$ (created *in situ* from **1**$_c$ (10 mM) and **2b** (1.0 equiv.) for 1 h) in $CDCl_3$.

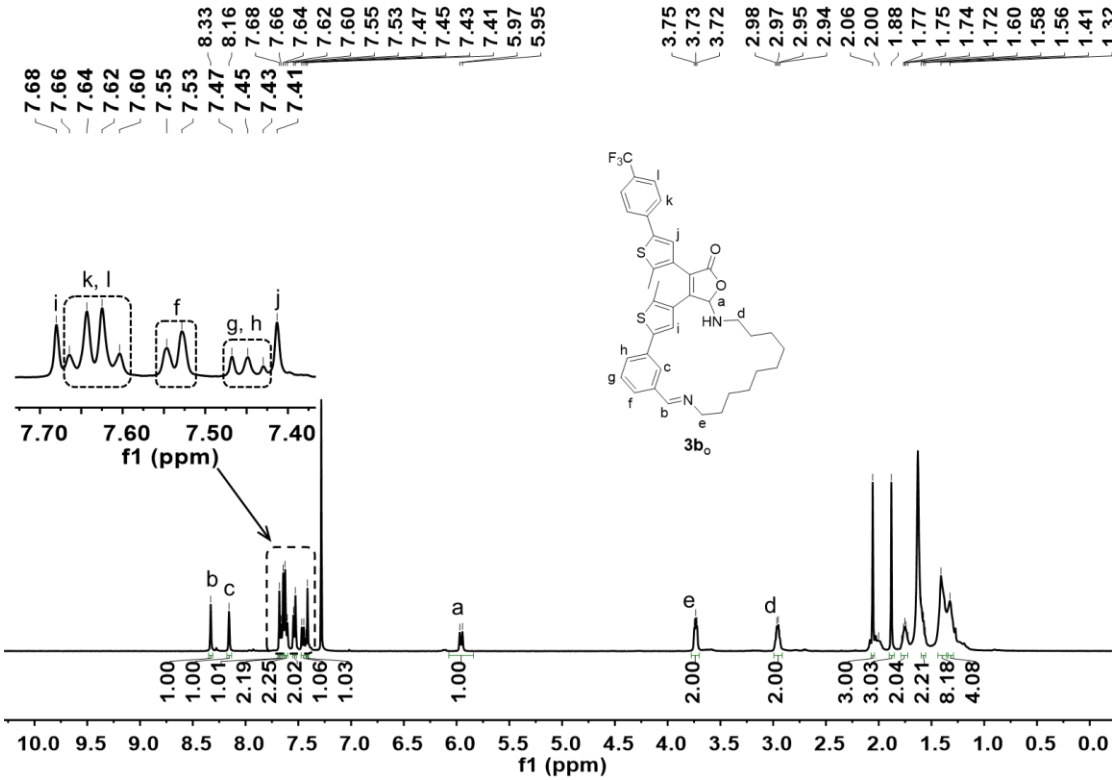

Figure S36. ^{1}H NMR spectra of **3b**$_o$ (10 mM, created by irradiation of **3b**$_c$ at 650 nm for 75 min) in $CDCl_3$.

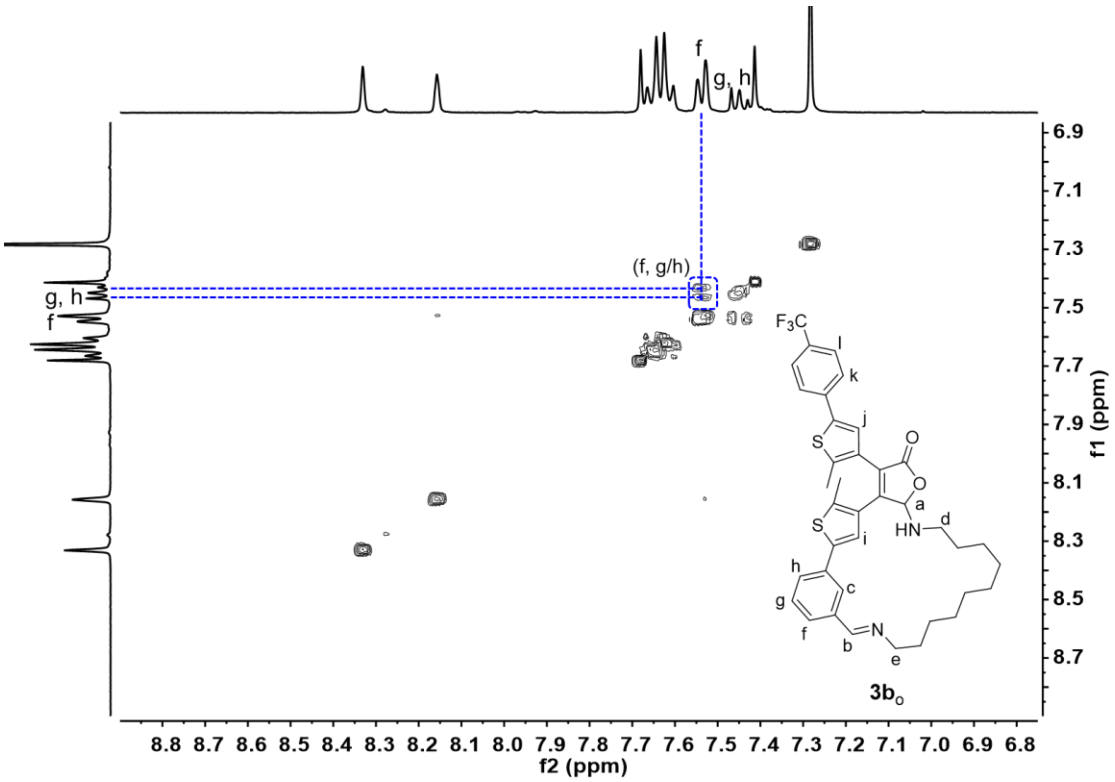

Figure S37. Partial 2D ^{1}H-^{1}H COSY NMR spectrum of **3b**$_o$ (10 mM, created by irradiation of **3b**$_c$ at 650 nm for 75 min) in $CDCl_3$.

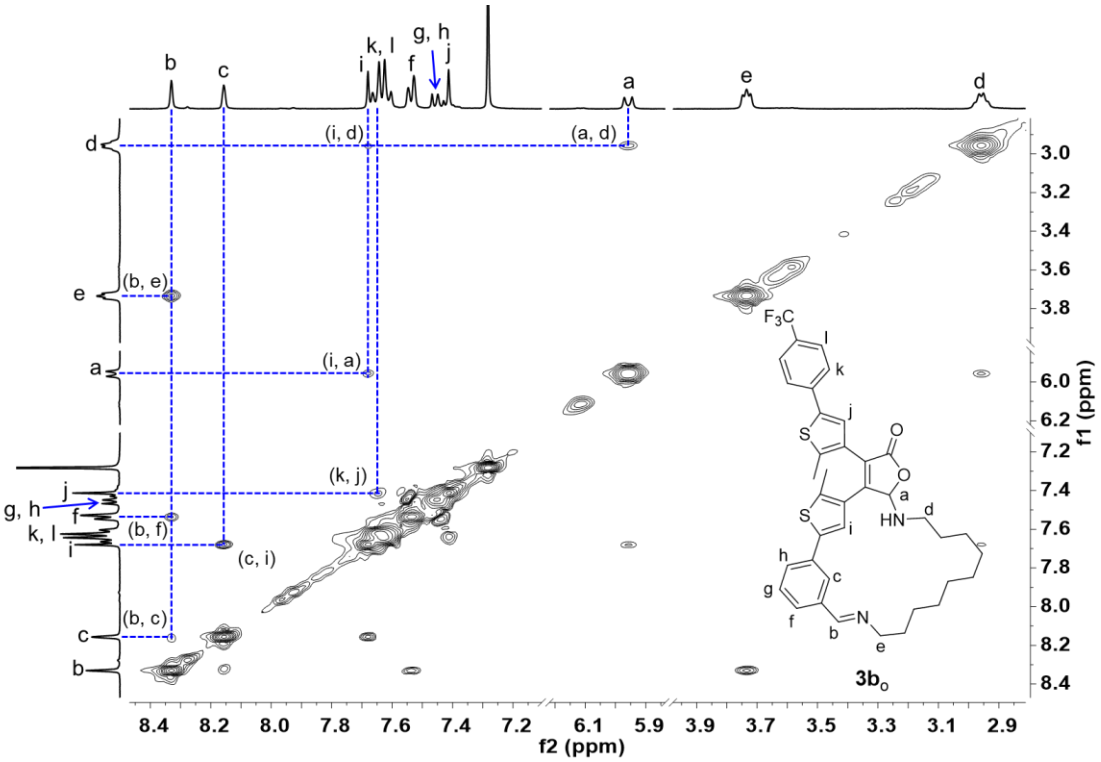

Figure S38. Partial 2D ^{1}H-^{1}H NOESY NMR spectrum of **3b**$_o$ (10 mM, created by irradiation of **3b**$_c$ at 650 nm for 75 min) in $CDCl_3$.

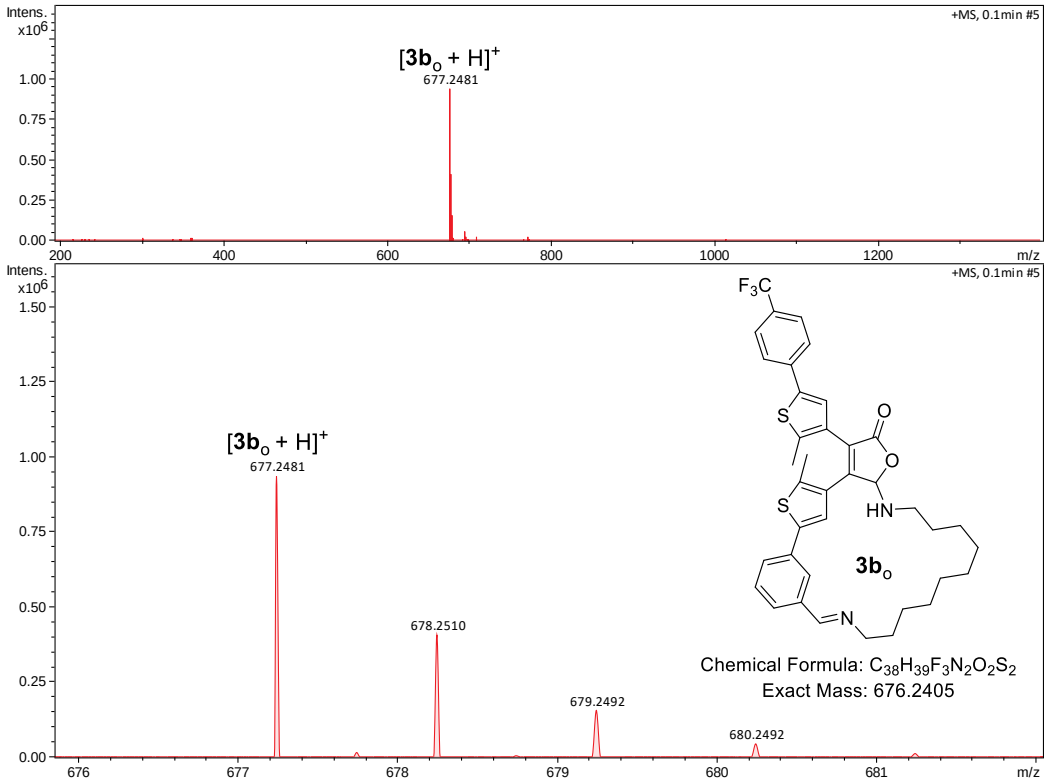

Figure S39. ESI mass spectrum of **3b**$_o$ (created by irradiation of **3b**$_c$ at 650 nm for 75 min).

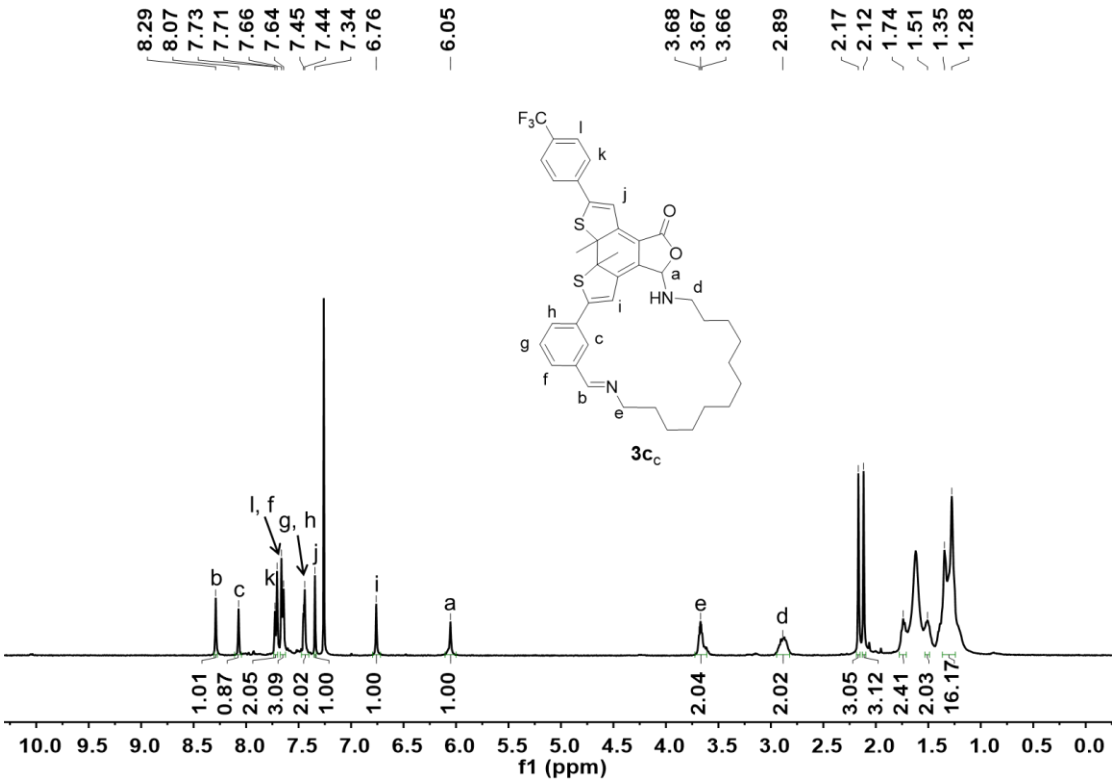

Figure S40. ^{1}H NMR spectra of **3c**$_c$ (created *in situ* from **1**$_c$ (10 mM) and **2c** (1,12-diaminododecane, 1.0 equiv.) for 1.5 h) in $CDCl_3$.

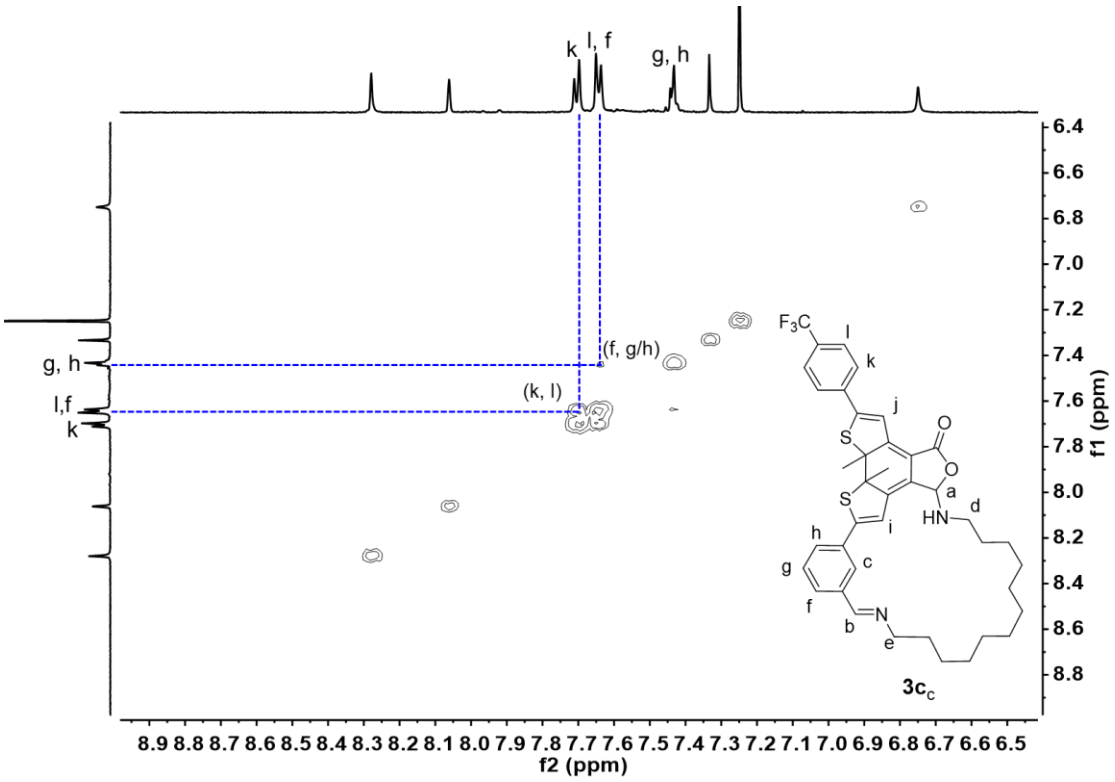

Figure S41. Partial 2D ^{1}H-^{1}H COSY NMR spectrum of **3c**$_c$ (created *in situ* from **1**$_c$ (10 mM) and **2c** (1.0 equiv.) for 1.5 h) in $CDCl_3$.

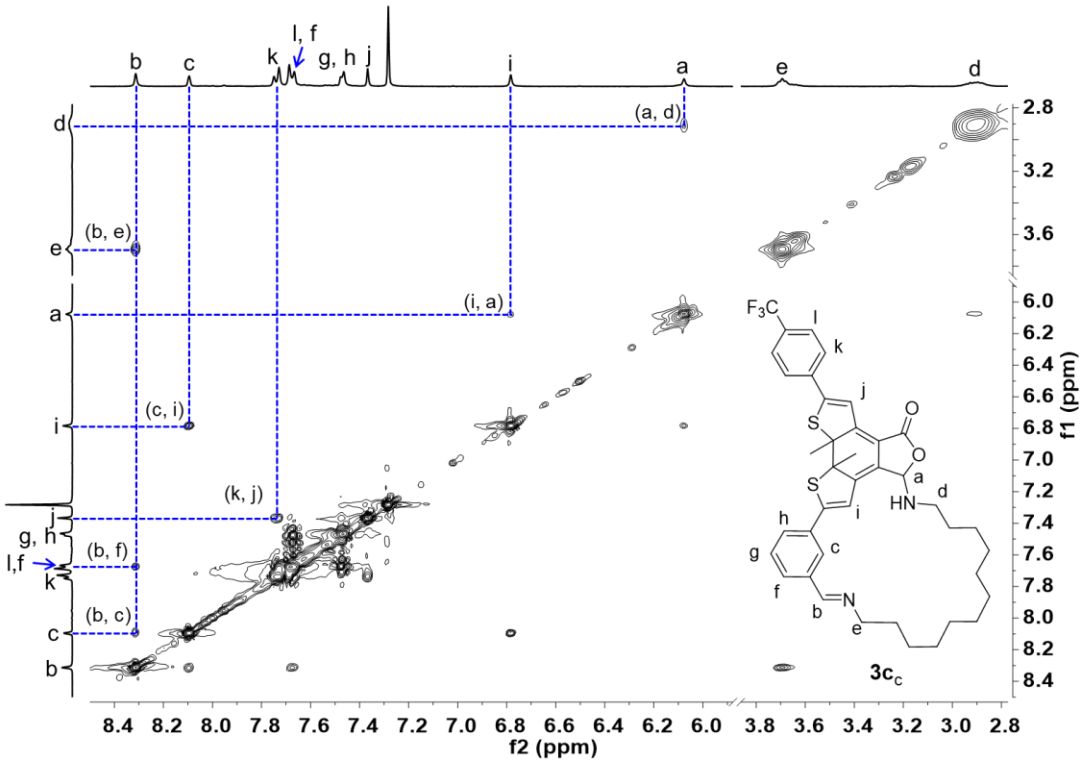

Figure S42. Partial 2D ^{1}H-^{1}H NOESY NMR spectrum of **3c**$_c$ (created *in situ* from **1**$_c$ (10 mM) and **2c** (1.0 equiv.) for 1.5h) in $CDCl_3$.

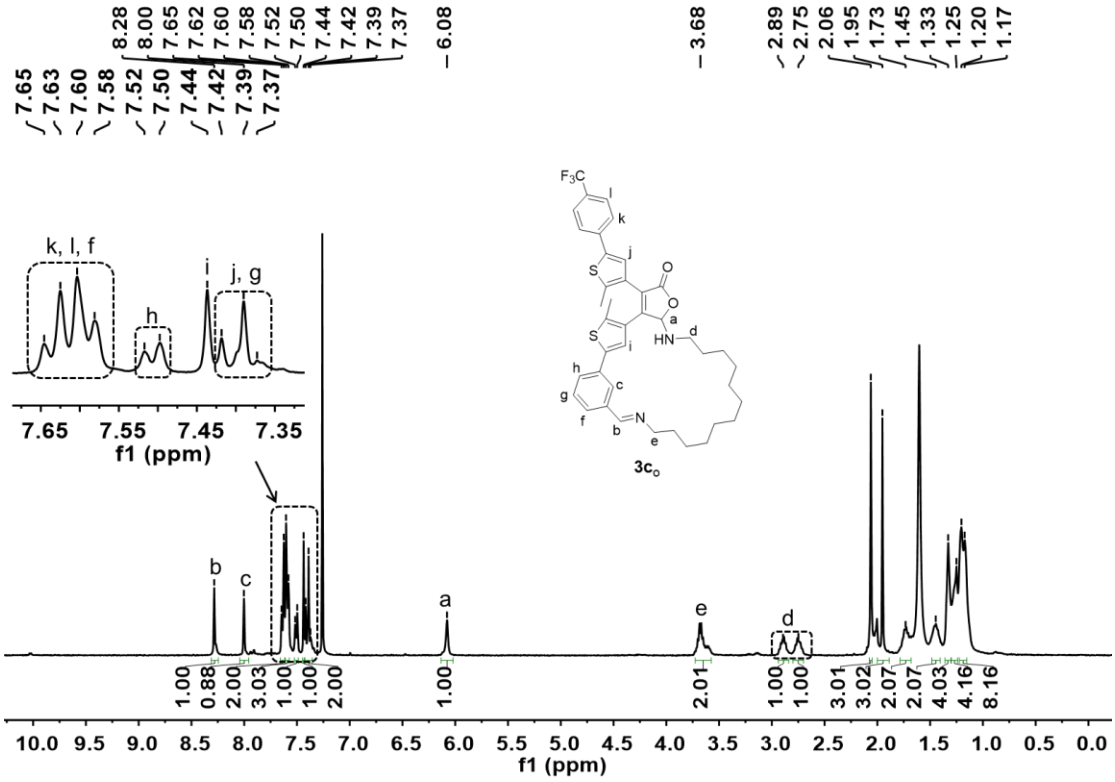

Figure S43. ^{1}H NMR spectra of **3c**$_o$ (10 mM, created by irradiation of **3c**$_c$ at 650 nm for 75 min) in $CDCl_3$.

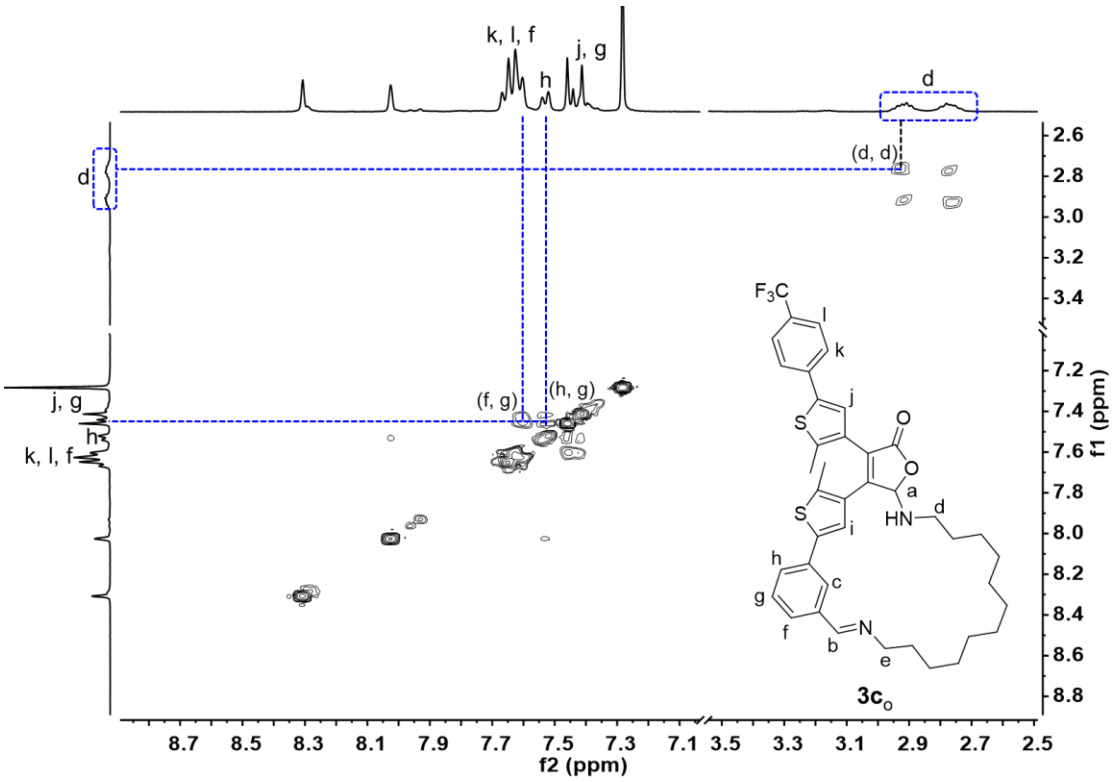

Figure S44. Partial 2D ^{1}H-^{1}H COSY NMR spectrum of **3c**$_{o}$ (10 mM, created by irradiation of **3c**$_{c}$ at 650 nm for 75 min in $CDCl_3$) in $CDCl_3$.

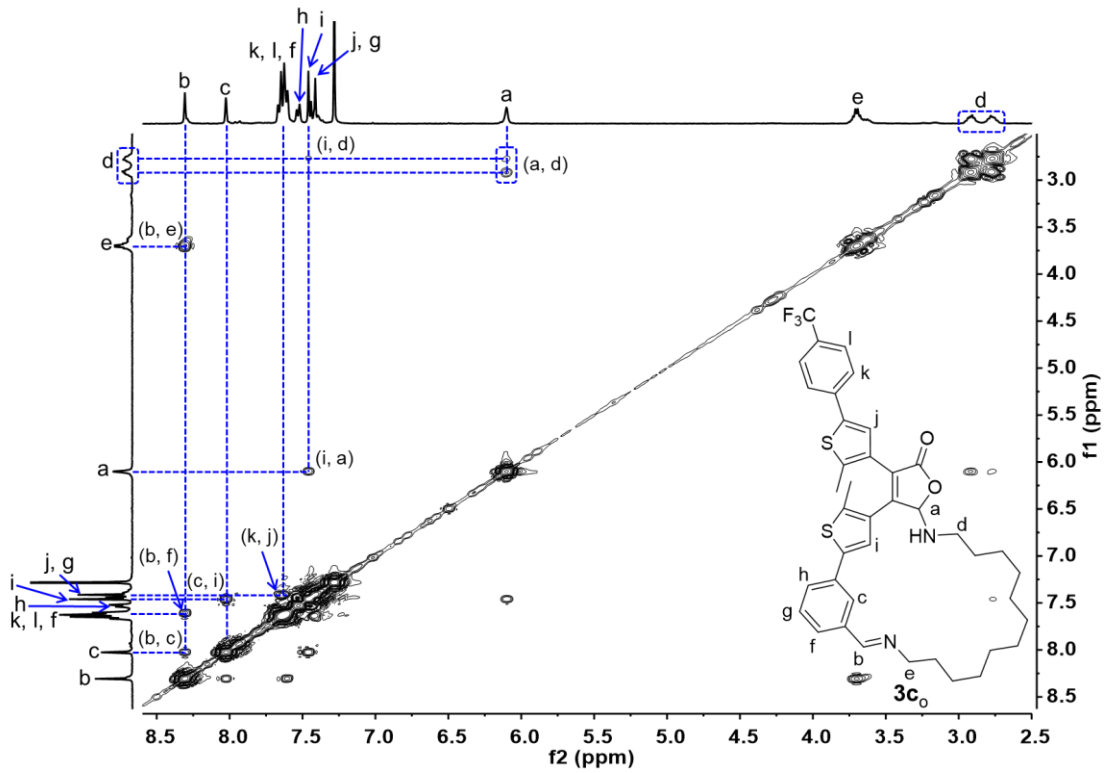

Figure S45. Partial 2D ^{1}H-^{1}H NOESY NMR spectrum of **3c**$_{o}$ (10 mM, created by irradiation of **3c**$_{c}$ at 650 nm for 75 min in $CDCl_3$) in $CDCl_3$.

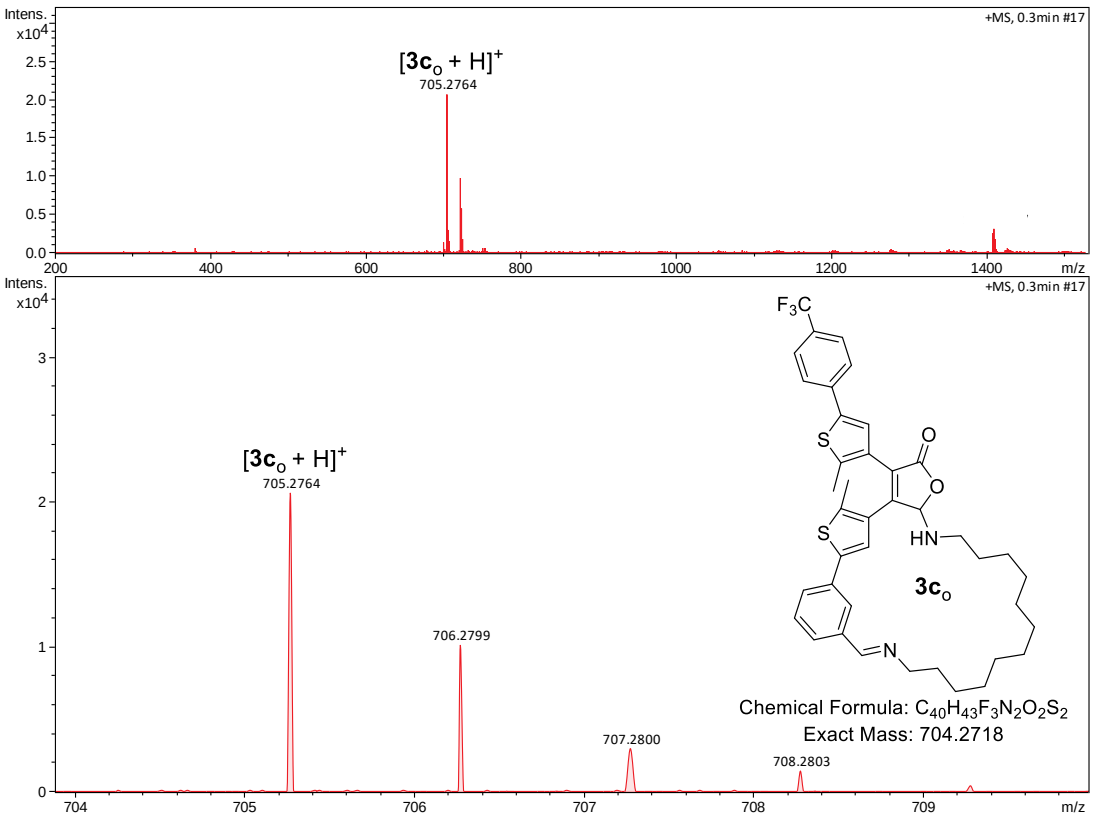

Figure S46. ESI mass spectrum of **3c**$_o$ (created by irradiation of **3c**$_c$ at 650 nm for 75 min in $CDCl_3$).

4. Regulation of [1+1] Macrocycles

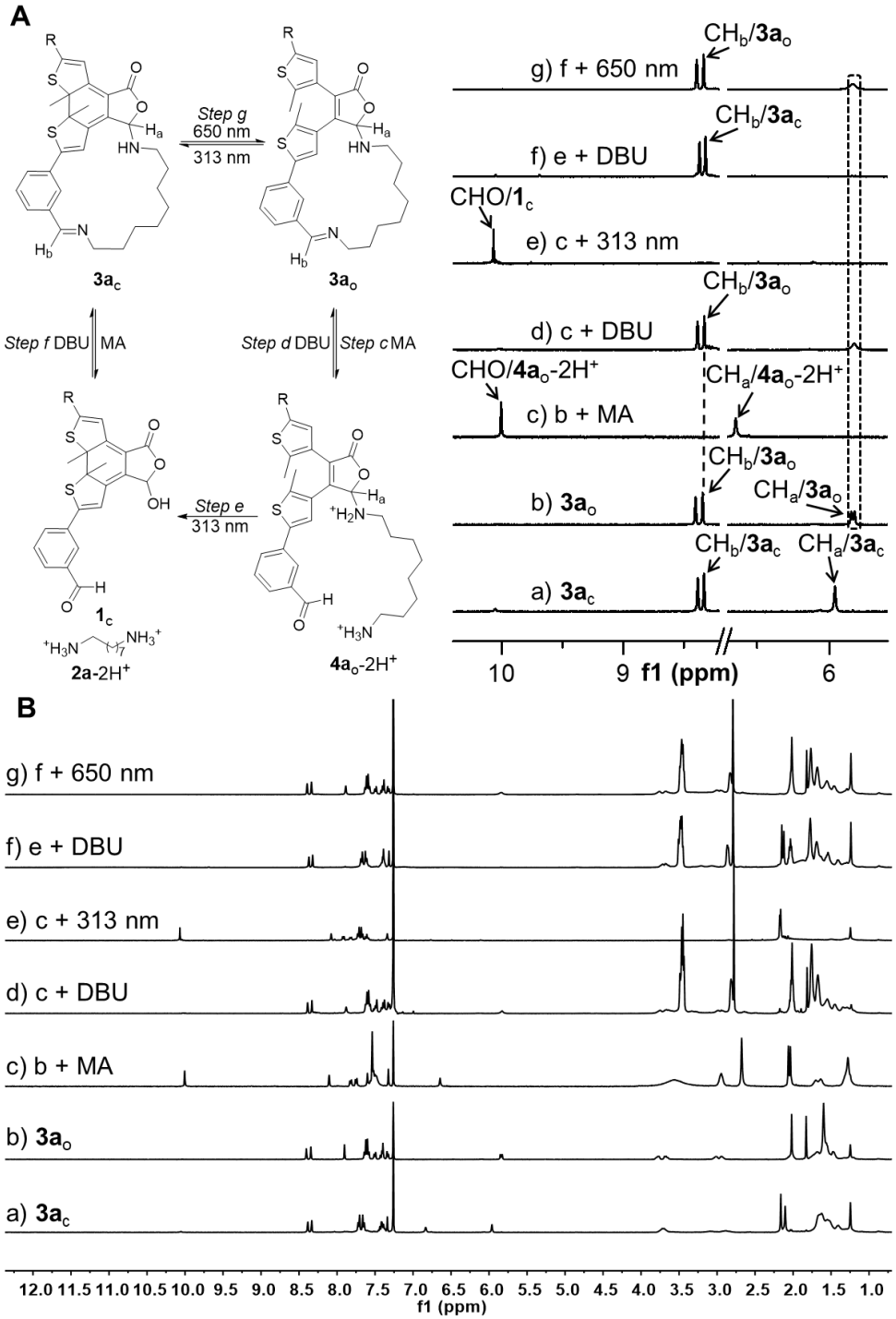

Figure S47. The regulation of [1+1] macrocycles. (A) ^{1}H NMR spectra of pre-formed macrocycle **3a**$_c$ (10 mM) in $CDCl_3$ (a), **3a**$_o$ (b), the addition of MA (2.0 equiv.) into **3a**$_o$ (c) and then DBU (2.3 equiv.) (d) to break/remake **3a**$_o$, as well as the irradiation at 313 nm for 150 min (e), followed by the addition of DBU (2.3 equiv.) (f) and then irradiation at 650 nm to restore **3a**$_o$ (g). (B) The full ^{1}H NMR spectra of A.

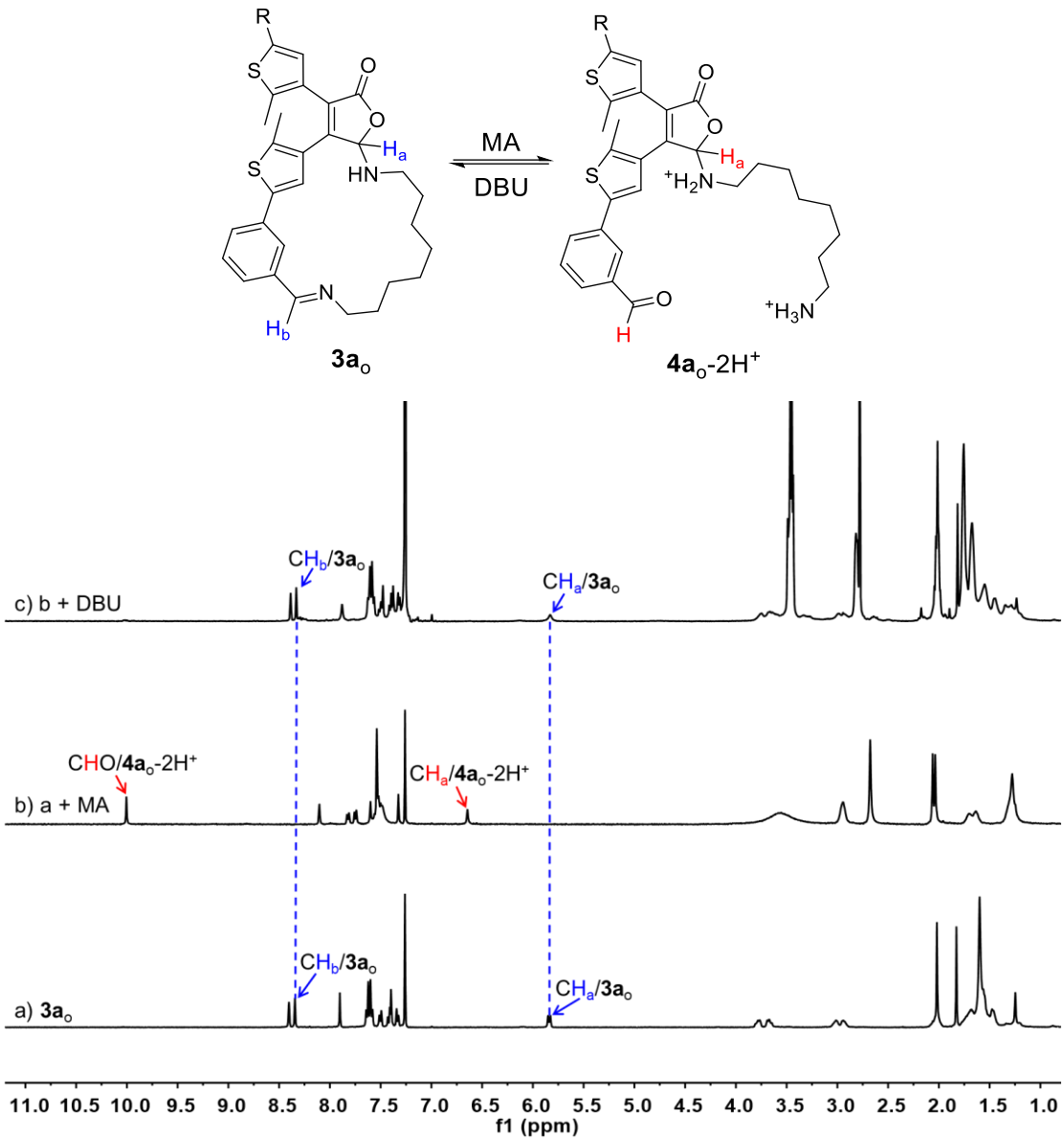

Figure S48. Precise formation/scission of *o*-[1+1] macrocycles with acid/base stimuli. (A) (a) ^{1}H NMR spectrum of **3a**$_o$ (10 mM) in $CDCl_3$; (b) The addition of MA (2.0 equiv.) to **3a**$_o$. **3a**$_o$ converted to **4a**$_o$-2H$^+$ immediately (3 min); (c) The addition of DBU (2.3 equiv.) to the panel b. **4a**$_o$-2H$^+$ converted to **3a**$_o$ after 80 h.

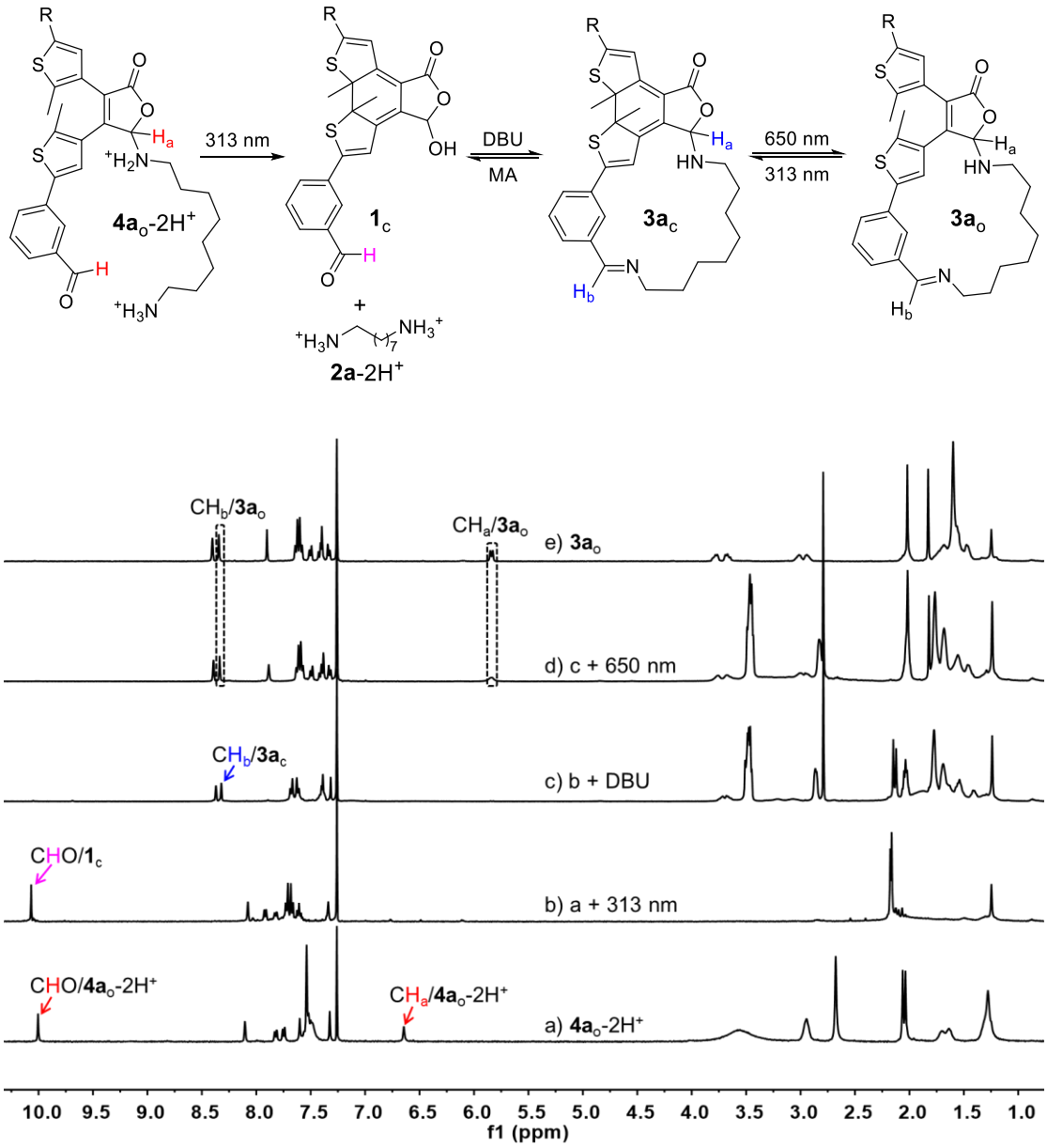

Figure S49. Precise formation/scission of [1+1] macrocycles through a combination of light and acid/base stimuli. (a) ^{1}H NMR spectrum of **4a**$_o$-2H$^+$ (10 mM) in $CDCl_3$, as generated in Figure S48; (b) Irradiation of panel a at 313 nm for 150 min. The hydrolysis of hemiaminal ether was turned on to afford **1**$_c$; (c) The addition of DBU (2.3 equiv.) to panel b. **1**$_c$ converted to **3a**$_c$ after 3 h, the ratio of **1**$_c$ and **3a**$_c$ is 4:96. Due to the basicity of the solution, the peak of CH$_a$/**3a**$_c$ disappeared; (d) Irradiation of panel c at 650 nm for 75 min to give **3a**$_o$; (e) ^{1}H NMR spectrum of **3a**$_o$ (10 mM) in $CDCl_3$ for comparison.

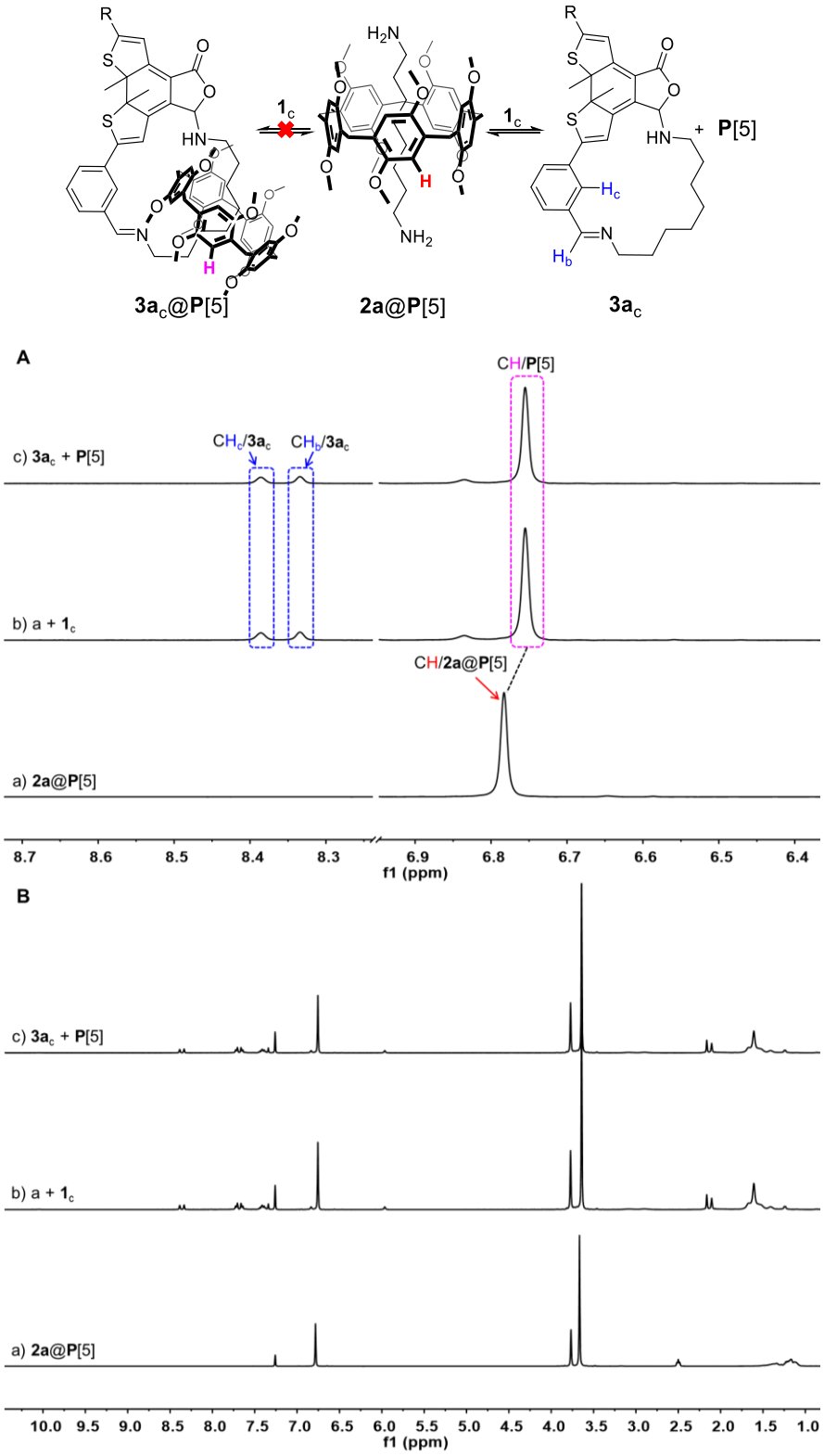

Figure S50. Dissociation of pseudorotaxane via construction of [1+1] macrocycles. (a) ^{1}H NMR spectrum of pseudorotaxane **2a**@**P**[5] (created by mixing P[5] (10 mM) and **2a** (1 equiv.) in $CDCl_3$); (b) The addition of **1**$_c$ (1.0 equiv.) to panel a. After 1 h, **2a**@**P**[5] and **1**$_c$ converted to the macrocycle **3a**$_c$ and free **P**[5]; (c) ^{1}H NMR spectrum of mixture of **3a**$_c$ (10 mM) and **P**[5] (1 equiv.) in $CDCl_3$. (B) The full ^{1}H NMR spectra of A.

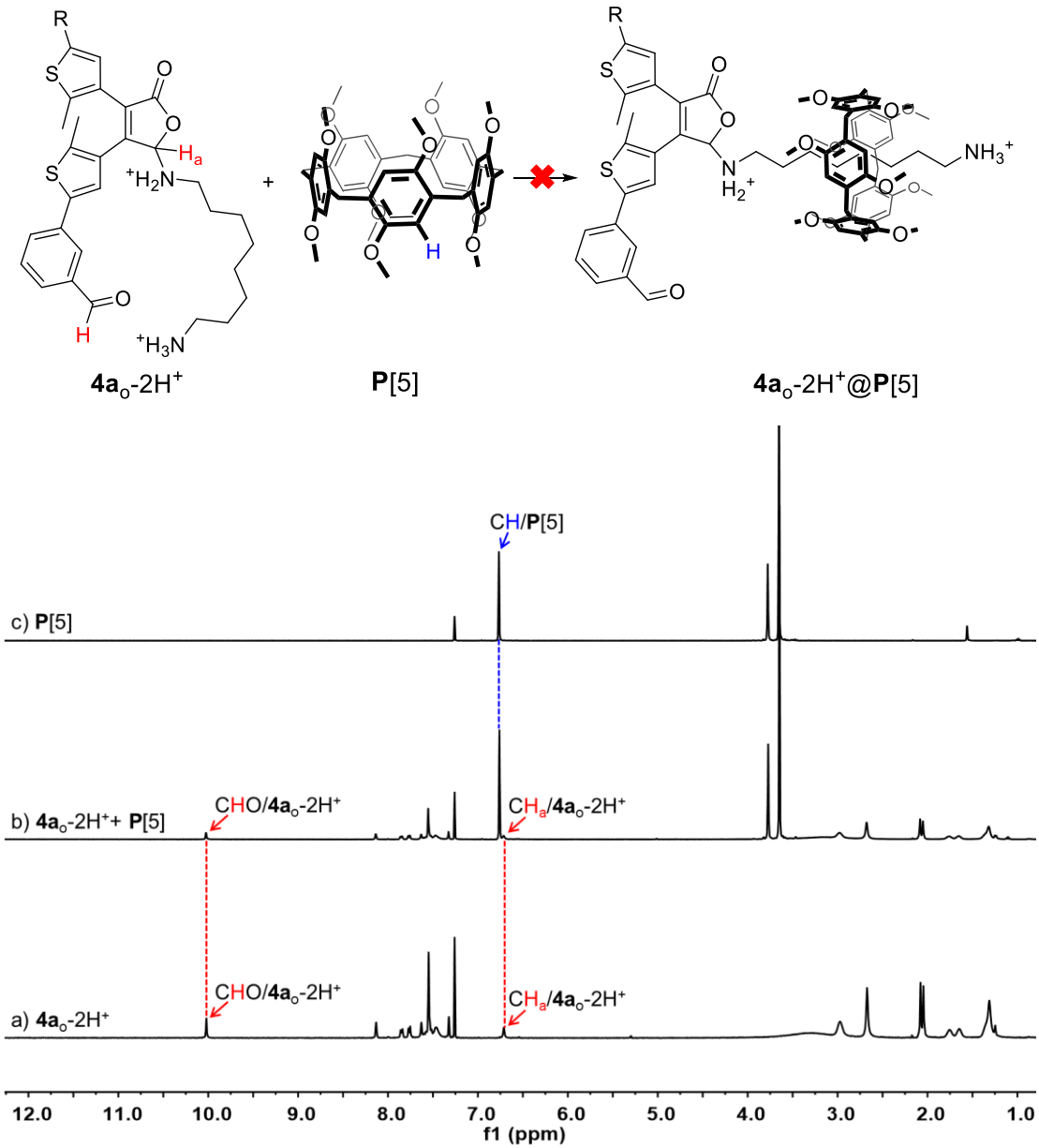

Figure S51. The addition of **P**[5] to the solution of **4a**$_o$-2H$^+$ (10 mM) in $CDCl_3$, as generated in Figure S48. (a) ^{1}H NMR spectrum of **4a**$_o$-2H$^+$ (10 mM) in $CDCl_3$; (b) The addition of **P**[5] (1.0 equiv.) to panel a; (c) ^{1}H NMR spectrum of **P**[5] (10 mM) in $CDCl_3$ for comparison. The formation of pseudorotaxane **4a**$_o$-2H$^+$@**P**[5] was not found.

5. Formation and Characterization of [2+1+1'] Macrocycles

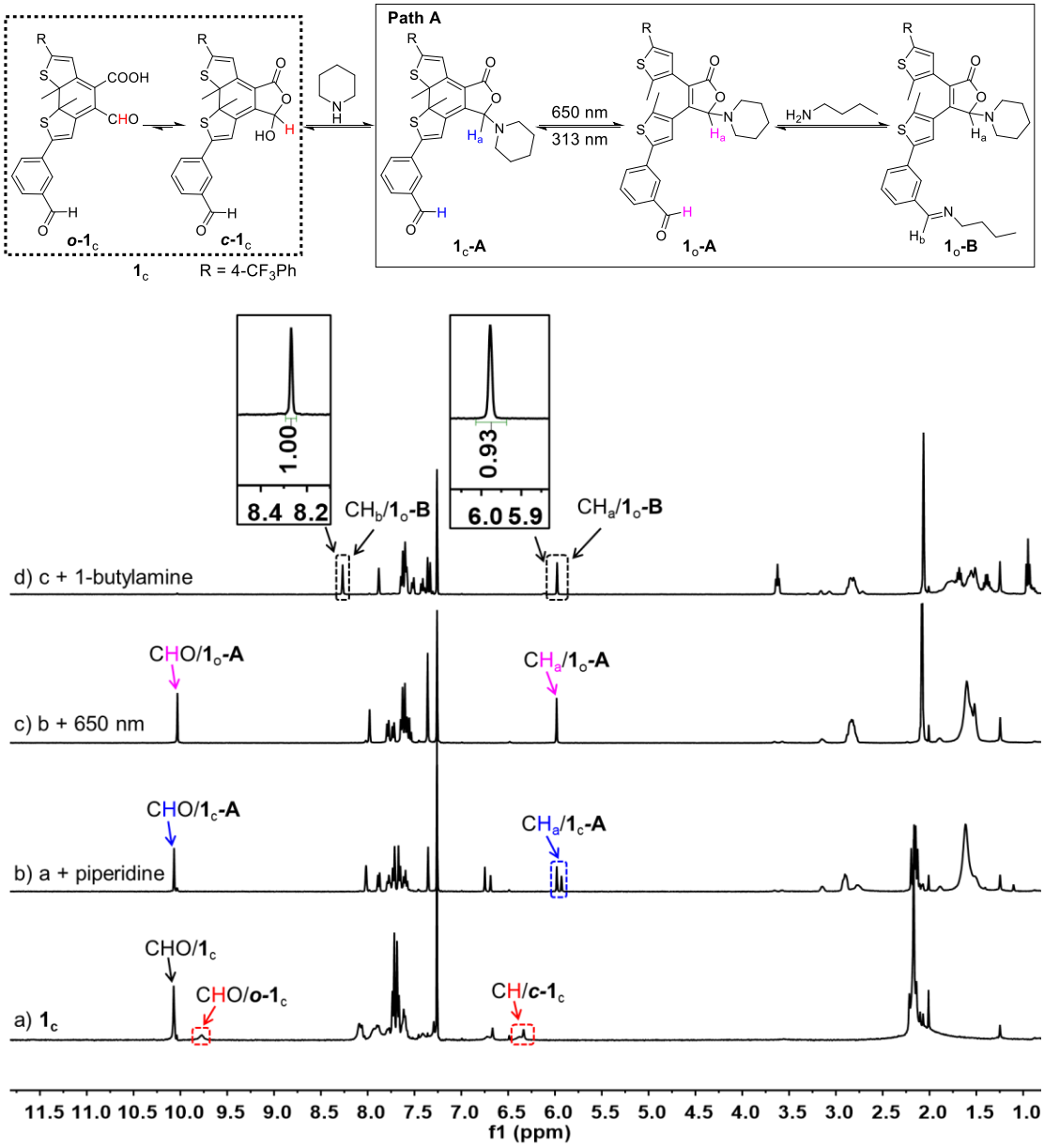

Figure S52. Creation of **1**$_o$**-B** by path A. (a) ^{1}H NMR spectrum of **1**$_c$ (10 mM, created from the irradiation of **1**$_o$ at 313 nm) in $CDCl_3$; (b) The addition of piperidine (1.1 equiv.) to panel a. After 12 h, **1**$_c$ converted to **1**$_c$**-A** completely; (c) Irradiation of panel b with visible light (650 nm, 150 min); (d) The addition of 1-butylamine (1.1 equiv.) to panel c. **1**$_o$**-A** converted to **1**$_o$**-B** after 5 days. The peaks at 6.0 and 8.3 ppm were assigned to cyclic hemiaminal ether and open imine methine protons, respectively. The integral ratio of imine CH peak and hemiaminal ether CH peak is 1:0.93.

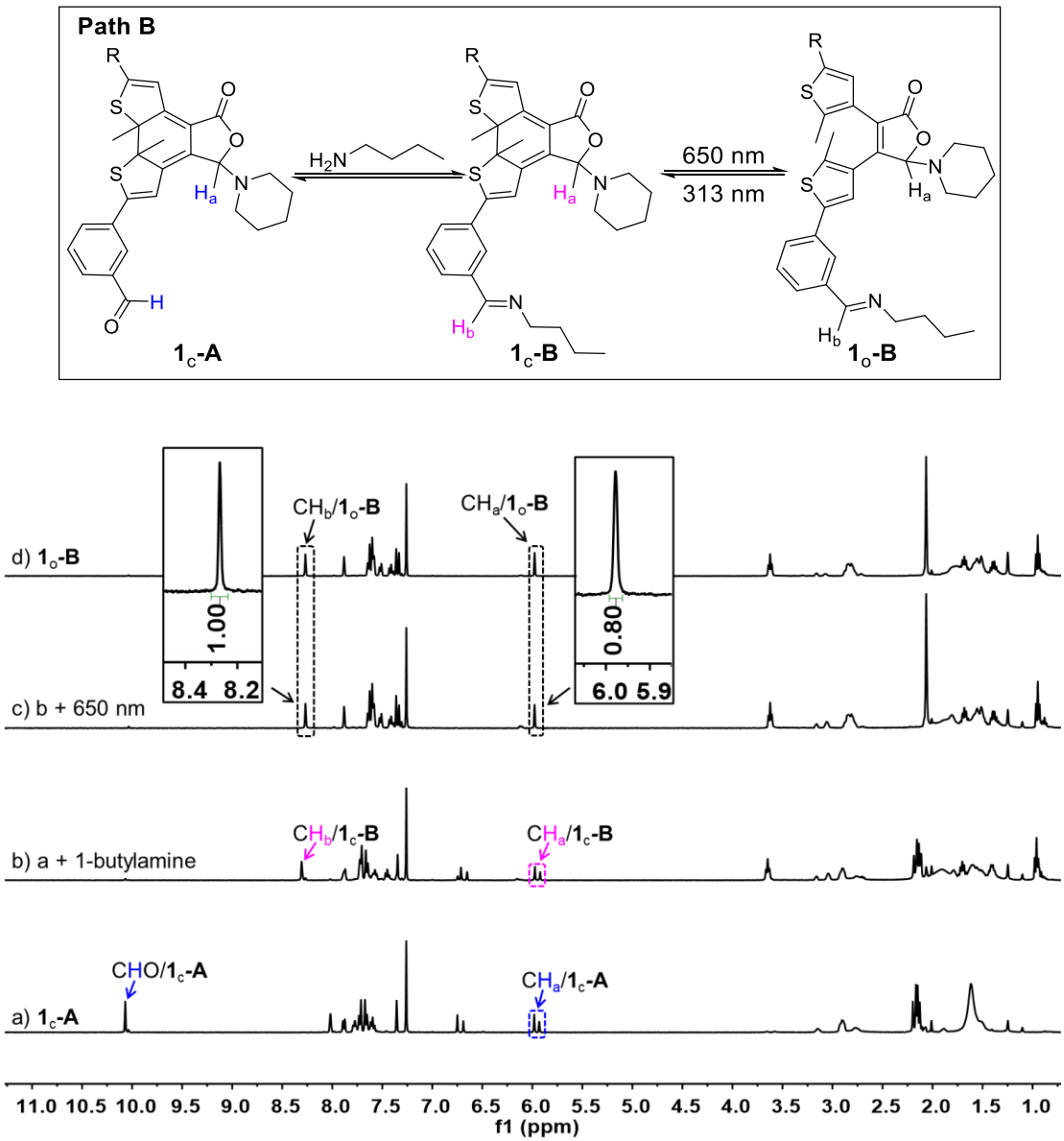

Figure S53. Creation of **1**$_o$**-B** by path B. (a) ^{1}H NMR spectrum of **1**$_c$**-A** (10 mM, created *in situ* from the reaction of **1**$_c$ and piperidine (1.1 equiv.)) in $CDCl_3$; (b) The addition of 1-butylamine (1.1 equiv.) to panel a. **1**$_c$**-A** converted to **1**$_c$**-B** after 5 days; (c) Irradiation of panel b with visible light (650 nm, 150 min); (d) ^{1}H NMR spectrum of **1**$_o$**-B** (10 mM, created by path A in Figure S52) for comparison. The peaks at 6.0 and 8.3 ppm were assigned to cyclic hemiaminal ether and open imine methine protons, respectively. The integral ratio of imine CH peak and hemiaminal ether CH peak is 1:0.8.

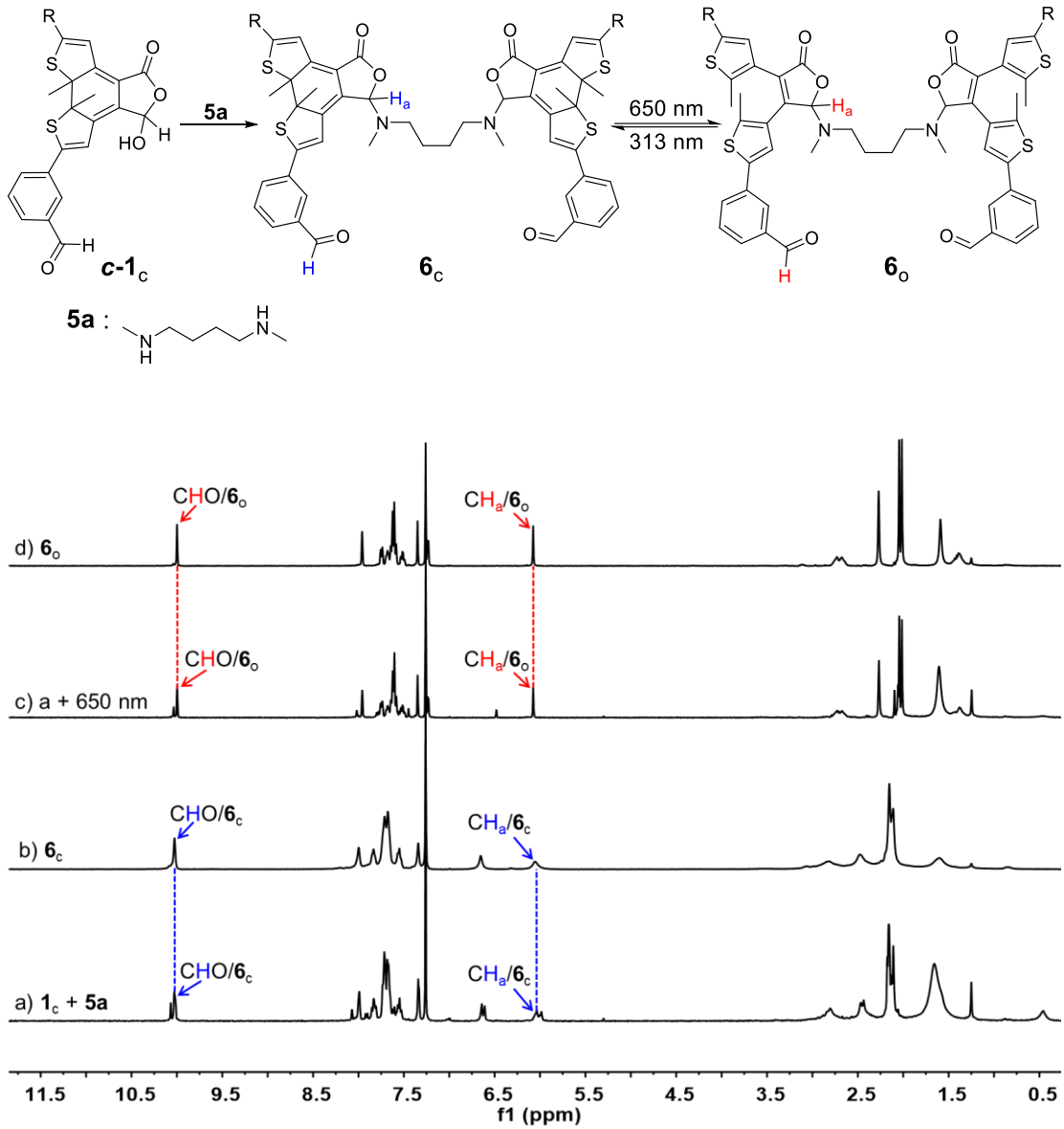

Figure S54. Creation of $\mathbf{6}_o$ by the reaction of $\mathbf{1}_c$ and **5a** *in situ*. (a) ^{1}H NMR spectrum of the reaction of $\mathbf{1}_c$ (10 mM) and **5a** (0.5 equiv.) in $CDCl_3$ in 5 days to give $\mathbf{6}_c$; (b) ^{1}H NMR spectrum of $\mathbf{6}_c$ (5 mM) in $CDCl_3$. The precipitates formed upon the reaction of $\mathbf{1}_c$ and 5a (0.5 equiv.) in CH_3CN for 12 h, which was collected and then dissolved in $CDCl_3$; (c) Irradiation of panel a with visible light (650 nm, 150 min). The yield of $\mathbf{6}_o$ is 75%; (d) ^{1}H NMR spectrum of $\mathbf{6}_o$ (5 mM, prepared and isolated as detailed in synthesis section) in $CDCl_3$ for comparison.

Scheme S4. (A) Synthesis of [2+1+1'] type macrocycles. (B) List of the dialdehydes, primary diamines, and [2+1+1'] type macrocycles.

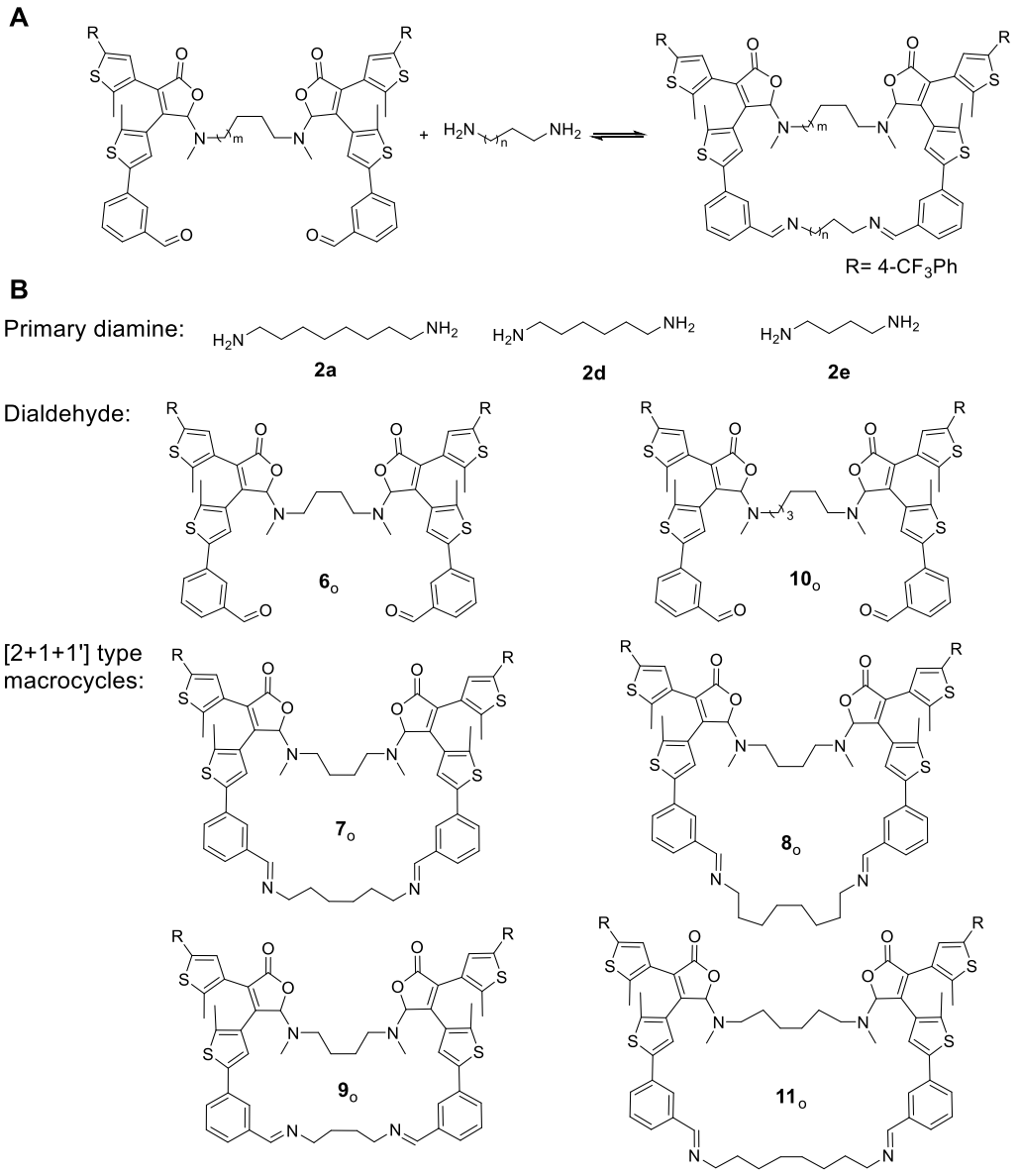

General methods: The [2+1+1'] type macrocycles were created *in situ*. The primary diamine (1 equiv.) was added into a solution of dialdehyde $\mathbf{6}_o$ or $\mathbf{9}_o$ (5 mM, $CDCl_3$) and the resulting mixture was stirred under dark at 40 ℃ for 12 h. The yield of [2+1+1'] type macrocycles was nearly quantitative.

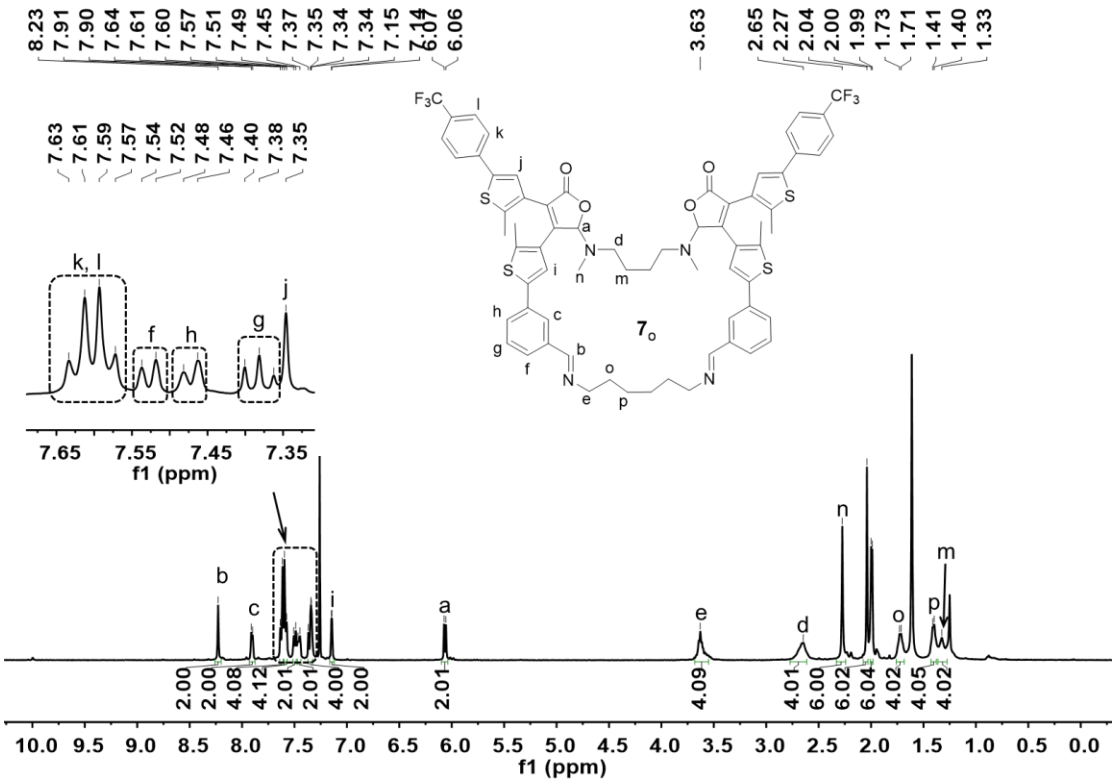

Figure S55. ^{1}H NMR spectra of $\mathbf{7}_o$ (created *in situ* from the reaction of $\mathbf{6}_o$ (5 mM) and **2d** (1,6-diaminohexane, 1 equiv.) at 40 °C for 12 h) in $CDCl_3$.

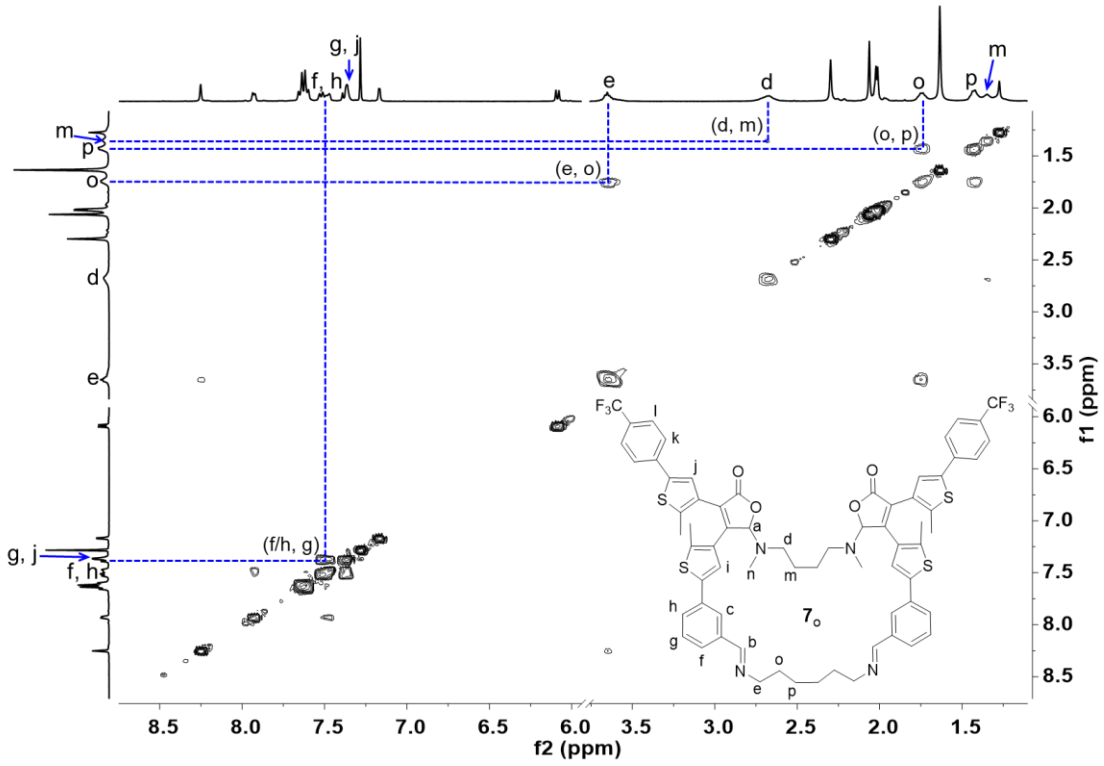

Figure S56. Partial 2D ^{1}H-^{1}H COSY NMR spectrum of $\mathbf{7}_o$ (created *in situ* from the reaction of $\mathbf{6}_o$ (5 mM) and **2d** (1 equiv.) at 40 °C for 12 h) in $CDCl_3$.

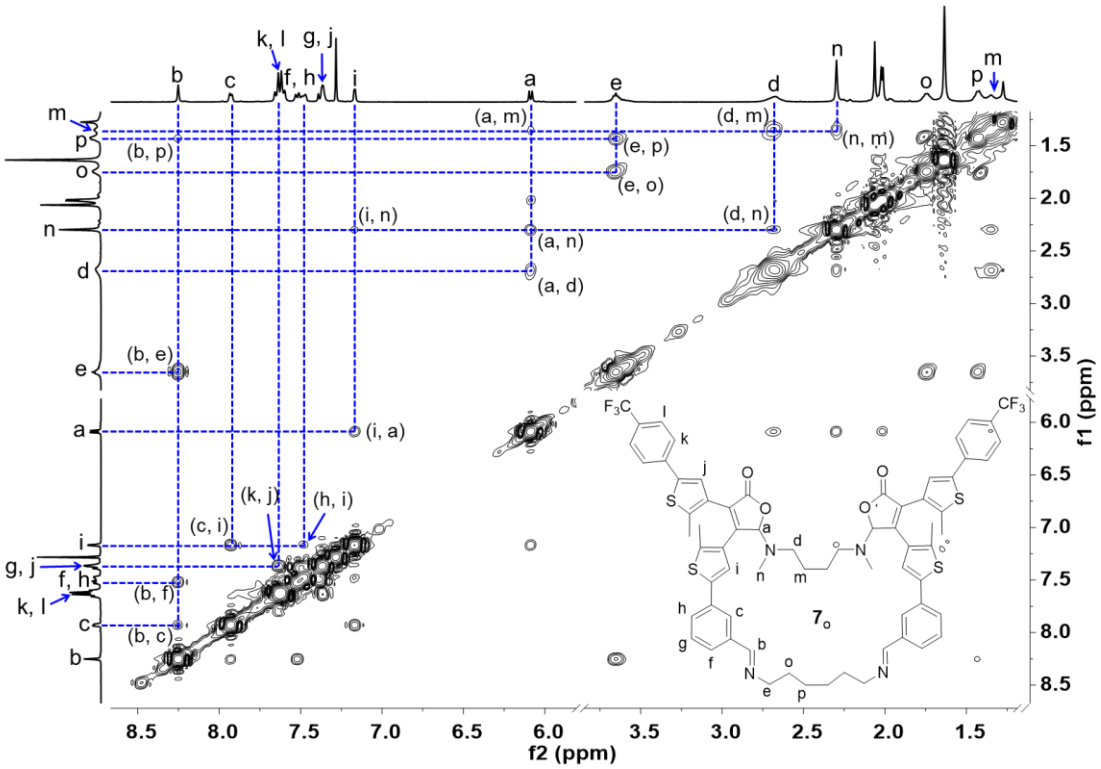

Figure S57. Partial 2D ^{1}H-^{1}H NOESY NMR spectrum of **7**$_o$ (created *in situ* from the reaction of **6**$_o$ (5 mM) and **2d** (1 equiv.) at 40 °C for 12 h) in $CDCl_3$.

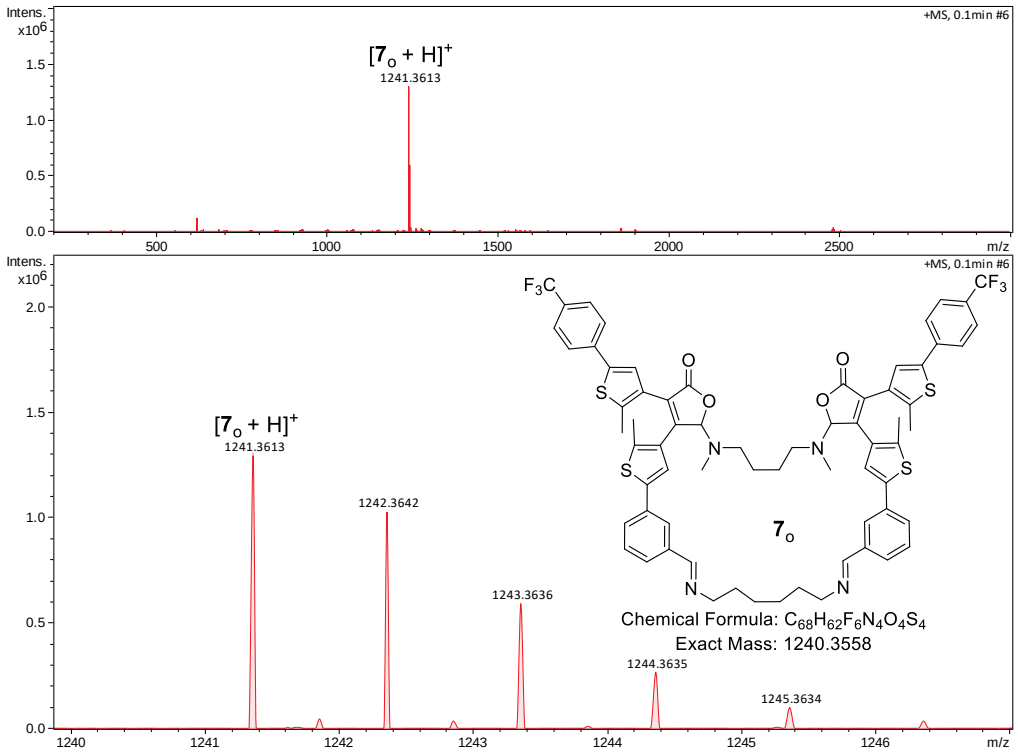

Figure S58. ESI mass spectrum of **7**$_o$ (created *in situ* from the reaction of **6**$_o$ and **2d** in $CDCl_3$).

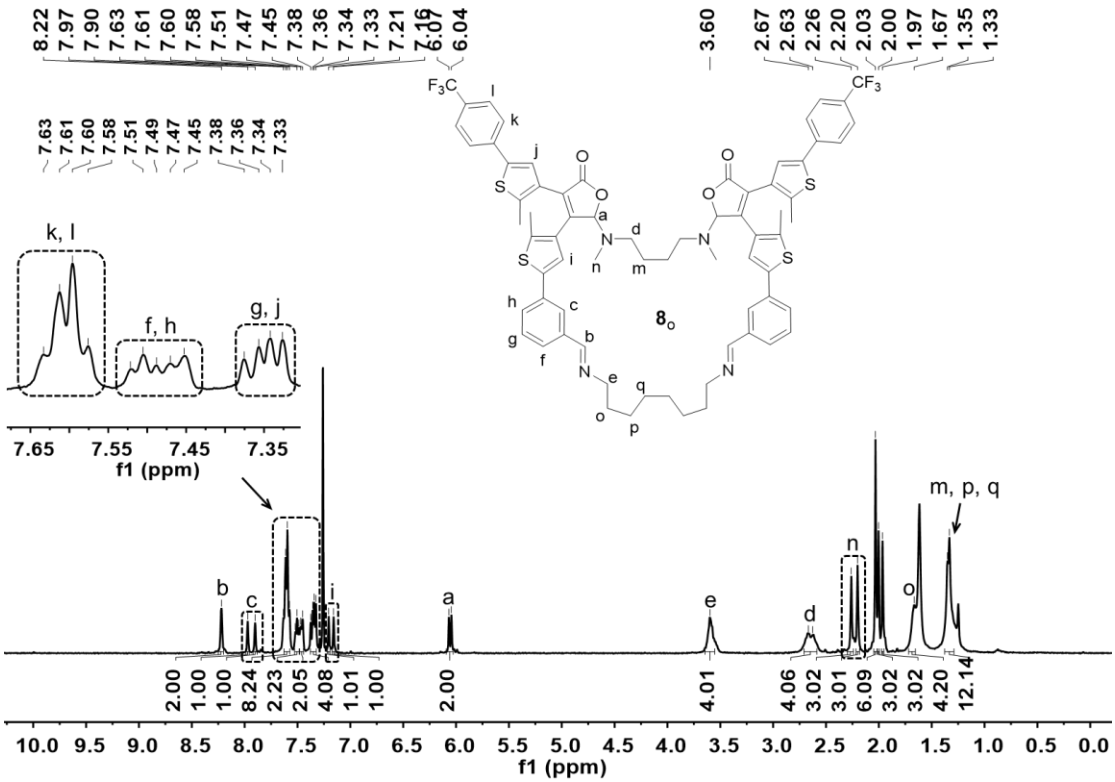

Figure S59. ^{1}H NMR spectra of **8**$_{o}$ (created *in situ* from the reaction of **6**$_{o}$ (5 mM) and **2a** (1,8-diaminooctane, 1 equiv.) at 40 °C for 12 h) in $CDCl_3$.

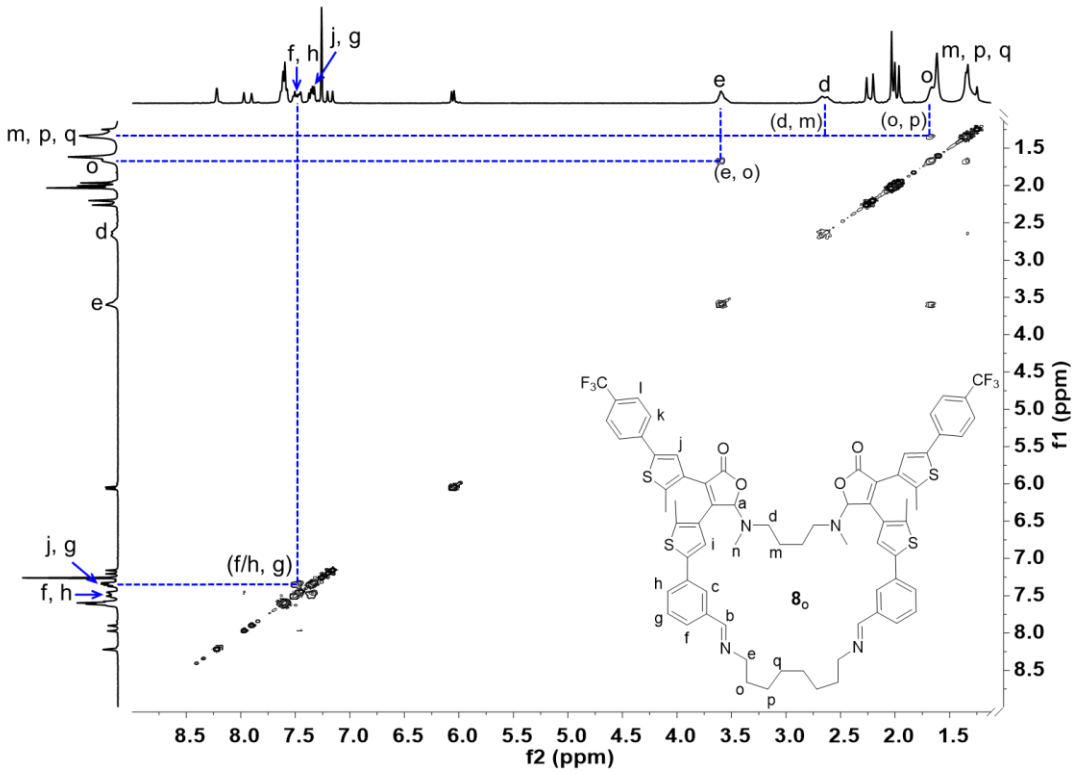

Figure S60. Partial 2D ^{1}H-^{1}H COSY NMR spectrum of **8**$_{o}$ (created *in situ* from the reaction of **6**$_{o}$ (5 mM) and **2a** (1 equiv.) at 40 °C for 12 h) in $CDCl_3$.

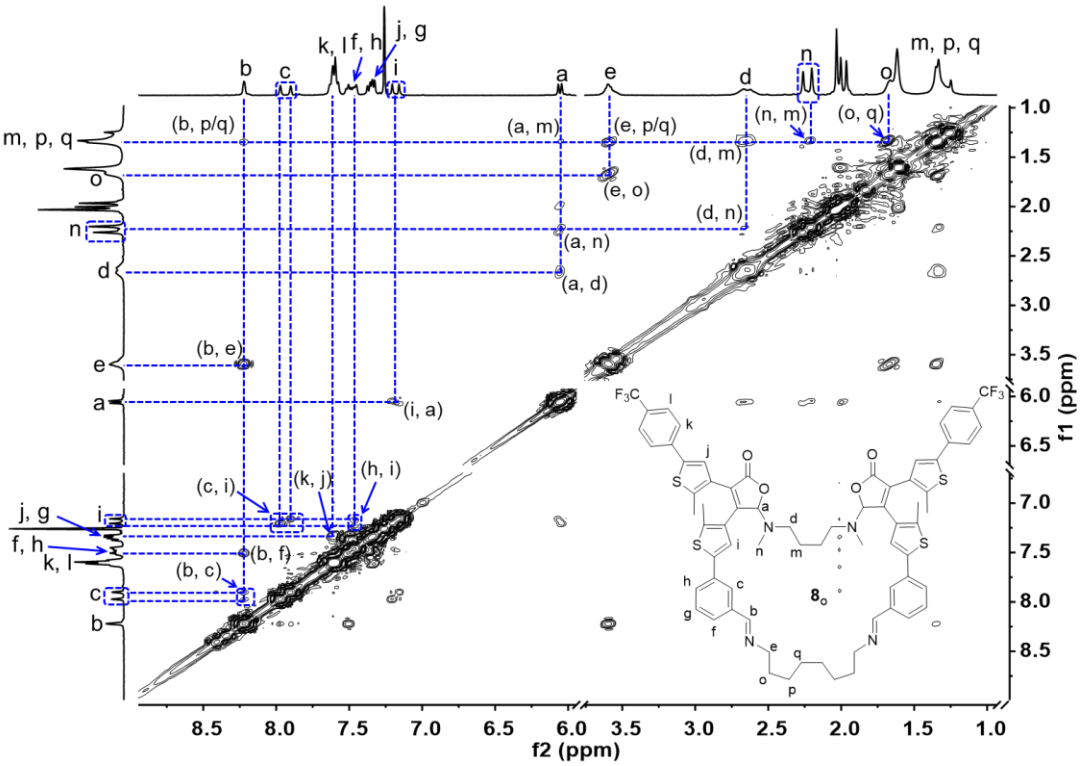

Figure S61. Partial 2D ^{1}H-^{1}H NOESY NMR spectrum of **8**$_o$ (created *in situ* from the reaction of **6**$_o$ (5 mM) and **2a** (1 equiv.) at 40 °C for 12 h) in $CDCl_3$.

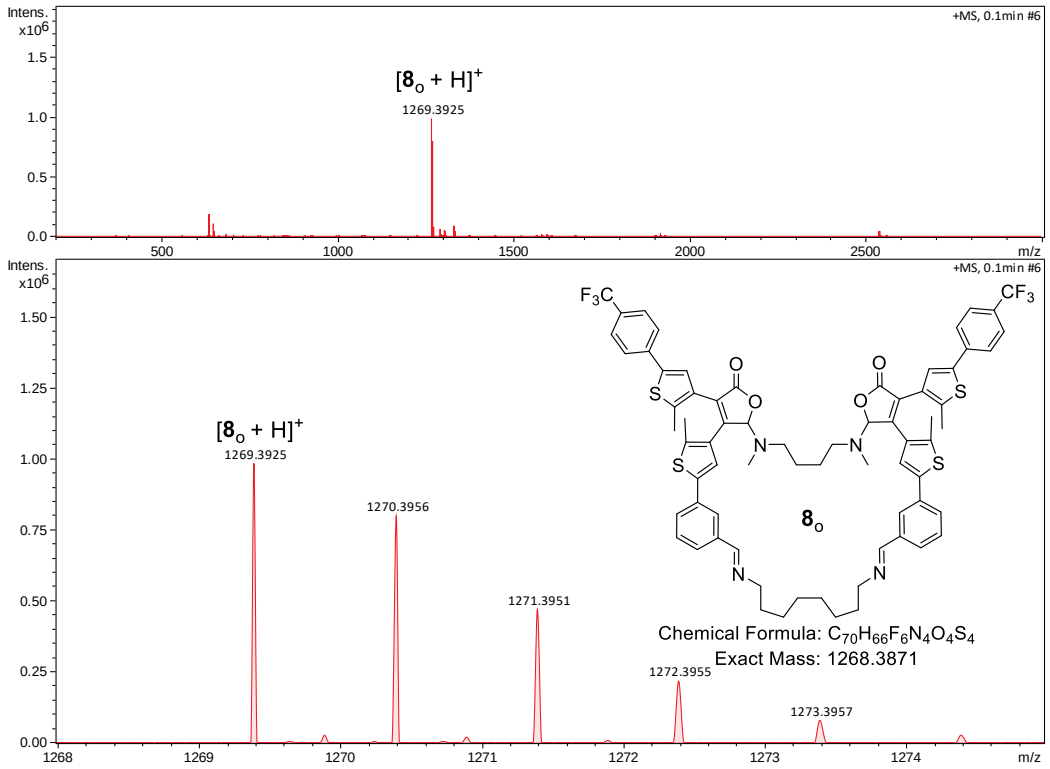

Figure S62. ESI mass spectrum of **8**$_o$ (created *in situ* from the reaction of **6**$_o$ and **2a** in $CDCl_3$).

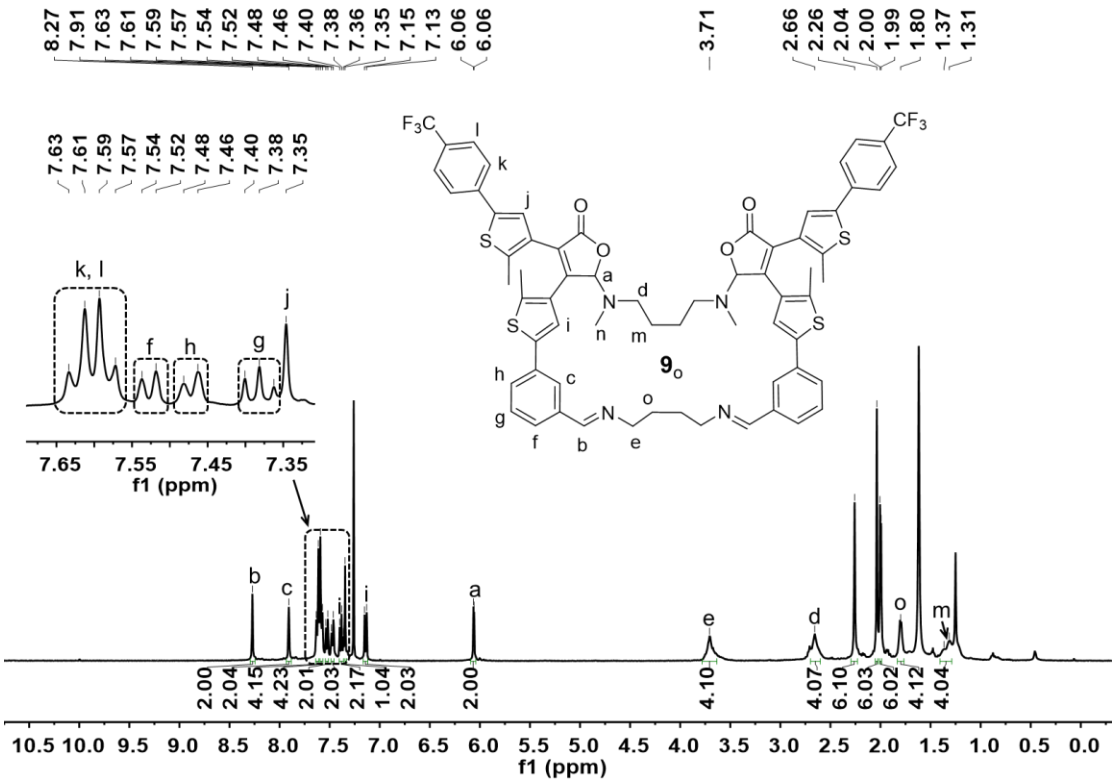

Figure S63. ^{1}H NMR spectra of $\mathbf{9}_{o}$ (created *in situ* from the reaction of $\mathbf{6}_{o}$ (5 mM) and **2e** (1,4-diaminobutane, 1 equiv.) at 40 °C for 12 h) in $CDCl_3$.

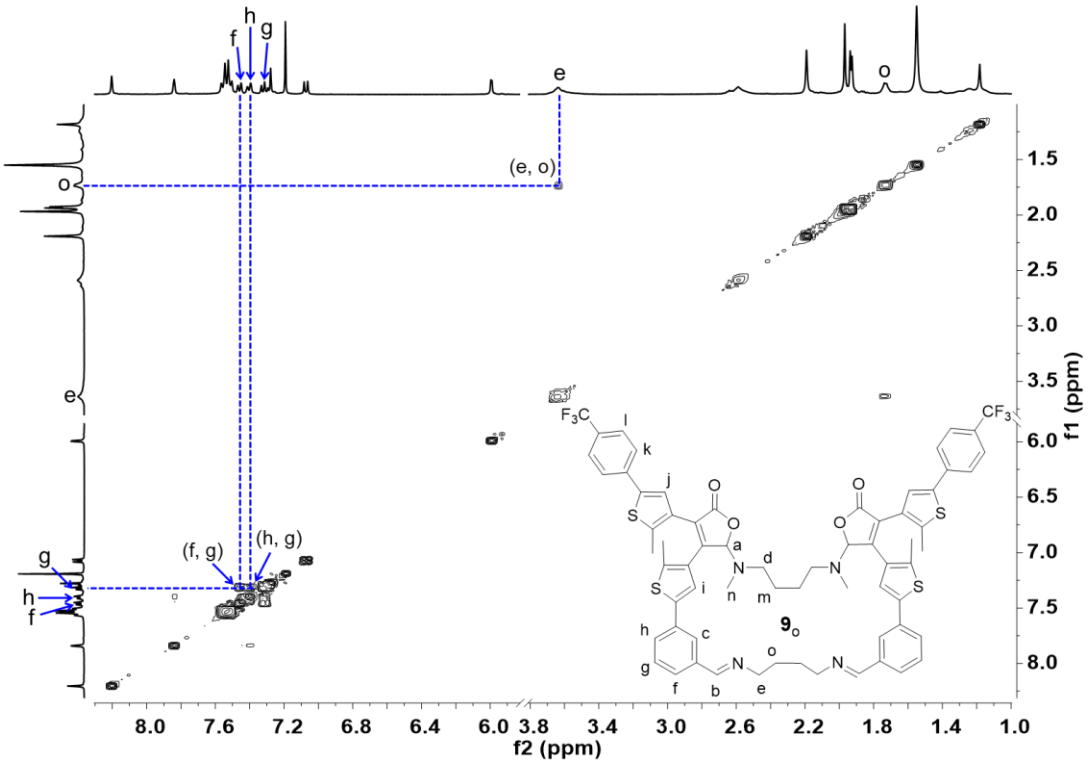

Figure S64. Partial 2D ^{1}H-^{1}H COSY NMR spectrum of $\mathbf{9}_{o}$ (created *in situ* from the reaction of $\mathbf{6}_{o}$ (5 mM) and **2e** (1 equiv.) at 40 °C for 12 h) in $CDCl_3$.

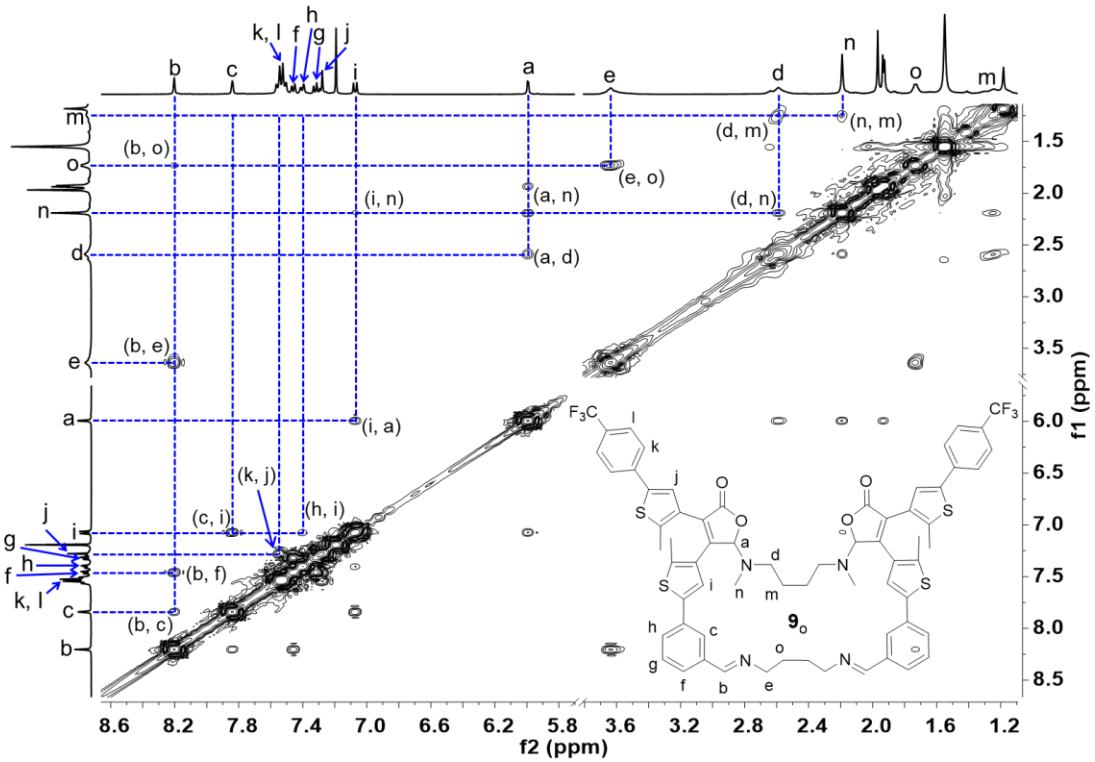

Figure S65. Partial 2D ^{1}H-^{1}H NOESY NMR spectrum of $\mathbf{9}_o$ (created *in situ* from the reaction of $\mathbf{6}_o$ (5 mM) and **2e** (1 equiv.) at 40 °C for 12 h) in $CDCl_3$.

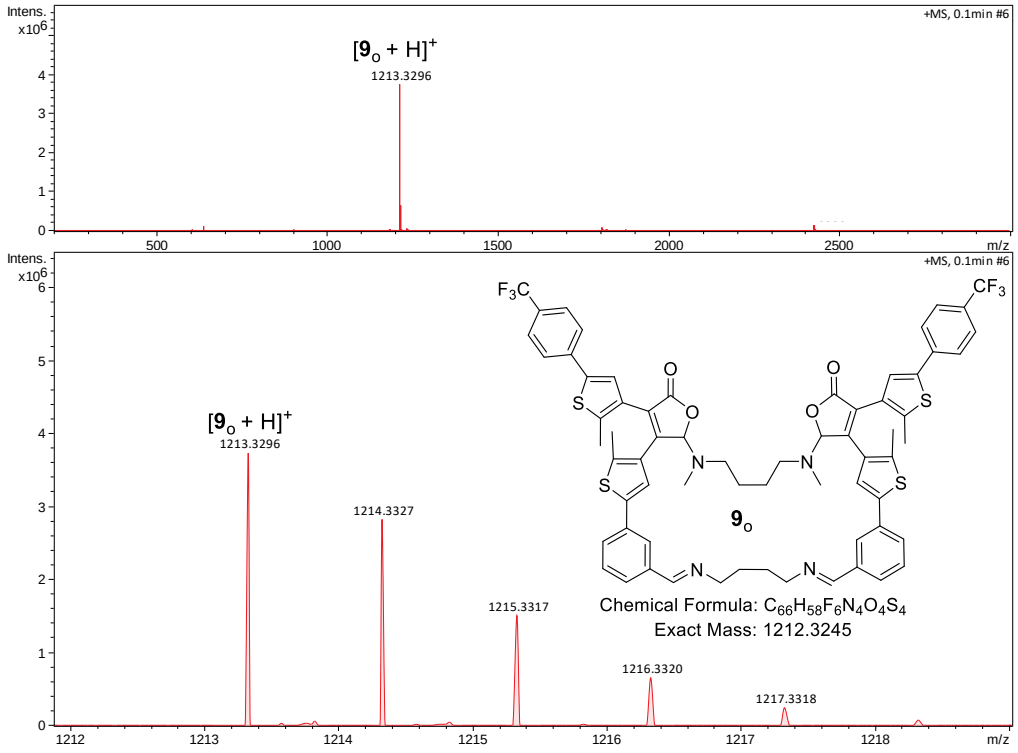

Figure S66. ESI mass spectrum of $\mathbf{9}_o$ (created *in situ* from the reaction of $\mathbf{6}_o$ and **2e** in $CDCl_3$).

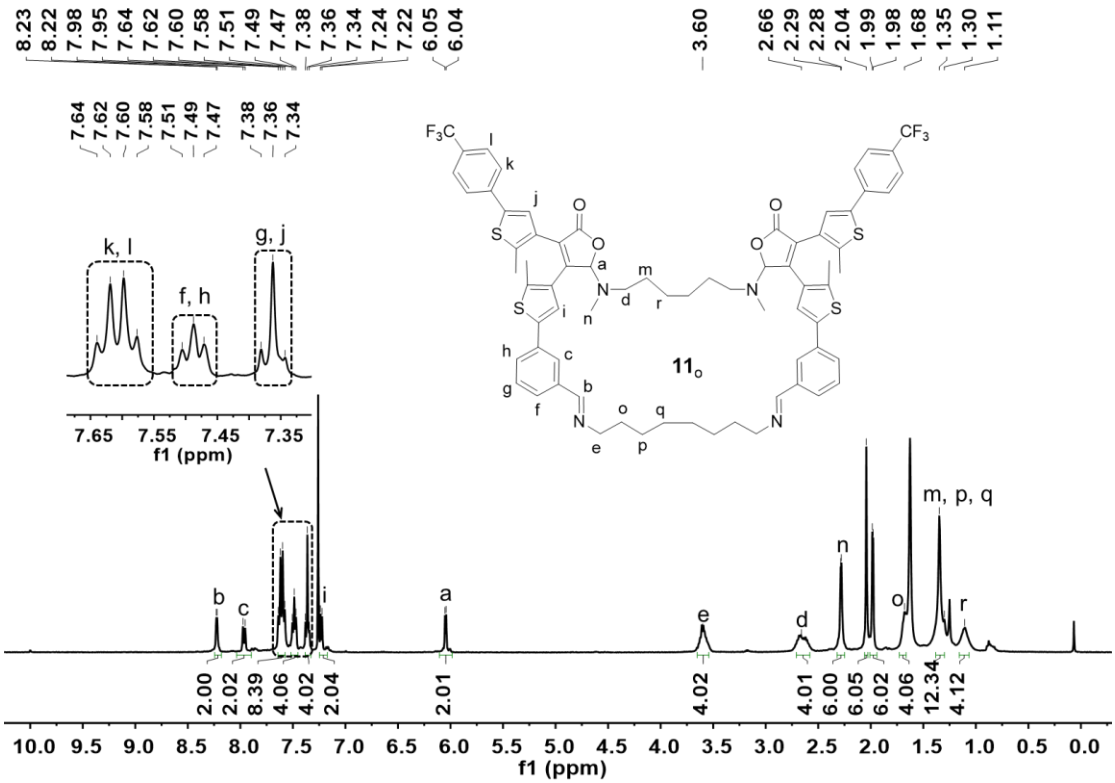

Figure S67. ^{1}H NMR spectra of **11**$_{o}$ (created *in situ* from the reaction of **10**$_{o}$ (5 mM) and **2a** (1,8-diaminooctane, 1.0 equiv.) at 40 °C for 12 h) in $CDCl_3$.

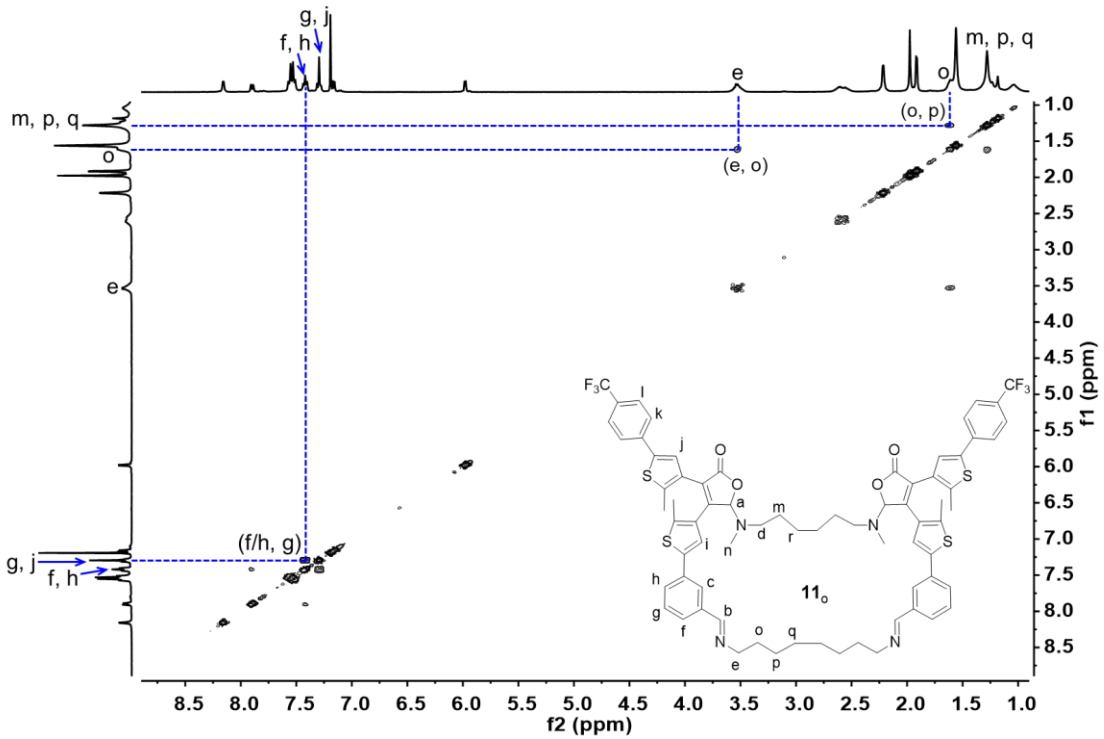

Figure S68. Partial 2D ^{1}H-^{1}H COSY NMR spectrum of **11**$_{o}$ (created *in situ* from the reaction of **10**$_{o}$ (5 mM) and **2a** (1.0 equiv.) at 40 °C for 12 h) in $CDCl_3$.

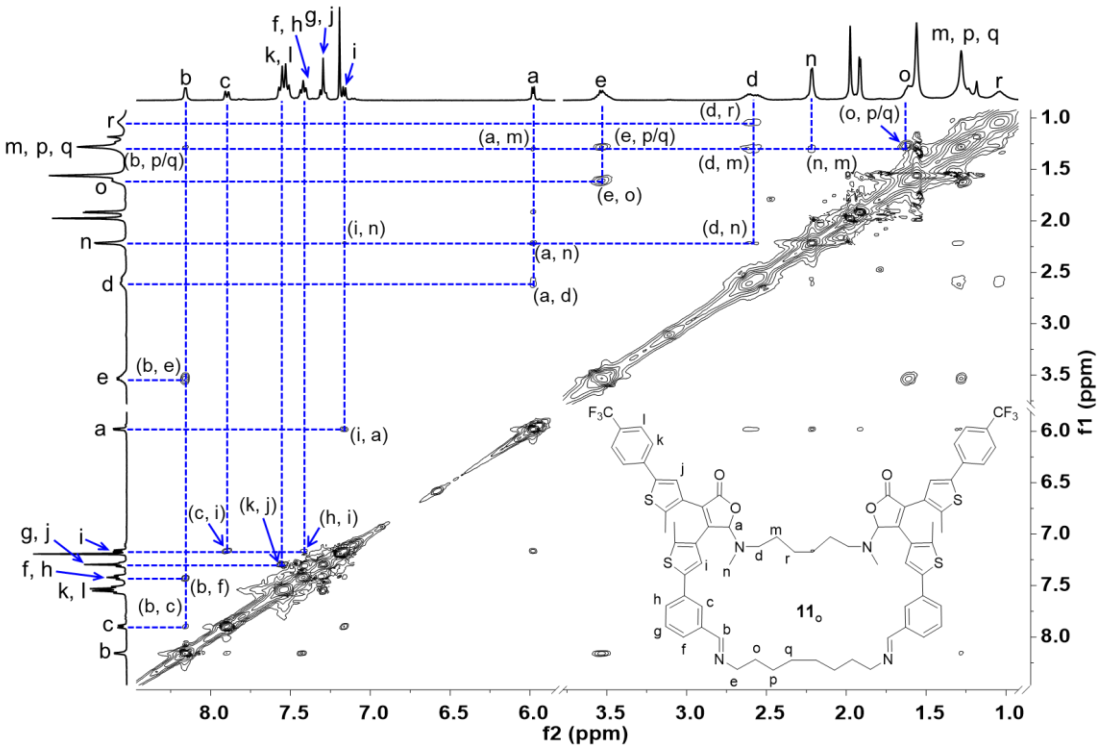

Figure S69. Partial 2D ^{1}H-^{1}H NOESY NMR spectrum of **11**$_o$ (created *in situ* from the reaction of **10**$_o$ (5 mM) and **2a** (1.0 equiv.) at 40 °C for 12 h) in $CDCl_3$.

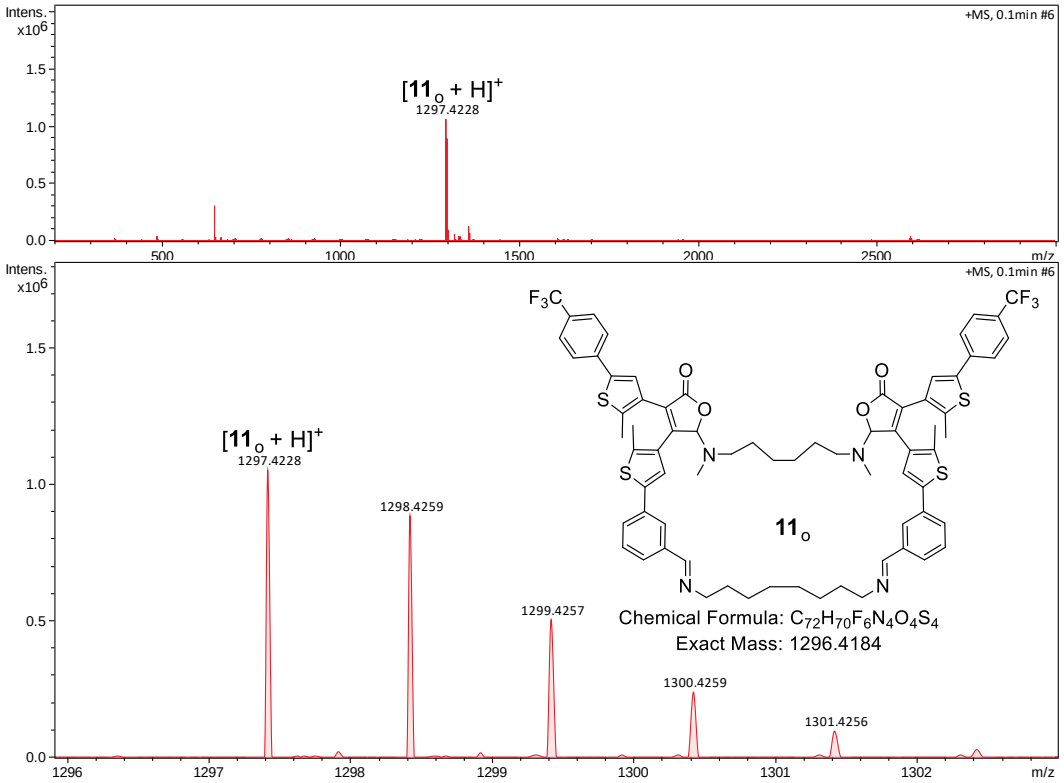

Figure S70. ESI mass spectrum of **11**$_o$ (created *in situ* from the reaction of **10**$_o$ and **2a** in $CDCl_3$.

6. Regulation of [2+1+1'] Macrocycles

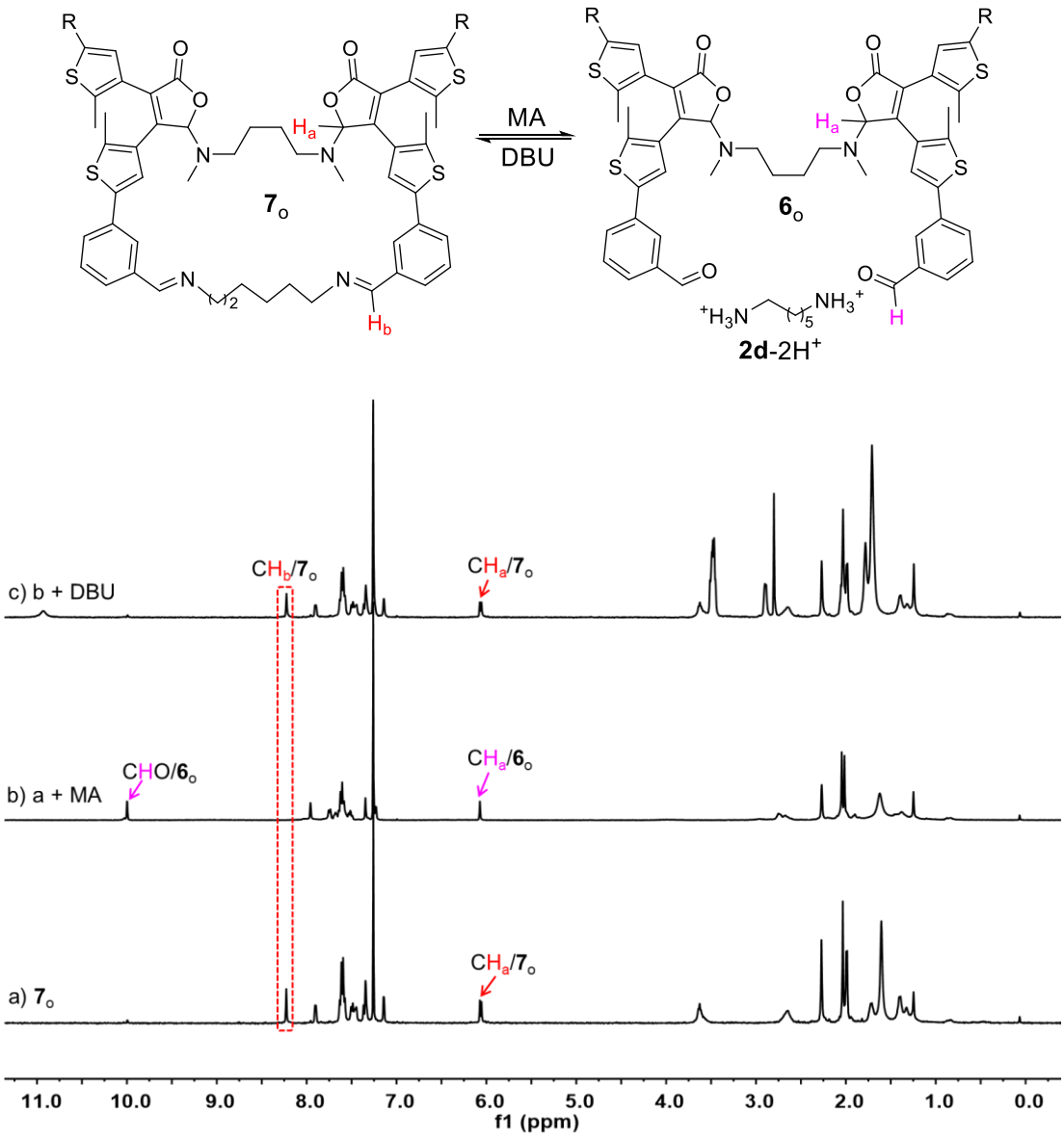

Figure S71. Precise formation/scission of [2+1+1'] macrocycles through acid/base stimuli. (a) ^{1}H NMR spectrum of $\mathbf{7}_o$ (5 mM, created *in situ* from $\mathbf{6}_o$ and **2d**) in $CDCl_3$; (b) The addition of MA (2 equiv.) to panel a. $\mathbf{7}_o$ converted to $\mathbf{6}_o$ and **2d**-2H$^+$ immediately (3 min); (c) The addition of DBU (2.3 equiv.) to panel b. $\mathbf{6}_o$ converted back to $\mathbf{7}_o$ in 80 h.

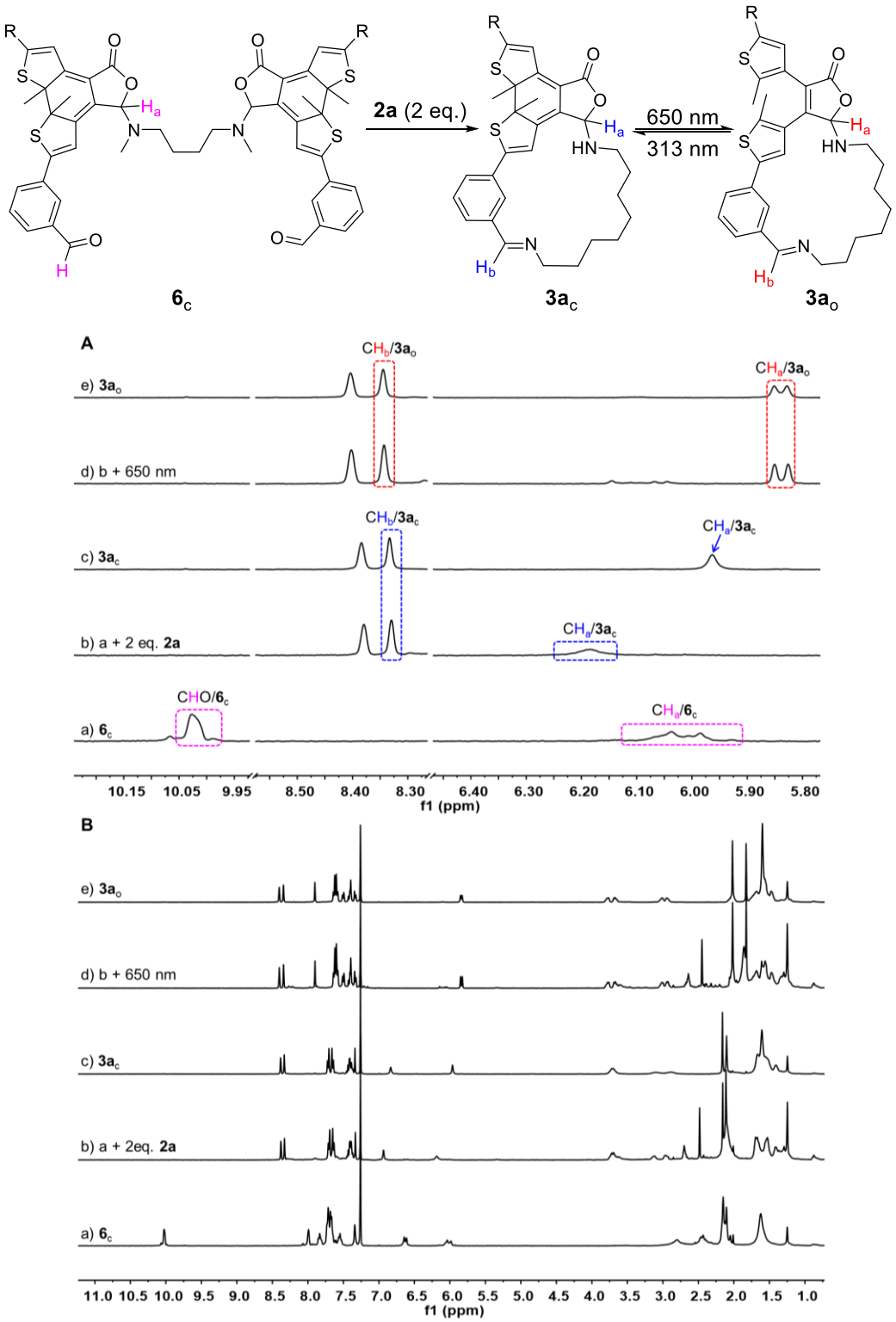

Figure S72. The addition of **2a** (2.0 eq.) to $\mathbf{6}_c$ (5 mM) to give mainly $\mathbf{3a}_c$. (A) (a) ^{1}H NMR spectrum of $\mathbf{6}_c$ (5 mM, created by irradiation of $\mathbf{6}_o$ at 313 nm for 150 min); (b) The addition of **2a** (2.0 eq.) to panel a. The system reached equilibrium in 2 h; (c) ^{1}H NMR spectrum of $\mathbf{3a}_c$ (10 mM, created *in situ* from the reaction of $\mathbf{1}_c$ and **2a** in $CDCl_3$) for comparison; (d) Irradiation of panel b at 650 nm for 150 min; (e) ^{1}H NMR spectrum of $\mathbf{3a}_o$ (10 mM, $CDCl_3$) for comparison. (B) The full ^{1}H NMR spectra of A.

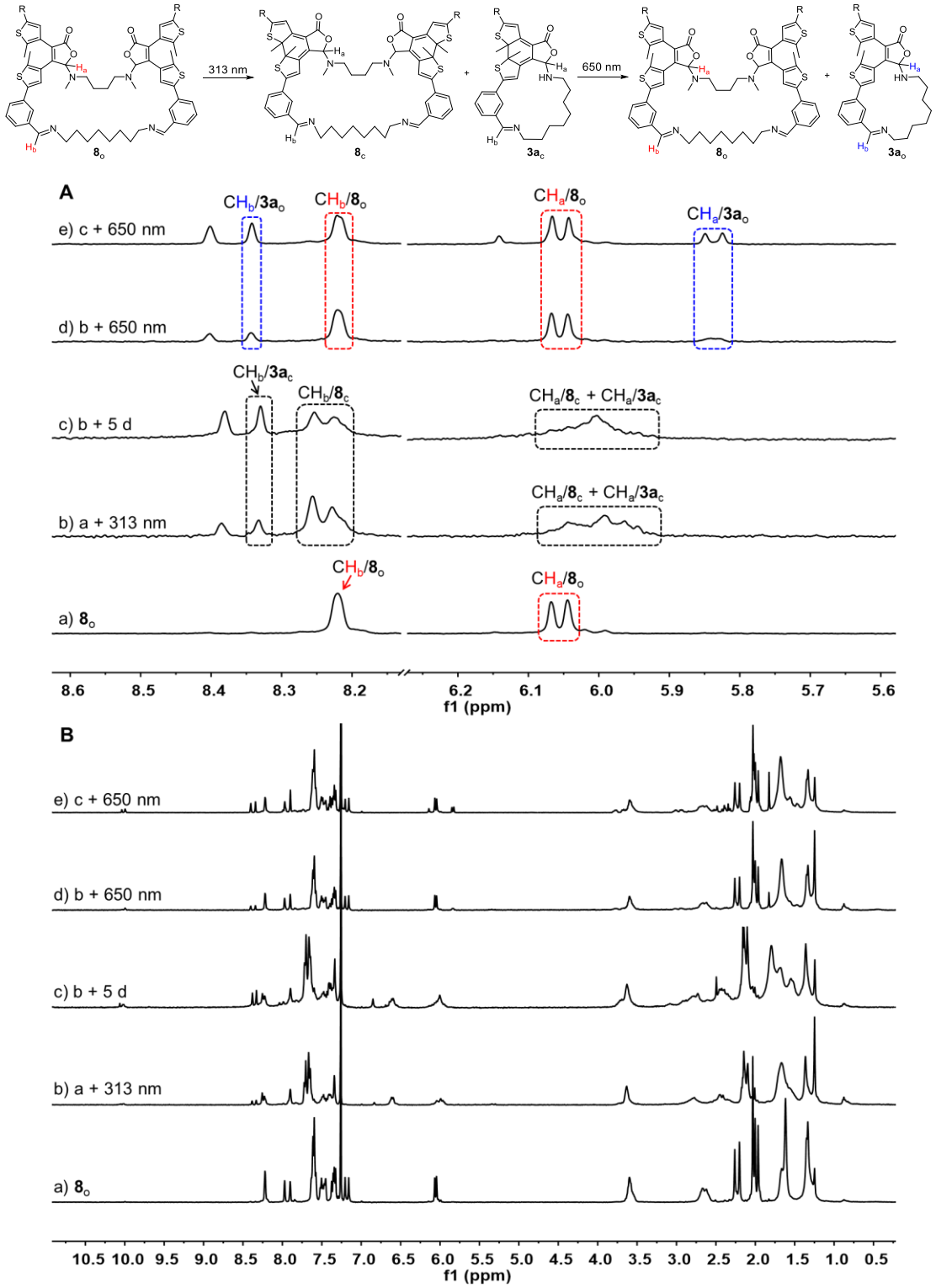

Figure S73. The changes of ^{1}H NMR spectrum of $\mathbf{8}_o$ with photoswitching. (A) (a) ^{1}H NMR spectrum of $\mathbf{8}_o$ (5 mM, created *in situ* from the reaction of $\mathbf{6}_o$ and **2a**) in $CDCl_3$; (b) Irradiation of panel a at 313 nm for 120 min; (c) After 5 days, the system reached equilibrium; (d) Irradiation of panel b at 650 nm for 150 min. The ratio of $\mathbf{8}_o$ and $\mathbf{3a}_o$ is 82:18; (e) Irradiation of panel c at 650 nm for 150 min, the ratio of $\mathbf{8}_o$ and $\mathbf{3a}_o$ is 59:41;. (B) The full ^{1}H NMR spectra of A.

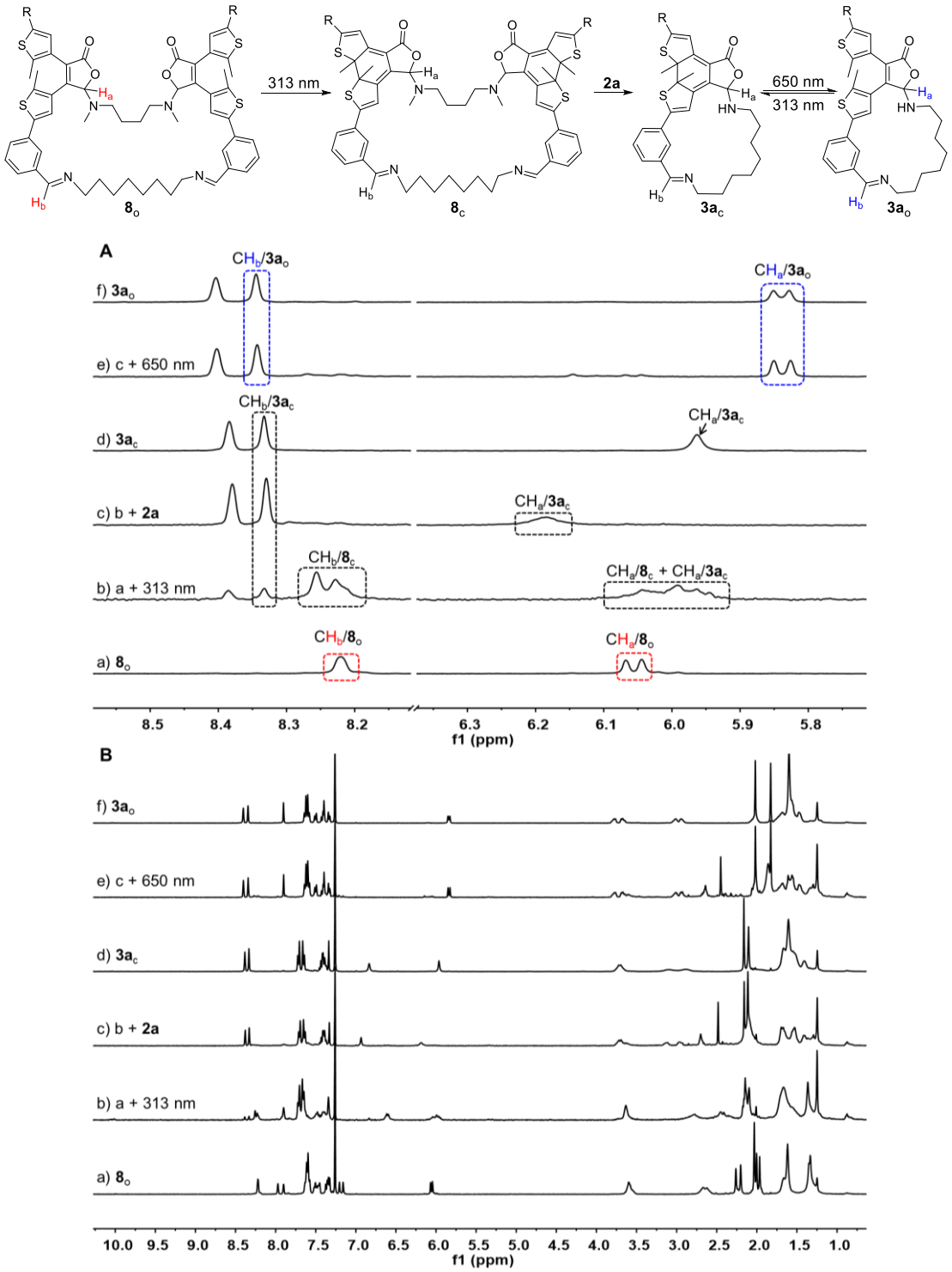

Figure S74. The conversation of $\mathbf{8}_c$ to $\mathbf{3a}_o$. (A) (a) ^{1}H NMR spectrum of $\mathbf{8}_o$ (5 mM, created *in situ* from the reaction of $\mathbf{6}_o$ and **2a**) in $CDCl_3$; (b) Irradiation of panel a at 313 nm for 120 min; (c) The addition of **2a** (1.0 equiv.) to panel b. $\mathbf{8}_c$ converted to $\mathbf{3a}_c$ in 120 min; (d) ^{1}H NMR spectrum of $\mathbf{3a}_c$ (10 mM, created *in situ* from the reaction of $\mathbf{1}_c$ and **2a**) in $CDCl_3$ for comparison; (e) Irradiation of panel b at 650 nm for 120 min; (f) ^{1}H NMR spectrum of $\mathbf{3a}_o$ (10 mM) in $CDCl_3$ for comparison. (B) The full ^{1}H NMR spectra of A.

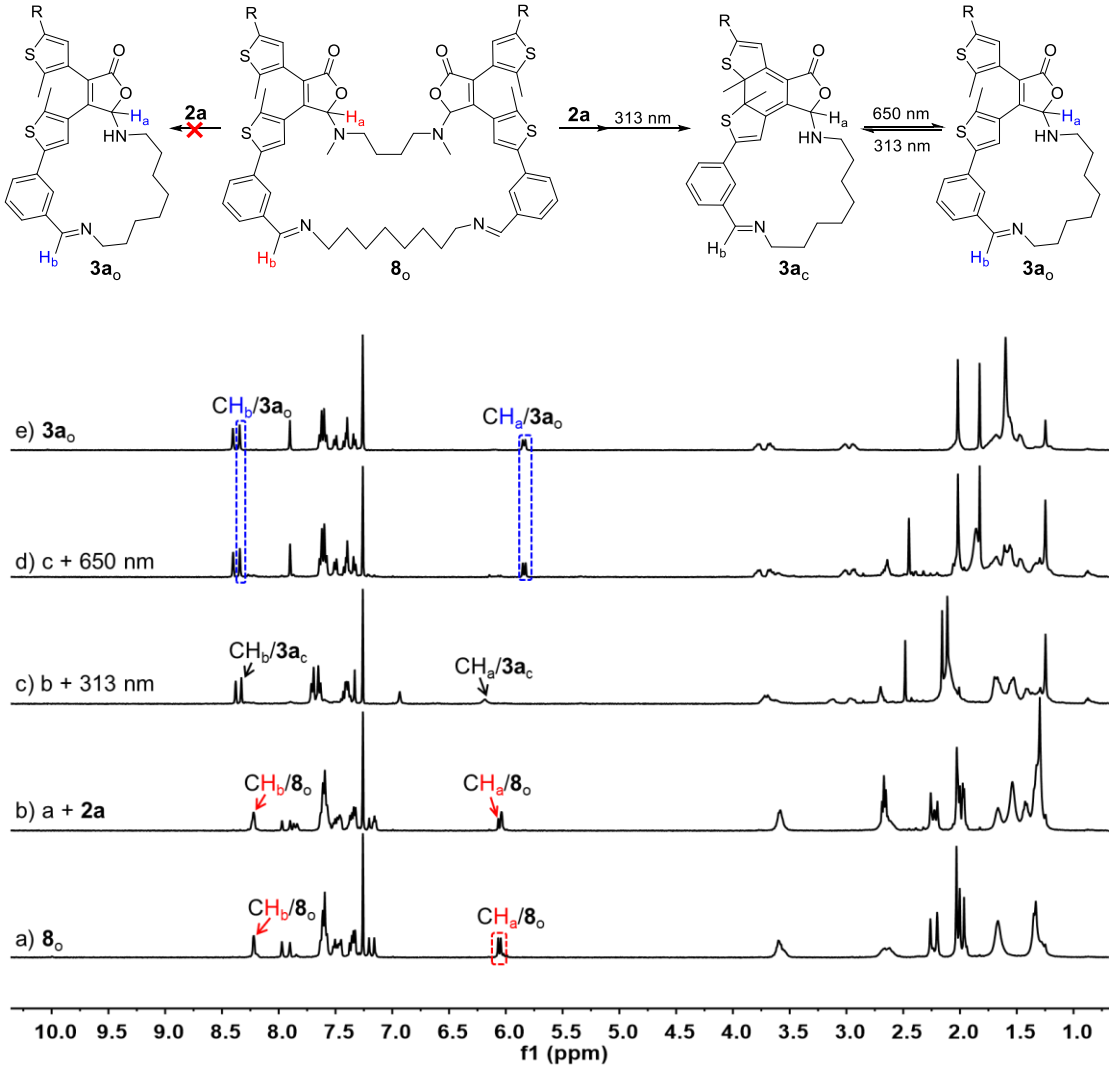

Figure S75. The conversation of **8**$_o$ to **3a**$_o$. (a) ^{1}H NMR spectrum of **8**$_o$ (5 mM, created *in situ* from the reaction of **6**$_o$ and **2a**) in $CDCl_3$; (b) The addition of **2a** (1.0 equiv.) to panel a. After 3 days, the peaks of CH_a/**3a**$_o$ and CH_b/**3a**$_o$ were not found though the exchange of imine b took place; (c) Irradiation of panel b at 313 nm for 120 min; (d) Irradiation of panel c at 650 nm for 120 min; (e) ^{1}H NMR spectrum of **3a**$_o$ (5 mM) in $CDCl_3$ for comparison.

7. Construction of Mechanically Interlocked Assemblies

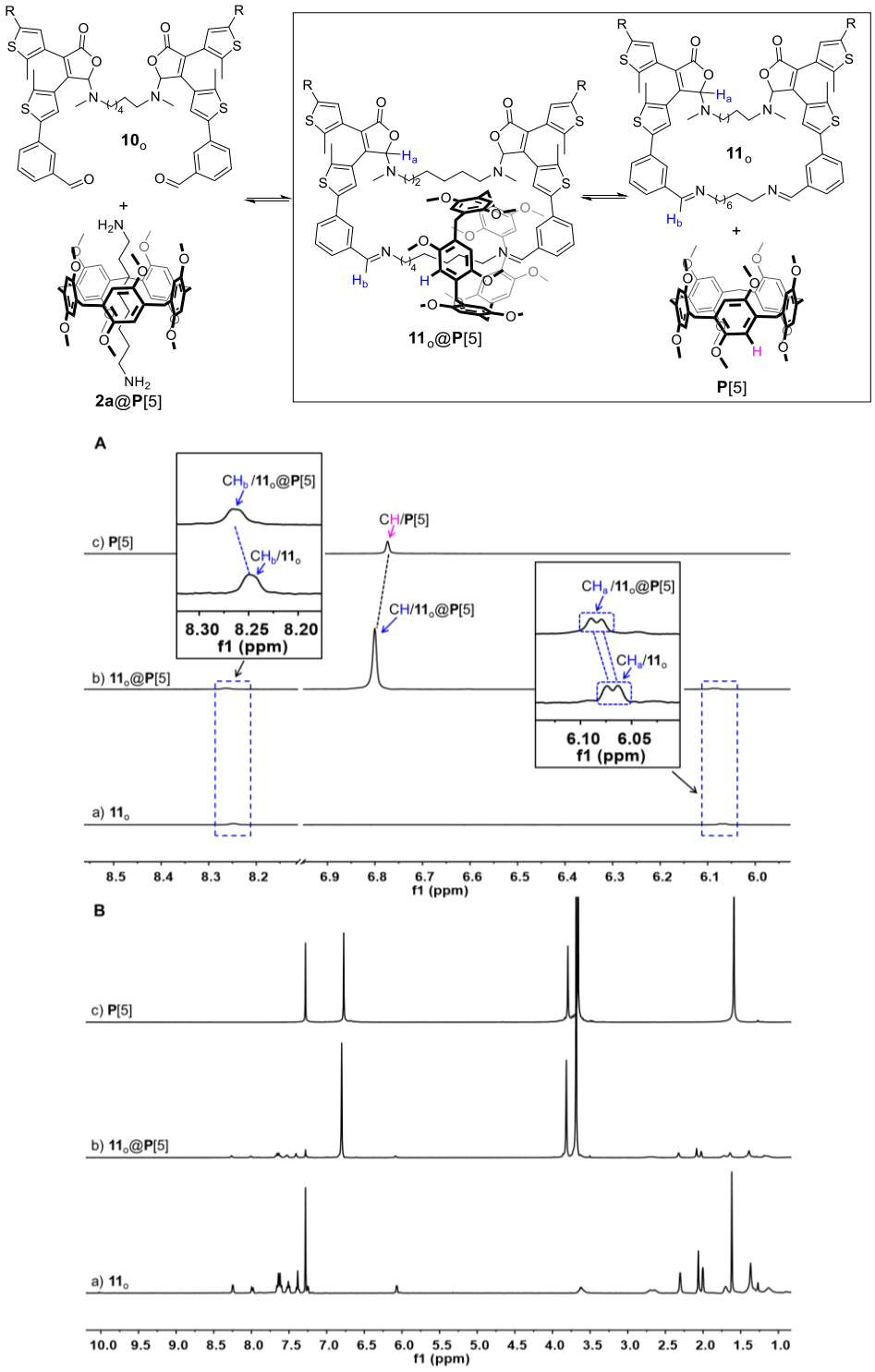

Figure S76. The creation of $\mathbf{11}_o$ and $\mathbf{11}_o$**@P**[5] from the reaction of $\mathbf{10}_o$ (7.5 mM), **2a** (1 equiv.), and **P**[5] (6 equiv.) *in situ* in $CDCl_3$ for 3 days. (A) (a) ^{1}H NMR spectrum of $\mathbf{11}_o$ (5 mM) in $CDCl_3$ for comparison; (b) ^{1}H NMR spectrum of the reaction mixture containing $\mathbf{11}_o$**@P**[5]; (c) ^{1}H NMR spectrum of **P**[5] (10 mM) in $CDCl_3$ for comparison. (B) The full ^{1}H NMR spectra of A.

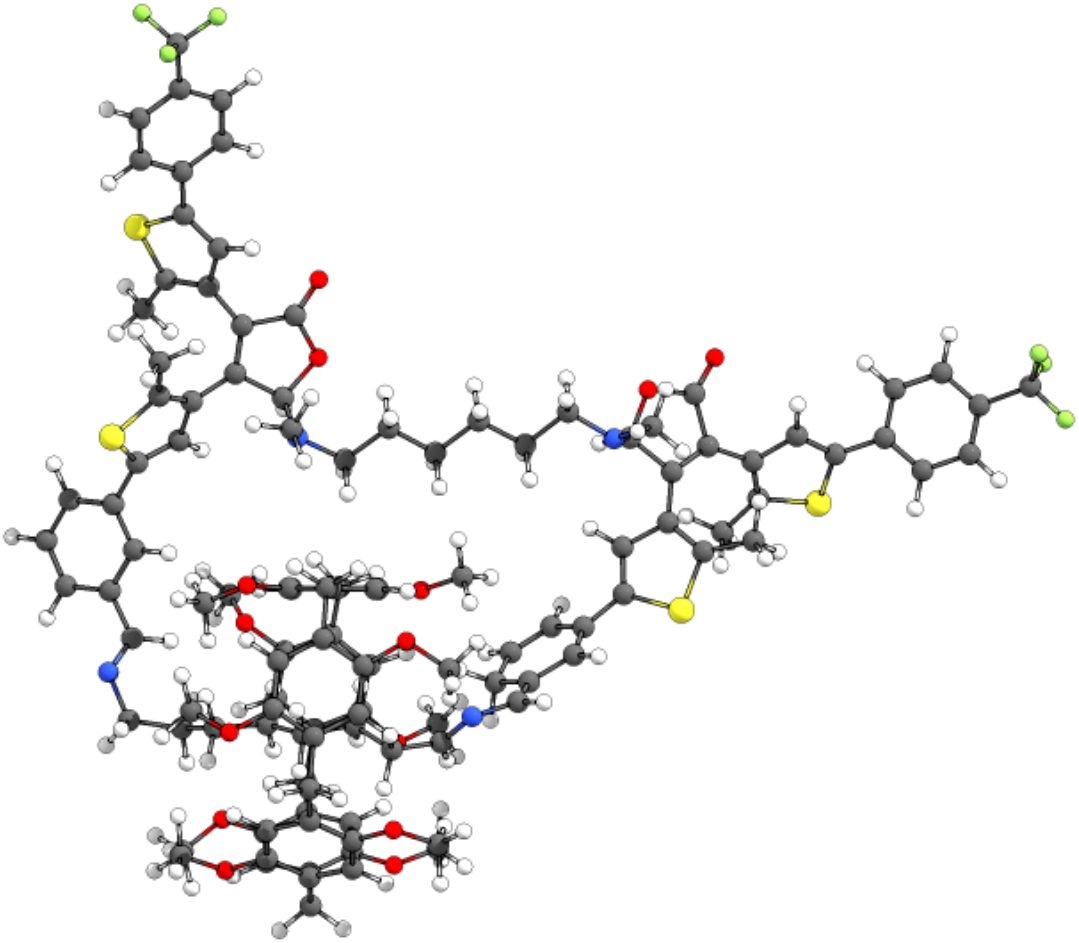

Figure S77. The geometry-optimized molecular model of **11**$_o$**@P**[5]. The geometry was optimized by PM3 method embedded in the Gaussian 09 (D.01).[S4]

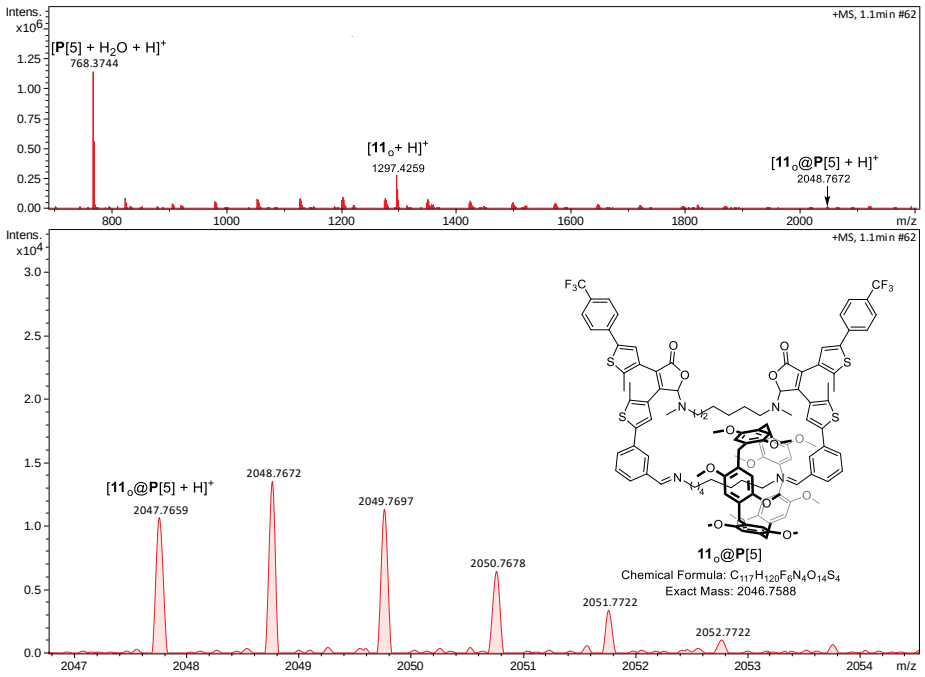

Figure S78. ESI mass spectrum of **11**$_o$ and **11**$_o$**@P**[5] (as generated in Figure S76).

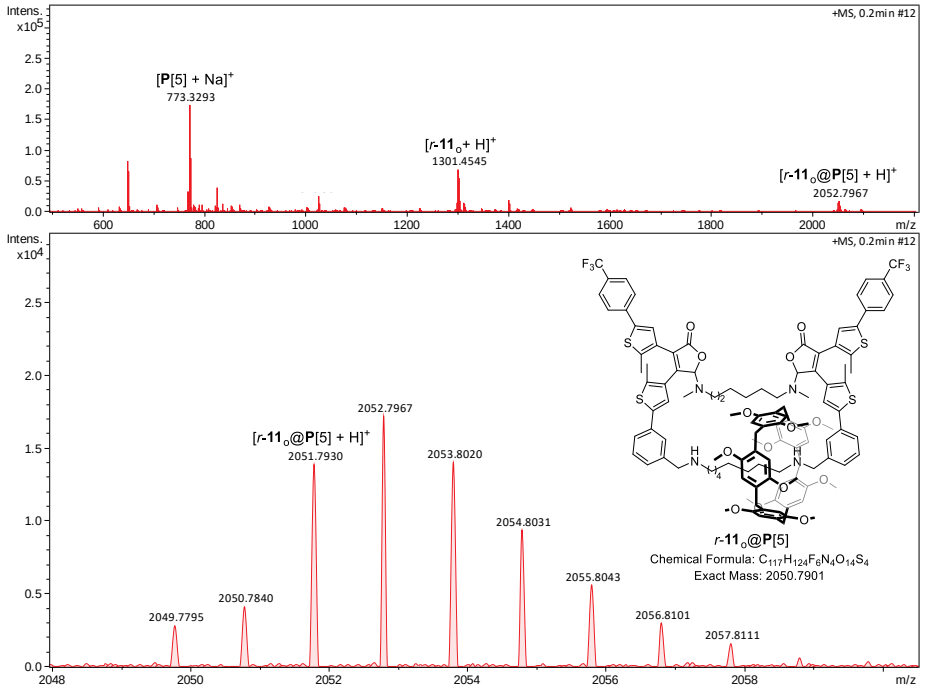

Figure S79. ESI mass spectrum of complicated mixture obtained by the reduction of **11**$_o$ and **11**$_o$**@P**[5]. The species *r*-**11**$_o$ and *r*-**11**$_o$**@P**[5] were detected. A solution of **11**$_o$ and **11**$_o$**@P**[5] (as the procedure in Figure S76) was generated from **10**$_o$ (71.5 mg, 60 mmol), **2a** (1 equiv.), and **P**[5] (6 equiv.) in $CHCl_3$ (6 mL). $NaBH_4$ (1 equiv.) and MeOH (0.1 mL) were then added. After 5 min the reaction was quenched with water. The extraction and evaporation *in vacuo* afforded the crude mixture, which was difficult to separate.

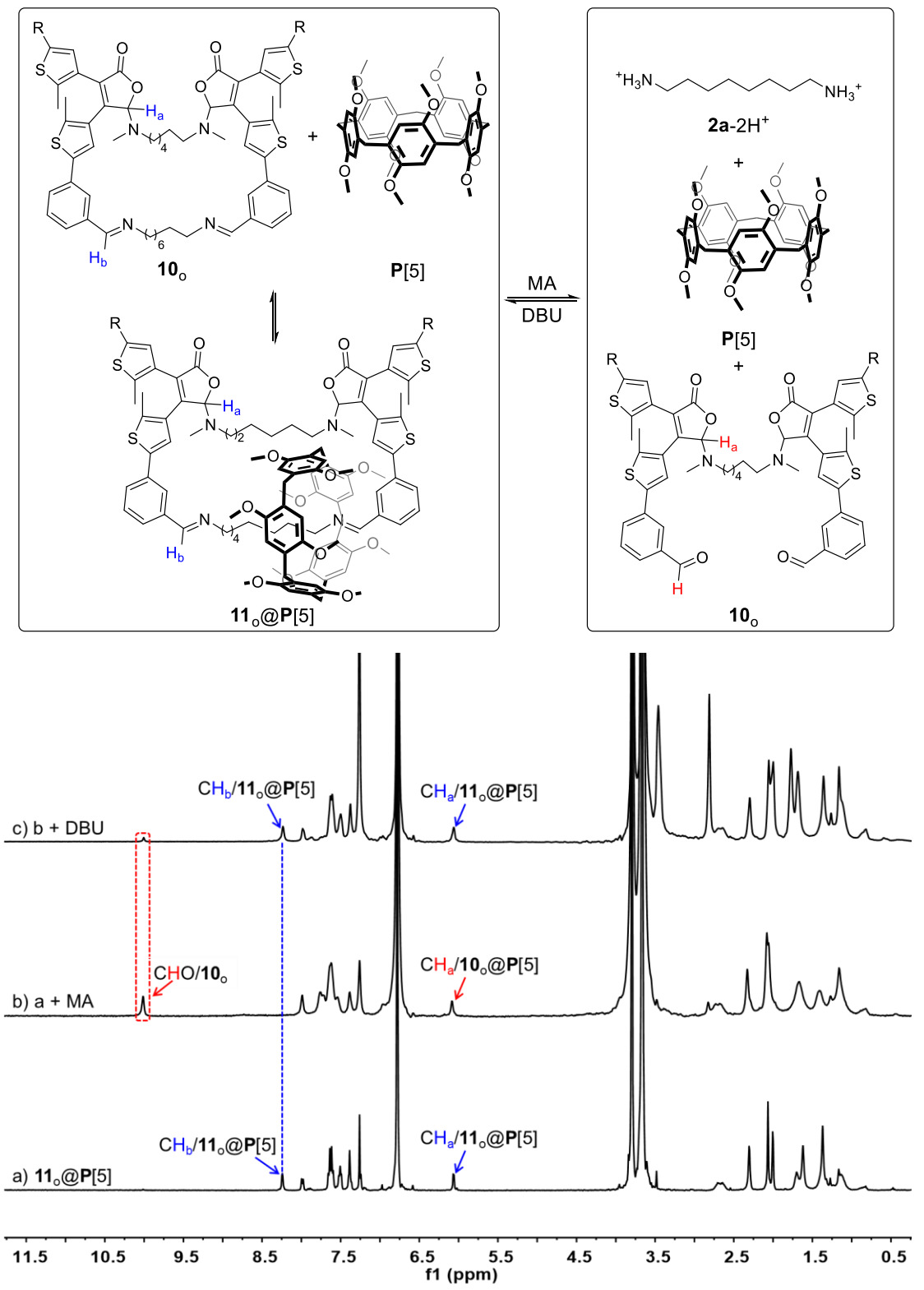

Figure S80. Controlled assembly/disassembly of catenane through acid/base stimuli. (A) (a) ^{1}H NMR spectrum of the mixture of **11**$_o$**@P**[5]; (b) The addition of MA (2 equiv.) to panel a. The assembly broken down immediately; (c) The addition of DBU (2.3 equiv.) to panel b. The integral ratio of CH$_b$/**11**$_o$**@P**[5] and CHO/**10**$_o$ is 87:13. The imine macrocycle was re-formed in 7 days.

8. References

S1. Moreno, J.; Schweighöfer, F.; Wachtveitl, J.; Hecht, S., Reversible Photomodulation of electronic communication in a π-conjugated photoswitch-fluorophore molecular dyad. *Chem.-Eur. J.* **2016**, *22*, 1070-1075.

S2. Lattmann, E.; Sattayasai, N.; Schwalbe, C. S.; Niamsanit, S.; Billington, D. C.; Lattmann, P.; Langley, C. A.; Singh, H.; Dunn, S., Novel anti-bacterials against MRSA: synthesis of focussed combinatorial libraries of tri-substituted 2(5H)-furanones. *Curr. Drug Discovery Technol.* **2006**, *3*, 125-134.

S3. Zhang, M.; Lu, H.; Ye, H.; Li, Z.; Hai, Y.; You, L., Photoinduced generation of carbocations enabled by the promotion of aromaticity. *Org. Chem. Front.* **2023**, *10*, 3889-3897.

S4. Frisch, M. J.; Trucks, G. W.; Schlegel, H. B.; Scuseria, G. E.; Robb, M. A.; Cheeseman, J. R.; Scalmani, G.; Barone, V.; Mennucci, B.; Petersson, G. A.; Nakatsuji, H.; Caricato, M.; Li, X.; Hratchian, H. P.; Izmaylov, A. F.; Bloino, J.; Zheng, G.; Sonnenberg, J. L.; Hada, M.; Ehara, M.; Toyota, K.; Fukuda, R.; Hasegawa, J.; Ishida, M.; Nakajima, T.; Honda, Y.; Kitao, O.; Nakai, H.; Vreven, T.; Montgomery, J. A., Jr.; Peralta, J. E.; Ogliaro, F.; Bearpark, M.; Heyd, J. J.; Brothers, E.; Kudin, K. N.; Staroverov, V. N.; Kobayashi, R.; Normand, J.; Raghavachari, K.; Rendell, A.; Burant, J. C.; Iyengar, S. S.; Tomasi, J.; Cossi, M.; Rega, N.; Millam, J. M.; Klene, M.; Knox, J. E.; Cross, J. B.; Bakken, V.; Adamo, C.; Jaramillo, J.; Gomperts, R.; Stratmann, R. E.; Yazyev, O.; Austin, A. J.; Cammi, R.; Pomelli, C.; Ochterski, J. W.; Martin, R. L.; Morokuma, K.; Zakrzewski, V. G.; Voth, G. A.; Salvador, P.; Dannenberg, J. J.; Dapprich, S.; Daniels, A. D.; Farkas, Ö .; Foresman, J. B.; Ortiz, J. V.; Cioslowski, J.; Fox, D. J. Gaussian 09, revision D.01; Gaussian, Inc.: Wallingford, CT, **2010**.